ESTABLISHING AND TESTING DETECTION METHODS FOR ANTI-ICING AND DEICING CHEMICALS USING SPECTRAL DATA

By

Gabriel Fulton, B.S.

A Thesis Submitted in Partial Fulfillment of the Requirements

for the Degree of

Master of Science

in

Civil Engineering

University of Alaska Fairbanks

August 2019

APPROVED:

Nathan Belz, Committee Chair
Franz Meyer, Committee Member
Svetlana Stuefer, Committee Member
Robert Perkins, Chair
Department of Civil Engineering
Bill Schnabel, Dean
College of Engineering and Mines
Michael Castellini,
Dean of the Graduate School

Abstract

Snow and ice accumulation on pavement reduce roadway surface friction and consequently result in diminished vehicle maneuverability, slower travel speeds, reduced roadway capacity, and increased crash risk. Though the use of chlorides and other freeze-inhibiting substances have been shown to reduce these negative factors, methods to quantify and analyze snow and ice remediation methods as well as the imposed loss of material are needed to allow state and municipal agencies to better allocate winter maintenance resources and funding.

The use and application of chlorides, sand, and their related mixtures have proven to be highly effective for controlling or removing the development of ice on the roadway surface. However, if the amount of salt in solution becomes too dilute, then it no longer retains the capacity to control the development of, or to melt, ice on the roadway and may prove to be more detrimental by allowing the previously melted material to refreeze with a smoother (i.e., more slippery) surface state. The goal of this project was to determine to what extent winter roadway surfaces can be analyzed using spectrometry to determine the longevity and coverage of various types of applications.

Using a systematically paired analysis of changes in spectrometric curves as solution concentrations change, relationships were generated which detected change in deicing and anti-icing compounds reliably in a lab setting. Field results were less reliable, suggesting that further comparisons and a more in-depth spectral library are needed.

TABLE OF CONTENTS

LIST OF FIGURES

LIST OF TABLES

LIST OF ABBREVIATIONS

AK	Alaska
AKDOT&PF	Alaska Department of Transportation and Public Facilities
Band Math	Mathematical Comparison of Wavelengths
CMA	Calcium Magnesium Acetate
HyLab	Hyperspectral Imaging Laboratory
KAc	Potassium Acetate
MDSS	Maintenance Decision Support System
NaCl	Sodium Chloride
NDVI	Normalized Difference Vegetation Index
NIR	Near infrared
NUV	Near ultraviolet
PNS	Pacific Northwest Snowfighters
PSR+	PSR+ 3500 Spectroradiometer
RWIS	Remote Weather Information Systems
USDOT	United States Department of Transportation
VIS	Visible

CHAPTER 1. INTRODUCTION

1.1.Problem Statement

Over 70% of roads in the United States are located in cold and snowy regions (*Snow and Ice*, 2017). The management of anti-icing and deicing efforts during winter months in these regions is critical for mobility and safety. Snow and ice accumulation on pavement reduces roadway surface friction resulting in lower vehicle maneuverability, slower travel speeds, reduced roadway capacity, and increased crash risk. The extent to which certain chemicals and practices are effective at mitigating the effects of snow and ice are, for the most part, well understood. However, little knowledge exists on the physical processes that affect the longevity of these applications. Methods to quantify and analyze snow and ice remediation methods as well as the imposed loss of material are needed. This information would allow state and municipal agencies to better allocate resources and funding.

1.2.Background

The use and application of salt, sand and their related mixtures, and derivatives have proven to be highly effective for controlling or removing the development of ice on the roadway surface. Ample research exists to indicate the way in which application method, application rate and efficacy of mix contents can vary depending on temperature and surface conditions. There is also substantial research on the environmental impacts of anti-icing and deicing applications on factors such as soil and groundwater as well as the corrosive properties of different types of chlorides. However, there is little if any research to suggest the longevity and dispersal of anti-icing and deicing compounds after they have been applied to the roadway surface (i.e., how long does it stay in place and where does it go after it has been applied?). It stands to reason that anti-icing and deicing compounds (e.g., salt and sand) are only effective at or above a certain

concentration. That is to say, if the amount of salt in solution becomes too dilute, then it no longer retains the capacity to control the development of, or to melt, ice on the roadway and may prove to be more detrimental by allowing the previously melted material to refreeze. The different methods for salt to be transported away from the location of application is demonstrated in Figure 1.1. Either tracking due to mechanical movement of vehicles or meltwater flow, lateral dispersion due to mechanical movement or meltwater flow, aerosolization of applied material due to application process or mechanical movement, or adherence to vehicles and deposition elsewhere.

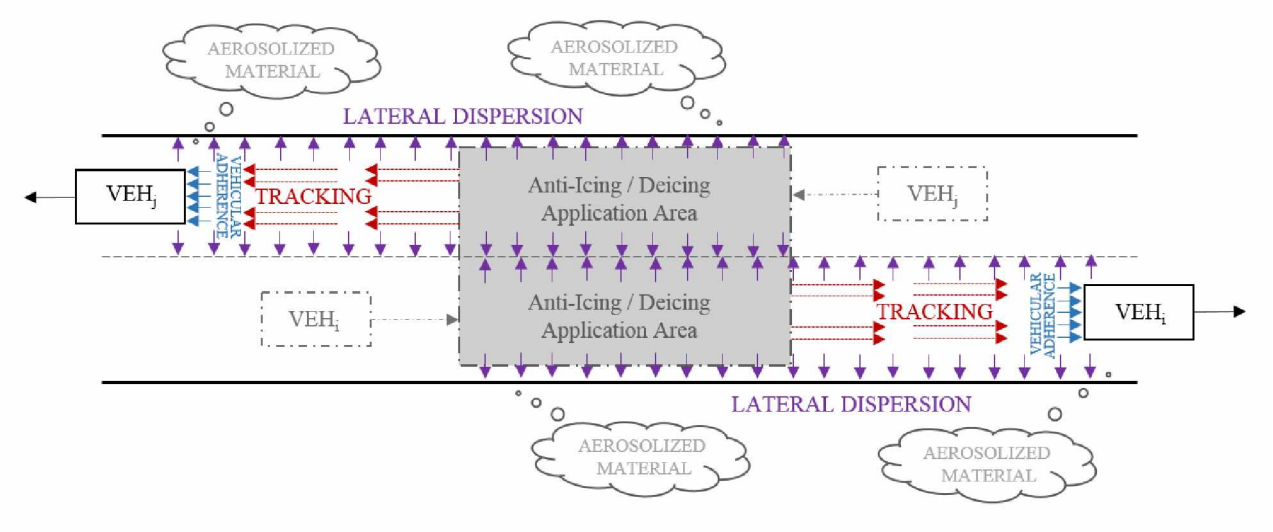

Figure 1.1 Methods of Anti Icing/Deicing Migration/Transport

1.3.Objectives

The goal of this project was to determine to what extent winter roadway surfaces can be analyzed using spectrometry to record the percentage reflectance at each wavelength. The results and deliverables of this research demonstrate broader applicability of spectral sensing technologies in the field of transportation. The findings of this research serve to quantify effects on visible and infrared reflectance of anti-icing and deicing chemicals and may provide information that can be used to better inform winter maintenance efforts and activities. Three

degrees of detection were attempted, 1) simple presence or non-presence of chemical, 2) percent surface coverage within the spectral unit's viewshed, and 3) the estimated amount or concentration of deicer present.

CHAPTER 2. LITERATURE REVIEW

There are roughly four million miles of roads and streets in the United States with more than 135 million registered motor vehicles. Over 70% of these roads are located in snowy regions, which the Federal Highway Administration (FHWA) classifies as locations that receive more than five inches of average snowfall annually (*Snow and Ice*, 2017). The accumulation of snow and ice on roads lowers pavement surface friction causing reduced vehicle maneuverability, slower travel speeds, reduced roadway capacity, and increased crash risk. Because of the negative effects of seasonal winter conditions on driving, fighting snow and ice is a priority for organizations tasked with the maintenance of public roads and highways (e.g., city and state maintenance divisions).

2.1. Organizations Responsible for Maintaining Safe Roads

The organization responsible for the maintenance of city streets is typically the Public Works Department and includes infrastructure related to sidewalks, traffic signals, signage, streetlights, storm drain systems, and during the winter months, snow plowing and street sanding[1]. For state highways, the Department of Transportation (DOT) is responsible for the development, implementation, and coordination of maintenance and operations activities for a given region within a state. Maintenance and operation responsibilities include all the activities required to keep a given state's highways, bridges, airports, buildings, and harbors in good condition and safe for the traveling public. During winter months in cold and snowy climates this includes anti-icing, deicing, snowplowing, snow hauling, and avalanche control and mitigation (Monteleone, 2012). The third major government organization supporting the safety of the traveling public is the FHWA whose goals established by Congress are increasing safety on

[1] City of Fairbanks Public Works Department

roads, insuring infrastructure is in good repair, congestion reduction, improving efficiency of surface transportation, and environmental sustainability (*Transportation Performance Management, 2017*).

These organizations analyze safety concerns of roadways on a local, state, and national level respectively. Only 70% of roads in the FHWA's classification are considered to be in snowy regions, however, all states can experience snowfall. In 2017 all 50 states in the nation experienced at least one inch of snowfall. Even if snow may not be a guarantee, it is imperative for all regions in the United States to have plans for responding to snow or ice accumulation (Dolce, 2017). The risks associated with winter roadway conditions are immediately apparent to the average motorist who has driven on icy or snow-covered roads. Reduced friction caused by ice and snow (and to some extent colder pavement conditions and colder tire rubber) leads to increased accident rates, increased time to accelerate or come to a stop, and reduced visibility. The problem is that these effects may not be visually apparent to a driver. In order to understand the restrictions imposed by winter roadway conditions the effects must be quantified.

2.2. Costs of Snow and Ice Accumulation

Roadway speeds can be reduced by up to 40% on snowy or slushy pavement (*Snow and Ice*, 2017). Reduced traffic speeds, while impactful on the average motor vehicle operator, are not the biggest risk associated with snow and ice. Or most concern is the prevalence and risk of crashes. Of the crashes reported to the FHWA in the last 10 years, there were on average 1,234,145 weather-related crashes per year which could be further broken down as 18% in snow/sleet, 13% on icy pavement, and 16% on snow/slushy pavement (*How Do Weather Events Impact Roads?,* 2017).

From a public safety perspective, managing snow and ice accumulation is a critical step in the prevention of such weather-related accidents. The costs associated with managing snow and ice accumulation can be significant. Winter road maintenance accounts for roughly 20% of DOT maintenance budgets, totaling almost 2.3 billion dollars annually (*How Do Weather Events Impact Roads?,* 2017). Perhaps more so than any other state in the nation, Alaska must deal with considerable snowfall and the longest periods of sub-zero temperatures, and by extension Alaska also reaches the coldest air and pavement temperatures. Alaska has 5600 miles of state-owned roadways, 845 bridges, 79 maintenance facilities, and the state itself has temperatures ranging from 100F to -80F and snowfalls as high as 974 inches of snow at Thompson Pass in a single year (Monteleone, 2012).

Responsibility for roadway maintenance in Alaska is divided into three Department of Transportation regions: Southcoast, Central, and Northern. The largest city in Alaska is Anchorage which is the home of Central region Alaska Department of Transportation. Anchorage has a population nearly 300,000 people and the city of Anchorage spent $16 million on snow maintenance in the winter of 2011 (*Winter Maintenance: Snow removal cost Anchorage*, 2017). These costs may seem astronomical for fighting snow and ice, however a study done by IHS Global Insight attempted to quantify the economic impact of a one-day snow-related shutdown. It was estimated a one-day shutdown for a state would cost $300-700 million for businesses, governments, and people, snow-related shutdowns would harm hourly workers the worst accounting for two thirds of direct economic losses (IHS Global Insight, 2014).

The economic impact of snow-related closures far exceeds the cost of snow removal. The efficacy of snow removal and control has been established by the FHWA, DOT, Public Works, and independent studies. In the late 1980's, research conducted at the Technical University of

Darmstadt in Germany compared winter road maintenance operations before and after bare road pavement policy was established, the results of the experiment are shown below in Figure 2.1. The rate of vehicular crashes is reduced almost immediately after the application of a chemical deicer (e.g., salt).

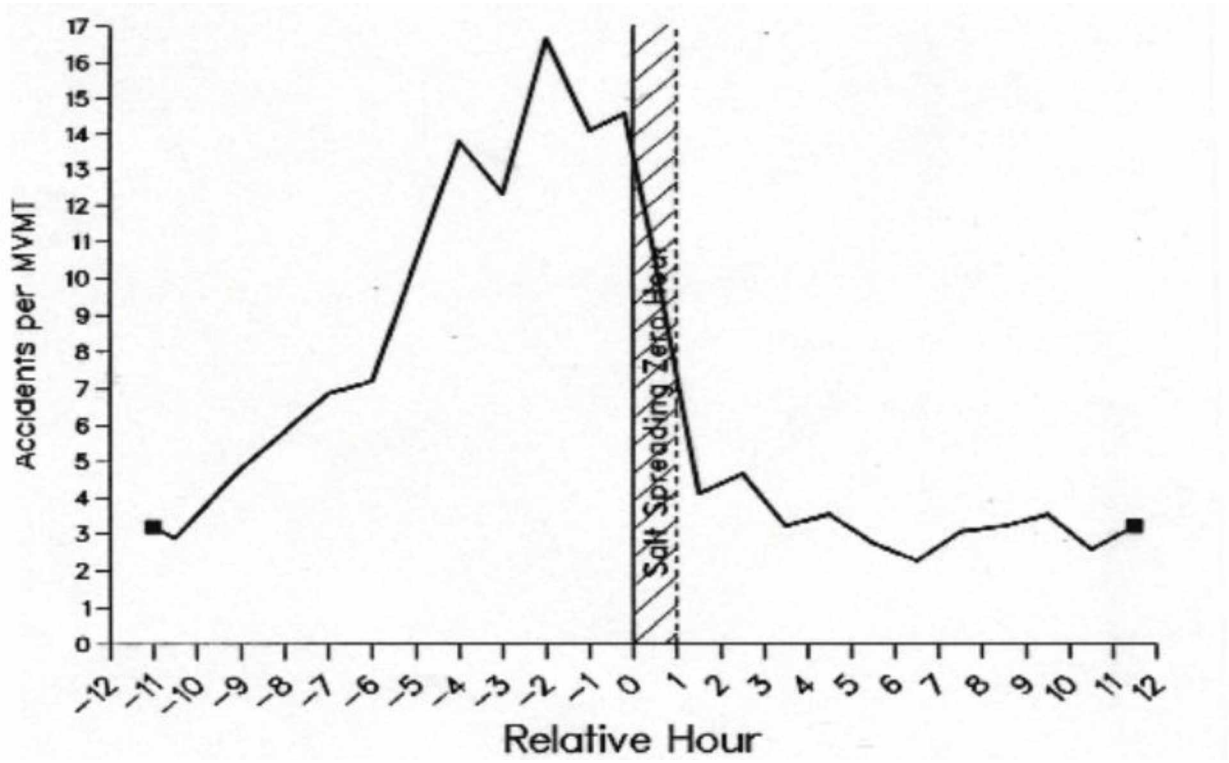

Figure 2.1 Traffic accident rates before and after salt spreading (Kuemmel & Hanbali, 1992).

2.3. Mechanical Snow and Ice Removal

There are many different methods of snow and ice control utilized by winter maintenance crews. Mechanical removal by plowing or blowing snow accumulation is most common. The procedure followed by winter maintenance crews and the time after a snowfall event when mechanical removal starts varies and is determined by local policies. Snow plows are used to scrape snow and ice from roadways and wasted into the shoulder or roadside in order to maintain safer driving conditions. Plowing is the quickest and most cost-effective way to remove snow

from roads. The Snow and Ice Control Environmental BMP Manual discusses the five main plow types and a brief description is shown in Table 2.1.

Table 2.1 Plow Types (Fay, Honarvarnazari, Jungwirth, Muthumani, Cui, Bergner, & Venner, 2015)

Plow Type and Description	Photo
The front end plow is most common type of plow, which offers good performance and versatility. The front end plow is mounted on the front of a vehicle and some have the option of changing the angle from side to side.	
The wing plow is often integrated with the front end plow to clear a wider road surface and transport snow further away from the roadway, which helps prevent snow from blowing and drifting on the road surface.	
A second configuration of the wing plow consists of the wing plow mounted further back from the front end plow.	
The tow plow is a large plow towed behind a vehicle. It is often used to span a wide road surface to minimize the number of passes and plow trucks needed to plow the width of the road. The use of tow plows significantly reduces the costs associated with labor and fuel.	
Underbody plows are typically installed on deicer spreader equipment to prevent reduced visibility of the road surface compared to front end plows. This gives the operator a better visual inspection of the roadway surface, which allows operators to remove any loose snow and ice immediately prior to deicer application.	

The optimal plow blade and design of a plow vehicle changes based on need and cost. The most common type of plow is the front-end plow, it is easily mounted on the front of a truck, the 14' wide version can completely clear 12' lanes in one pass reducing the need a second pass and therefore reducing exposure between traffic and snow plow trucks (*Best Practice for Road Weather Management*, 2012). The side-wing plow is effectively the same as a front-end plow, however miniature plows are attached to the side as wing. The side-wing plow requires a truck with higher horsepower due to the increased snow load being moved, this wider plow allows for two full highway lanes to be cleared in a single pass, reducing operator time. (Conger, 2005). The underbody plow is a blade located underneath an operator's vehicle, it gives the operator a clear line of sight. Construction graders are commonly used as underbody plows in municipal and residential snow removal. A tow plow is a unit towed by a vehicle, the unit can be tilted to travel into an adjacent lane and plow snow. Tow plows are used in conjunction with a front-end plow in order to clear multi-lane roadways, reducing operator time (*Best Practice for Road Weather Management*, 2012).

There are numerous plowing techniques, and each has benefits and associated costs. Depending on the needs of a road and constraints put on winter maintenance crews, different plow types are preferable. The Table 2.2 below depicts the four most common plowing techniques by maintenance crews in the United States in 2015, associated costs, and corresponding benefits.

Table 2.2 Costs and Benefits of Plowing Techniques (Fay et al., 2015)

Technique	Costs	Benefits	Reference
Using wider front plows and tow plows	Conversion to 14-ft plow: $400/foot Tow plows reduce equipment investment by 20% to 30%	Reduced number of passes required Fuel savings Reduced labor required Increased snow removal efficiency	Lannert, 2008
High speed snow plow	Potential roadside damage	Reduced chemical usage Improved level of service due to flexible cutting edge	Gruhs, 2008
Use of underbody plows and improved overall plowing practices	Total costs including pre-wetting equipment: $53,700	Total savings from salt reduction $151,200	Environment Canada, 2000
Tow Plow	$93,000	20-30 % savings Plow 50% more miles 6-7 year return on investment Increased service life of 20-30 years compared to typical 12-15 years Operates at 40% of the cost of standard plow	Behnan, 2014 Michigan DOT

One of the issues associated with all of the discussed plowing techniques is where the snow goes after being mechanically removed. Repeated plowing throughout the winter allows for significant amounts of snow to accumulate along the sides of traveled ways. This accumulation can create many issues such as visual obstruction for motor vehicles, facilitate easier formation of snow drifts on roads, or the creation of ramping conditions when snow accumulates near guardrails or bridges effectively allowing vehicles to unintentionally slide over guard barriers. Loading, hauling, and dumping of snow is necessary in certain areas but can be time intensive

and costly. The most cost effective and easily mobilized snow removal operation for plowed snow is to use a loader to fill a conventional dump truck with excess snow, the dump truck can then haul the snow to a designated storage or melting site (*Synthesis of Best Practices*, 2003). Snow blowers are typically used for post-storm snow removal. One of the main advantages of snow blowers is that the location of the blown snow has a lot more control over that of a plow, the snow can be blown directly into a dump truck, or farther away from roads so as not to create the line of sight problems associated with using plows. The drawbacks that prevent snow blowers from common use is the extra cost of maintaining the blowers and the slower clear speed.

2.4. Snow and Ice Remediation Applications

Instead of physically or mechanically removing snow and ice from roads, chemical-based remediation methods can be used. Many materials can be applied to roadway surfaces by winter maintenance crews in order to make roads safer for motorists. Chemicals, such as chlorides and other salt derivatives, can be applied to melt the ice by lowering the temperature at which ice forms. These salts can have admixtures added to them in the form of different carbohydrates that can further enhance their efficacy, such as beet juice. Dry abrasives, such as gravel or sand, can also be applied to add traction to icy roads. Applying these different materials can drastically increase safety on roads by increasing traction of road surfaces, and if used appropriately without too much associated cost.

Chemical removal of ice and snow is most commonly achieved using chlorides and facilitated by physical application as a solid or be dissolved in water to form a liquid brine. The three most widely used snow and ice control salts are sodium chloride (NaCl), magnesium chloride ($MgCl_2$), and calcium chloride ($CaCl_2$) (Fay et al., 2008). The goal of applying these

chlorides to a roadway surface is lowering the freezing point of water. By reducing the freezing point of water, the accumulation of ice can be avoided as well as releasing the bond between ice and the pavement surface. The deicer which is best suited for a given region, city, or winter maintenance crew is determined through many factors such as melting capacity, temperature performance, environmental impacts, corrosion impacts, and consistency issues. The effects of the five most common deicing chemicals on the freezing point of water is shown in Figure 2.2. The effects of deicing chlorides can be improved with additives such as carbohydrates.

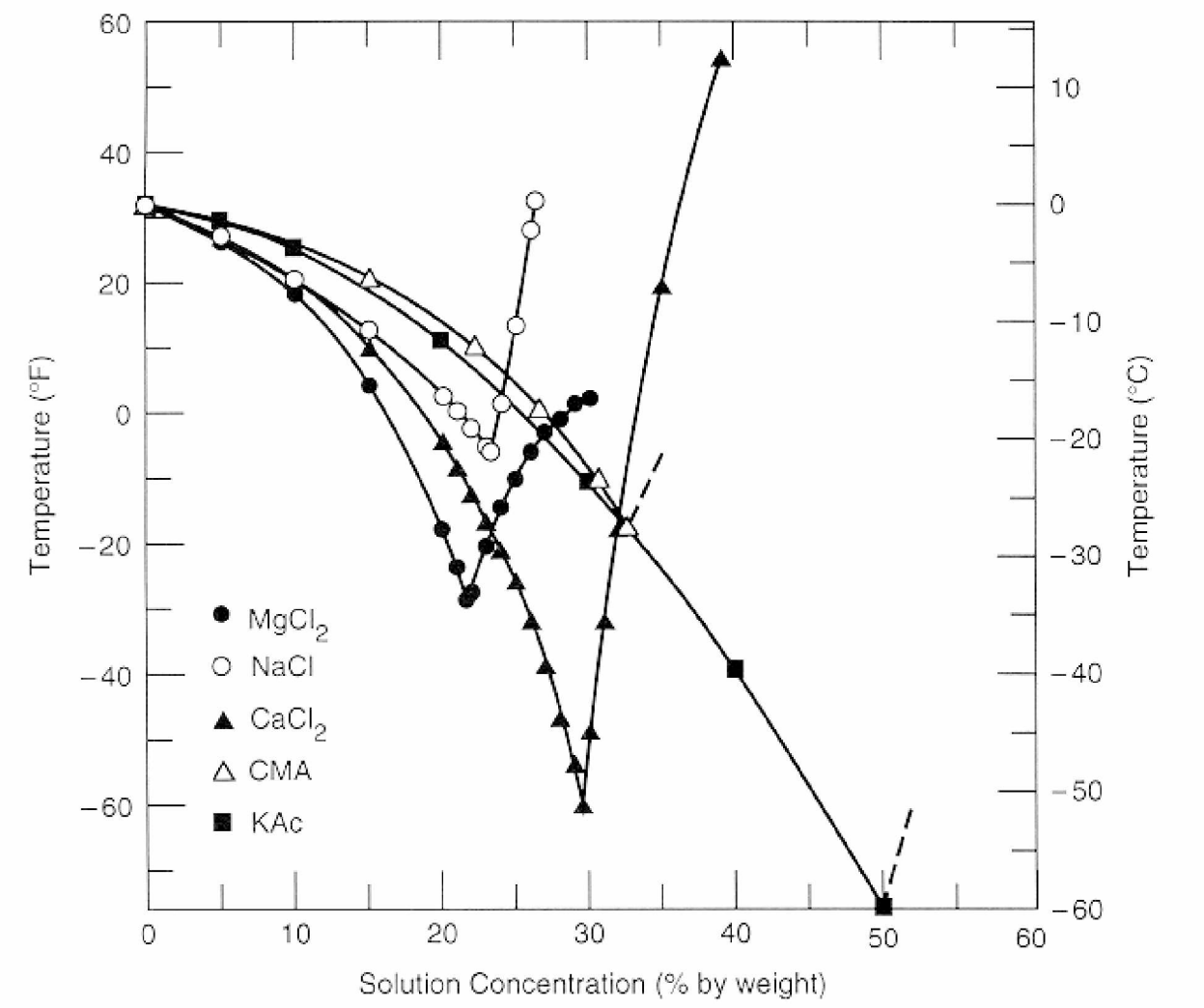

Figure 2.2 Relative Temperature of Efficacy by Concentration for Chemical Deicers (*Manual of Practice for an Effective Anti-Icing Program,* 1996)

For most deicing compounds, the freezing point temperature is lowered as the concentration of the respective chemical is increased. This relationship holds true until a temperature known as the *eutectic point* when the freezing temperature subsequently increases. Falling below the deicer temperature curves means the solution has frozen and only a mixture of solids and ice will remain. Practically speaking, when applying deicing compounds, winter maintenance crews strive to achieve a concentration as near to, but not exceeding, the eutectic point as possible. Conversely, it is important that the concentration does not fall to such a low point that freezing can occur. Balancing the concentration of deicer has profound implications when it comes to determining likely performance of an ice-control product on the road. It is not only the quantity of snow or ice that a product can melt, but also the rate at which it melts and how long it will be before the melted ice and remaining deicer will refreeze, and how much winter events or repeated driving of motorists will spread deicer off of the road that must be considered when using deicing compounds (Nixon, Kochumman, Qiu, Qiu, & Xiong., 2007).

Calcium magnesium acetate (CMA) and potassium acetate (KAc) both need significantly higher concentrations than sodium chloride in order to remain effective (Figure 2.2). Because of this reduced melting capacity, calcium magnesium acetate and potassium acetate conservatively need 1.4 times the concentration to remain equal in temperature performance to sodium chloride. A higher volume requires more operator time to transport and apply and therefore have considerably higher costs per application treatment (*Manual of Practice for an Effective Anti-Icing Program,* 1996).

However, chemical deicers have operational, environmental, and infrastructural drawbacks. One of the main operational concerns about the application of deicing liquids on highways is the potential for the deicer to create a slick surface. One of the causes of slickness

associated with deicers occurs when the chloride liquid dries out and leaves a chemical slurry that reduces road surface friction (Nixon et al., 2007). Winter maintenance crews can avoid this effect by not applying chemicals to the road surface when temperatures are above 40 degrees Fahrenheit.

All deicing compounds that are placed on roads will eventually be transported away from the road and end up in nearby soils, enter storm drains, ultimately residing somewhere in the surrounding environment. It is the responsibility of those applying these compounds to consider the deleterious effects of these substances. Excessive use of deicing compounds has the potential to negatively impact the environment. Damage to the environment should be weighed against the positive effects such as reducing vehicle accidents (e.g., a car crash) which create environmental damage in the form of leaked gasoline, oil, and coolant that may disperse far from the scene of the crash. The Pacific Northwest Snowfighters (PNS) requires that toxicity tests be run on deicing compounds including a Rainbow Trout or Flathead Minnow Toxicity Test, Ceriodaphnia Dubia Reproductive and Survival Bioassay, and Selenastrum Capricornutum Algal Growth whose procedures are described by the EPA and American Public Health Association (Nixon et al., 2007).

Water quality, air quality, soil quality, and land and water-based plants and animals can be negatively affected by deicers. A study done by the USGS Wisconsin Water Science Center did an investigation into the effects of deicer material runoff on aquatic toxicity surrounding an airfield and found that chloride and sodium analyses demonstrated the influence of urban runoff in the nearby watershed, especially downstream from the airport where concentrations of these road-salt-derived contaminants increased due salting of roads, parking lots, and sidewalks downstream from airport drainage (Corsi et al., 2008). Between November 1996 and April 2007,

47 samples were collected to check for chlorides. The study found that 68% of samples exceeded the hourly average USEPA water-quality criterion (860 mg/L) and 91% of samples exceeded the 4-day average criterion (230 mg/L). It was concluded that salt runoff from roads has a considerable effect on aquatic life in the watershed near the tested airport (Corsi et al., 2008). A study prepared for the Illinois Department of Transportation by Atmospheric Environment Section of the Illinois State Water Survey did tests regarding the atmospheric dispersion of deicing salt through aerosolization. The data was collected by using continuous high-volume aerosol samplers, a dichotomous aerosol sampler, and through collection of snow samples at different distances from Interstate 55 (Williams, Stensland, Peters, & Osborne, 2000). The results were that the salt deposition pattern near a treated roadway, as determined by snow samples, decreased consistently with distance from a road. The average deposition per length of a roadway was 300 pound per mile which is similar to the typical salt application done by Illinois Department of Transportation in 1994 (Williams et al., 2000). The research concludes that no source of aerosolized deicer material can be determined from the research done so far, only confirming that indeed deicer is dispersed into the area surrounding the sides of the road. This suggests the need for additional studies on detection and tracking of deicing materials and is one of the motivating factors for the research presented in this thesis.

Deicer products have the potential to damage many aspects of the transportation infrastructure such as pavement, rebar, metals, roadside equipment, and vehicles. Deicers can affect concrete both physically and chemically. Physical effects are typically manifested as cracking and scaling. The chemical effects result from reactions involving hydration products, aggregates, or corrosion of the reinforcing steel (Sumsion & Guthrie, 2013). The deicer ions react chemically with concrete and leach calcium hydroxide from the paste, decalcify the

calcium silicate hydrate, convert the magnesium silicate hydrate, and form brucite, complex salts, and oxychlorides. An alkali-silica reaction and alkali-carbonate reaction can be initiated and accelerated by alkalis from deicers, as well as the accumulation of critical concentrations of chloride ions around steel can initiate corrosion (Sumsion & Guthrie, 2013). Using information gathered by various sources the Utah Department of Transportation came to the conclusion that sodium chloride should be utilized by engineers responsible for winter maintenance wherever possible instead of CaCl, $MgCl_2$, CMA, and only to utilize the amount needed to ensure the safety of the traveling public (Sumsion & Guthrie, 2013). Use of deicers, in most amounts, can be damaging to vehicles and the infrastructure upon which they travel. However, using deicing compounds such as sodium chloride can be extremely beneficial to ensure safe winter roadways.

One option other than chlorides and chemicals are sands and gravels. These abrasives provide temporary but immediate traction on icy roads. Abrasives are most effective for vehicles traveling 30 mph or less. If vehicles are traveling greater than 30 mph, there are diminishing returns on traction and additional costs related to clean-up (*Guidelines for the Selection of Snow and Ice Control*, 2007). Consequently, the most effective places for abrasives to be applied are on low volume roads near hills, curves, and intersections where speeds are relatively low. Yet, the use of abrasives may also be warranted when other ice remediation methods are less effective. One of the key problems with applying abrasives is that it does not easily stay on the road. Repeated wear and tracking from passing vehicles will cause loose abrasives to migrate, spreading along the roadway and off the sides of the road. If another snowfall event occurs much of the abrasives will be plowed or blown away. Without enough abrasives present the effectiveness will be greatly reduced therefore reapplication of abrasives will be necessary. To prevent scatter and ensure the abrasives will remain on the roadway surface as long as possible,

there are three general approaches that can be used: pre-wetting sand with liquid deicers, pre-wetting sand with hot water at 30% by weight mix, or heating sand to 356 degrees Fahrenheit (Vaa, 2004; Staples et al., 2004; Lysbakken and Stotterud, 2006; MTO, 2008; CTC & Associates, 2008). These methods effectively cause the ice surrounding the abrasive to partially melt allowing the abrasive to penetrate the surrounding ice and upon freezing locks the abrasive in place.

2.5. Information Assisstance Systems

In addition to applying materials to roadways, information gathering techniques can also aid in making winter roadways safer for motorists and help maintenance operations make better and more informed decisions. Stations devoted to gathering information for the DOT are known as Road Weather Information Systems (RWIS). These stations provide real-time weather data such as atmospheric data: air temperature, humidity, visibility distance, wind speed, precipitation type and rate, cloud cover, and air quality. RWIS also measures roadway data such as pavement temperature, freezing point, roadway condition, and soil temperature. An Alberta Infrastructure and Transportation (2006) cited by Clear Roads, studied the pros and cons of utilizing RWIS and anticipated that RWIS would deliver $5.38 in benefits for every dollar spent (e.g., more efficient use of winter maintenance equipment and deicing chemicals, reduced rate of vehicle collisions, and reduced labor costs). A survey conducted by Clear Roads indicated that of the organizations that have implemented weather forecasting systems, 90% indicated having improved or expanded upon current systems and 77% indicated having expanded their RWIS or weather station networks (Fay et al., 2015). The survey provides evidence that weather and pavement information systems are becoming more widely used for winter maintenance operations. RWIS stations can be used in conjunction with a Maintenance Decision Support Systems (MDSS). The

MDSS assists maintenance personnel in the decision-making processes of determining roadway maintenance activities by providing real-time and post-storm analysis to evaluate materials used, rate of application, and timing of application (Fay et al., 2015). A study conducted in Indiana found that by using MDSS the salt savings in the winter of 2008 was about 228,470 tons ($12,108,910) and if normalized for winter conditions based on storm severity, the total salt savings were 188,274 tons ($9,978,536) (McClellan et al., 2009). Reducing salt usage while also maintaining safe roads is a keen interest of those who utilize it for winter maintenance purposes. The benefits of information gathering, and processing are demonstrated not only from the increased safety and cost savings reported but also from the personnel using MDSS endorsing its efficacy. If new information gathering technology could be added to these RWIS stations that could accurately measure deicer concentration the efficacy and cost effectiveness of winter maintenance practices would be greatly benefitted.

2.6. Spectrometry and Applications to Detect Deicers

The research presented here sought to apply spectrometry and related methodologies to detect elements of deicers. Hyperspectral imaging is a form of remote sensing that quantifies the reflectance of a target surface. Remote sensing methods are advantageous because it negates the need for physically sampling or, depending on the method of data collection, physically occupying areas that would be unsafe, untimely, or otherwise inaccessible. Spectral imaging can take many forms from physical contact reading where the device must be pressed against a surface, to field units capable of distances of up to several feet, to drone and airplane mounted devices, to units housed in satellites.

Spectral analysis often requires the use of "band math" which is a form of mathematical analysis used to interpret reflectance spectra gathered from spectral imaging units. A reflectance

spectra records specified wavelengths and their corresponding reflectance values. Band math compares the relative amount of reflectance at one wavelength to the amount at other wavelengths. Depending on which wavelengths are available a number of mathematical ratios and comparisons can be employed to gather information and make assumptions. One of the most well-known band math equations is the Normalized Vegetation Difference Index (NDVI) which is used to analyze vegetation. The NDVI looks at the ratio of NIR and red bands [(NIR-RED)/(NIR+RED)], and the resulting values can be interpreted to determine vegetation health (Schuckman, n.d.). NDVI analysis was developed and works because of the knowledge inherent to the materials being analyzed. Healthy vegetation reflects more NIR and green light compared to other wavelengths, conversely healthy vegetation absorbs more red and blue light. Using NDVI the image Figure 2.3a can be analyzed and the subsequent result will have each pixel assigned a value from -1 to 1 in Figure 2.3b, green representing proximity to NDVI of 1 or healthy vegetation. A value closer to 1 would signify a healthy vegetation, a value closer to 0 will signify unhealthy vegetation, and a negative value would indicate the presence of water, since water is highly absorptive to NIR. Other forms of band math can be used and will depend on the inherent reflectance of the surfaces and materials being analyzed.

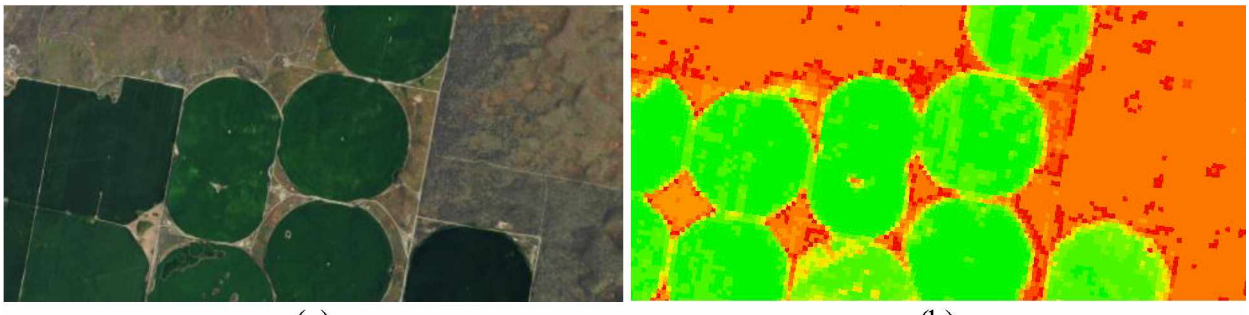

(a) (b)

Figure 2.3 (a) Pre NDVI Processing (b) Post NDVI Processing (*What is NDVI*, 2018)

Reflectance analyses like these are particularly useful for monitoring temporal trends in phenomena of interest. For example, NDVI is useful for farmers monitoring locations where vegetation is most healthy versus least healthy for future agricultural management. NDVI can also be applied to monitoring forest fires and the resulting burn scars. The possibilities and applications of spectrometry are growing and future research, such as the study presented here, should be done to identify the extent to which it can be applied. Band math such as NDVI is one of the many available for interpreting spectral imaging and the uses for band math are only growing as research into new comparisons are conducted. Nonetheless, the use of band math in this research is expected to detect and quantify changes in reflectance due to the addition and subsequent recession of deicing compound applications.

2.7. Conclusion / Research Need

As new ways to measure, process, and plan for winter storm events emerge, new efficiencies in the form of cost savings, environmental protection, or safety can be discovered. The research presented herein attempts to utilize existing methods in spectrometry to track dispersal and concentrations of deicers. Based on the recorded reflectance and adsorption peaks which are unique to substances, materials can be identified and cataloged. For example, chloride and sodium molecules have specific wavelength peaks, and can be identified when comparing water and sodium chloride in aqueous solution. The specific application being presented here is the application of wavelength analysis to monitor the dispersal and transport of deicer (e.g., surface concentrations, surface coverage, and migration).

CHAPTER 3. SPECTRAL DATA AND METHODS

3.1. Setting and Samples

3.1.1. Labratory Preparation

This research employed the use of facilities and equipment available through the University of Alaska Fairbanks (UAF) Hyperspectral Imaging Laboratory (Hylab), specifically spectral imaging unit instrumentation (e.g., HySpex VNIR-1800 and SWIR-384 pushbroom HS cameras). The Hylab has an ASD Fieldspec and a PSR+ 3500, which can be used for field and lab-based measurements and has accessories for calibration, normalization, and analysis. The PSR+ 3500 hyperspectrometer has a wavelength range from 350 nm to 2500 nm, which encompasses the near infrared, visual, and near ultraviolet wavelengths. This was critical to this project because without an established relationship, a wide range of wavelengths would maximize the likelihood of finding the strongest relationships possible. In order to maximize accuracy and consistency of data recorded by the PSR+ 3500, the UAF Hylab has a halogen lamp (Figure 3.1a) that mimics the spectrum and consistency of intensity that natural sunlight creates (Figure 3.1b).

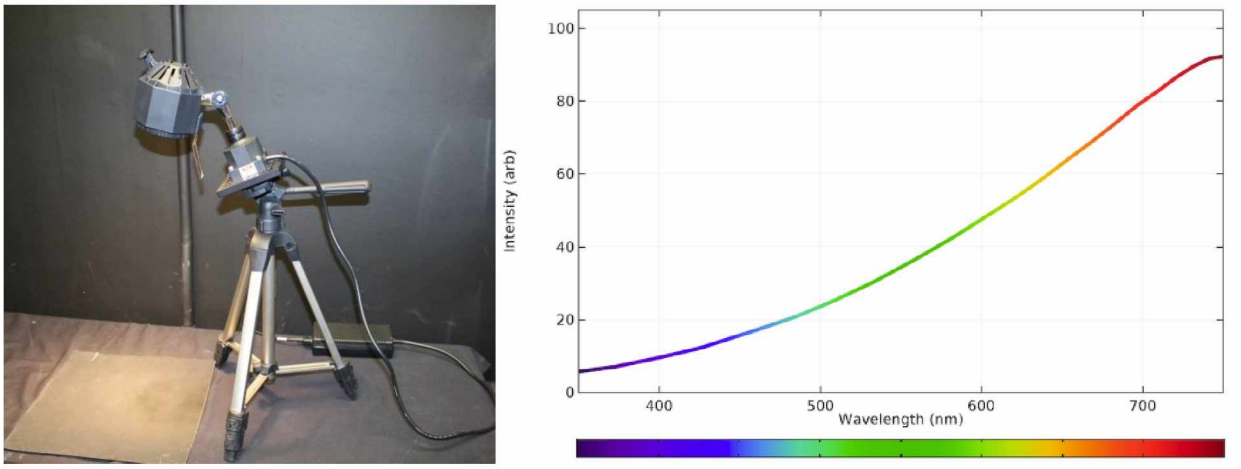

(a) (b)

Figure 3.1 (a) Halogen Lamp Spectra (*Illumination*, n.d.) (b) Halogen Lamp in UAF Hylab

The natural sunlight spectrum (Figure 3.2) can be compared to the halogens' spectrum, both curves have complete coverage of the wavelengths unlike most sources of light.

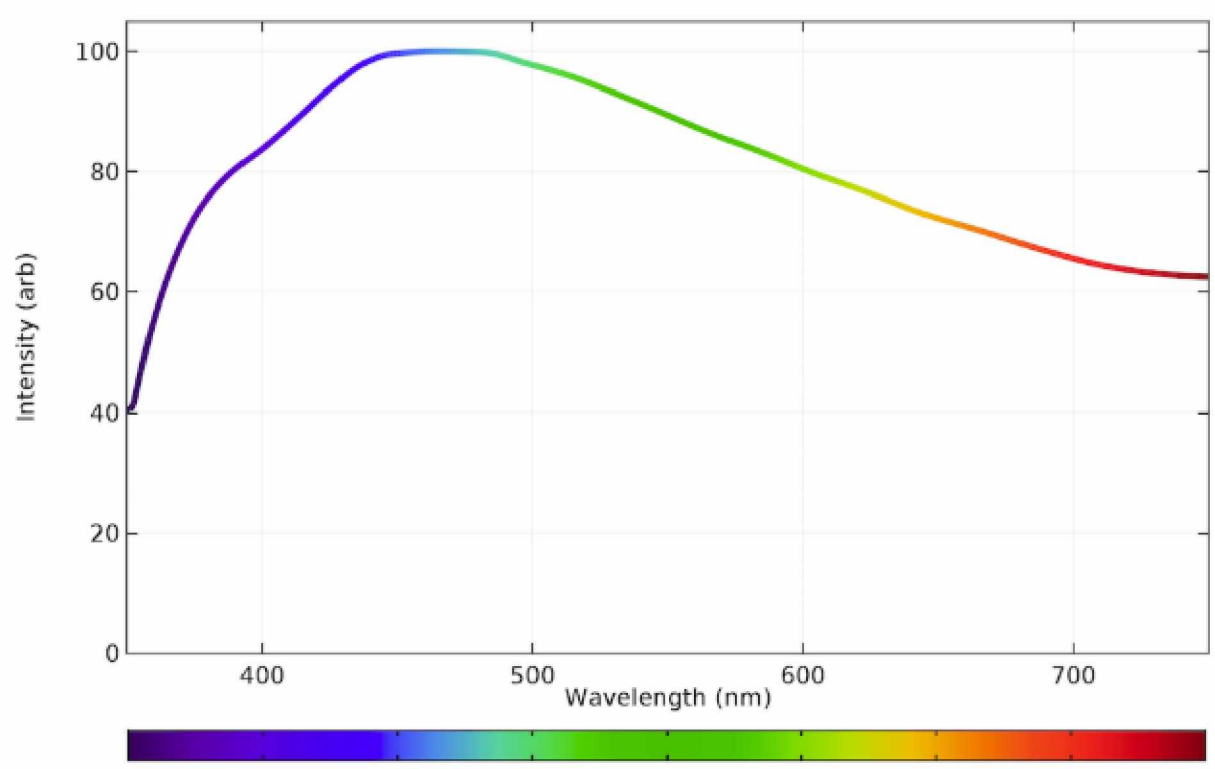

Figure 3.2 Sunlight Spectra (*Illumination*, n.d.)

The PSR+ 3500 collects reflectance of surfaces in the wavelength range of 350 to 2500 nm. The walls, ceilings, and surfaces of the lab are either painted in black paint or covered in black material to minimize extraneous scatter or reflectance. The imaging background is a specially painted black matte board with a flat reflectance spectrum. Extraneous light from outside of the lab is mitigated by restricting access to the lab during imaging. Occupancy of the spectral lab is indicated by closing the door to the small testing room and by turning off the lights in the adjoining room. Light emitted from LED (Figure 3.3a) and fluorescent tube (Figure 3.3b) lights do not have a continuous spectrum like natural sunlight or halogen lamps and could contaminate

observations. If some sections of wavelength do not have any illumination, or if there are sporadic peaks, the reflectance of a target surface can be inaccurate (*Illumination*, n.d.).

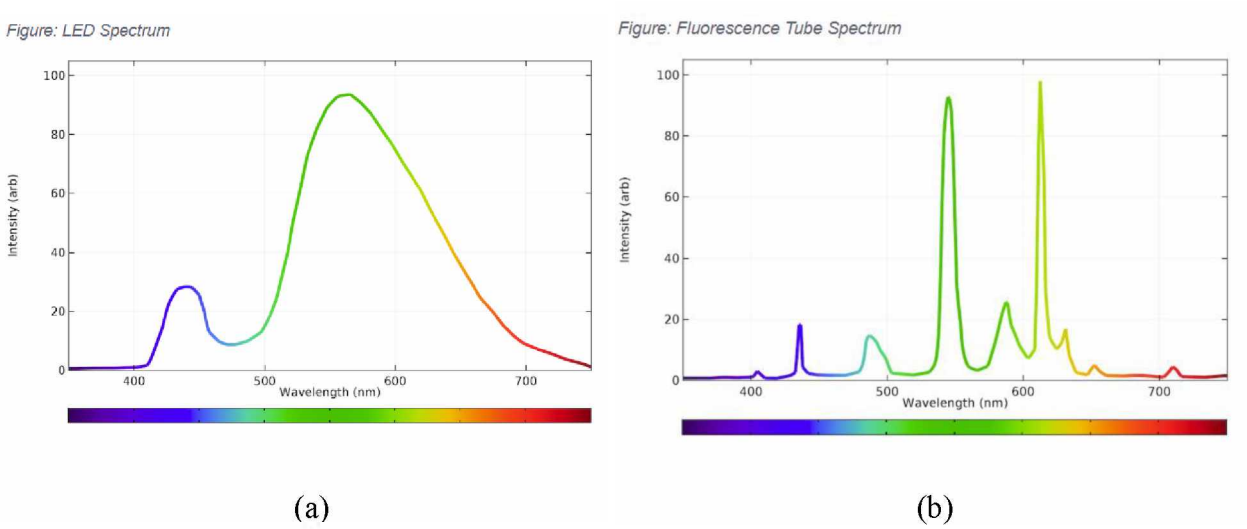

(a) (b)

Figure 3.3 (a) LED Spectra and (b) Fluorescent Tube Spectra (*Illumination*, n.d.)

3.1.2. Lab Sample Preparation

Samples were generated in the lab to simulate field conditions of different concentrations of a deicer brine and a deicer beet-brine mixtures. These samples went through several iterations as the testing procedures were refined. The first set of data were a proof of concept and were comprised of the individual components that would normally be found on a roadway during winter remediation. These materials include asphalt pavement, sodium chloride-based rock salt, ice, traction sand, and water. These materials were imaged in the lab and compared to established spectral curves where available.

After the baseline values for the individual components were recorded, permutations and mixtures that would be found in real world situations were explored. Brine application rates obtained from AKDOT&PF Northern Region are found below in Table 3.1. A concentration of 23.3% sodium chloride is mixed with a carbohydrate beet juice at an 80:20 ratio to generate real world application scenarios.

Table 3.1 AKDOT&PF Northern Region Application Rates

Pre-wetting sand or salt:	8 to 14 gallons of brine or brine with additive per ton of material
Aggregate:	400-750 pounds per lane mile
Salt:	75-300 pounds per lane mile (condition dependent)
Brine or Brine with additive:	20-30 gallons per lane mile when anti-icing; 30-50 gallons per lane mile when deicing

Variations in the amounts and concentrations of these chloride solutions may occur for several reasons. First, deicing materials applied by AKDOT&PF are not done so ubiquitously and evenly across the transportation network. Key locations such as curves, bridges, bridge approaches and intersection are typically a higher priority. AKDOT&PF applies brine at a concentration of 23.3%, which, as it is designed to do, would slowly melt ice and snow and therefore begin to dilute over time. For lab experimentation, a range of brine solutions were fabricated using tap water and included concentrations at 5%, 10%, 15%, 23.3%, and an oversaturated mixture, which is approximated at 40%. This set of concentrations encompass the AKDOT&PF application as well as the subsequent stages of dilution. The oversaturated concentration was used to simulate conditions when either solid salt was applied or evaporation of the ice and snow melt resulted in a high-concentration brine or salt residue. The generated concentrations were fabricated in surface thicknesses of 3.6 mm, 1.6 mm, and 0.8 mm in a petri dish. A film thickness of 0.8 mm was the thinnest achievable thickness on a petri dish due to cohesion and adhesion, the water would stick to itself rather than spread evenly across the dish unless enough liquid was present. The 3.6 mm film thickness was the first achieved volume added to petri dish to achieve full surface coverage without mechanical movement of the liquid in the petri dish to reach full coverage. The 1.6 mm film thickness was then chosen as a midpoint for comparison between the 3.6 mm and 0.8 mm film thicknesses. These concentrations were extrapolated and used to prepare a clone of the AKDOT&PF beet mixture (23% brine solution mixed with 20% beet juice

carbohydrate by volume) at different dilutions at surface thicknesses of 3.6 mm, 1.6 mm, and 0.8 mm. Additionally, pure beet juice mixtures were prepared with water and analyzed.

Recording the interactions of the spectral reflectance of these individual components (as they would be present on a roadway surface) is the ultimate goal of this project. However, to control for potential confounding variables, research started by simulating these field conditions in the lab such that each element can be analyzed individually and then in combination. The simulated winter roadway (Figure 9) was constructed and housed in a black PVC endcap that acted as a container for each material layer (i.e., pavement, ice, and brine). An asphalt pavement sample was compacted using a gyratory compactor in the UAF Asphalt Lab using typical Alaskan roadway specifications. The asphalt pavement sample was then cored to a 3-inch diameter and cut at a thickness that would allow an ice layer to be fabricated on the surface once placed in the PVC cap. The height of the fabricated roadway surface was adjusted in relation to container rim to reach a desired ice layer thickness by inserting washers underneath the pavement core. Desired volumes of water were applied on the pavement core surface and frozen to create ice layers of varied thickness. This simulated road (Figure 3.4), was then treated with deicing compounds and/or aggregate at volumes and weights specified by AKDOT&PF.

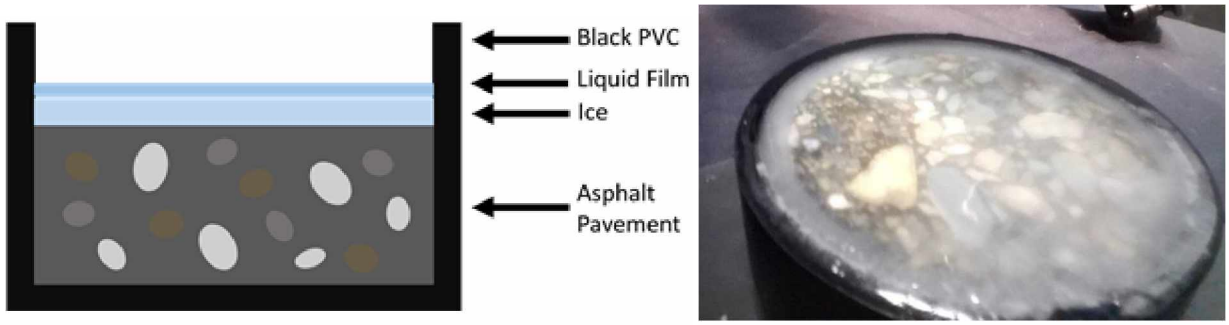

Figure 3.4 (a) Designed Road Simulation (b) Fabricated Road Simulation

During the initial phase of lab testing a field-truthing problem became apparent. Ice layer thicknesses, such as those found on regularly treated and maintained roads, were impossible to achieve on the simulated roads. The correct ice thickness could be created, however, ultimately it could not survive the room temperature environments for a long enough time to get accurate results with the testing methods in the UAF Hylab. At this stage in the experiment, it was not possible to utilize the spectrometer in the UAF Cold Room laboratory due to the transition of engineering buildings at UAF from Duckering to ELIF. The thicker the ice layer that was fabricated, the longer it would take for the surface to melt. However, once the ice layer thickness approached (0.4 mm) they no longer accurately represented a regularly deiced or maintained roadway. This is not expected to affect the overall experiment because the research is primarily concerned with the liquid film above the ice layer, which contains the deicing material. Ideally, having a lab background identical to a specified pavement surface type in Alaska would help with calibration issues. Additionally, generating a complete library of all permeations of asphalt- and concrete-based pavements (e.g., levels of wear and aggregate types) would be unrealistic in the scope of this project. Using the pavement background in the created form was at least a good first step in relating lab results to field conditions.

3.1.3. Field Setting and Field Sample Preparation

In a lab setting most aspects of the experiment could be regulated and kept constant (e.g., light source and intensity, angle of light, sources of lighting or reflectance interference, background continuity, and material concentration). In a field setting many of these factors could change on a day to day or even an hour by hour basis. Because of these changing features, steps were taken in the procedure to minimize the severity and impact of these factors, which ultimately results in limited testing times. In order to satisfy the need for limited atmospheric

interference due to cloud coverage (Figure 3.5), thickness of atmosphere penetrated by sunlight, angle of sunlight, and ambient air temperature, the appropriate time frames for data collection were sometimes limited to as little as a couple hours per week.

(a) (b)

Figure 3.5 Example of ideal testing condition with (a) clear skies and non-ideal conditions with (b) cloudy skies

The reason for prioritizing days with no cloud cover is because cloud coverage is a form of interference that can block, or at least obfuscate, key wavelength reflectance values, possibly reducing or eliminating wavelength pairs that would otherwise show relationships for the sodium chloride and beet juice mixtures being recorded in the field. The limitations taken to maximize consistency of recorded data ultimately impacted locations and times usable for field collection. To achieve the best possible consistency, data gathering was restricted to days with clear skies to avoid unnecessary scattering due to cloud coverage and snowfall and at times when the sun is near its zenith to minimize the angle at which the sunlight penetrates the atmosphere reducing atmospheric interference. The background used for field testing was taken at two different qualities, regularly travelled pavement in a poor and a well-maintained status. Poor maintained conditions were qualified as white hardpack present on the surface while well-maintained conditions showed minimal ice or snow coverage. The clear ice coverage, asphalt pavement, and

hardpack surfaces allowed much thinner volumetric applications to be applied compared to lab testing. Liquid doses as miniscule as 0.5 mL could be applied via perfume spray bottle to ensure complete coverage.

The final location for field testing was a parking lot on UAF campus. As a location the UAF parking lot satisfied the greatest number of criteria for a winter roadway without requiring closure of a road: a location with a background of asphalt pavement (Figure 3.6), driven on repeatedly by vehicles, plowed, clear line of sight to sun, easy access, utilizable without fully obstructing traffic flow.

(a) (b)

Figure 3.6 Testing conditions with (a) hardpack present and (b) hardpack removed to simulate a well-maintained road.

The parking lot had a couple of issues that had to be worked around to get data accurate to traveled winter roadways. The most obvious problem was amount of snow or ice found on the surface, unlike most roads actively treated with deicer, the parking lot was not plowed to asphalt surface. The parking lot could accumulate hardpack as thick as 2 inches in some locations, which is not an accurate representation of roads regularly treated with deicer even in the poorest conditions. The solution to this was to mechanically remove hardpack (Figure 3.6b) and to pour

boiling water to melt down to surface asphalt layer, if excavated location smelled of oil or other foreign material a new location was selected to minimize possible contaminants that could impact initial relationships established.

3.2. Obtaining Data

3.2.1. Lab Data

Setting up the PSR+ spectroradiometer unit begins with removing the PSR+ portable spectrometer, white 99% reflectance panel, fully charged 7.4V Li-ion battery packs, pistol grip fiber optics holder, and 1.5-meter fiber optic cable from compact carrying case or storage. PSR+ unit is then connected to the pistol grip with the fiber optic cable as shown in Figure 3.7.

Figure 3.7 PSR+ Unit

The halogen lamp must then be turned on an allowed to warm up for thirty minutes to allow the bulb temperature and emitted wavelengths to stabilize (Figure 3.8). Letting the bulb reach constant temperature ensures emitted spectrum will remain constant throughout testing.

Figure 3.8 Hylab Halogen Lamp

The spectroradiometer is then connected to a computer and the DARWin software is opened.

The DARWin software is used to monitor and control data collection (Figure 3.9).

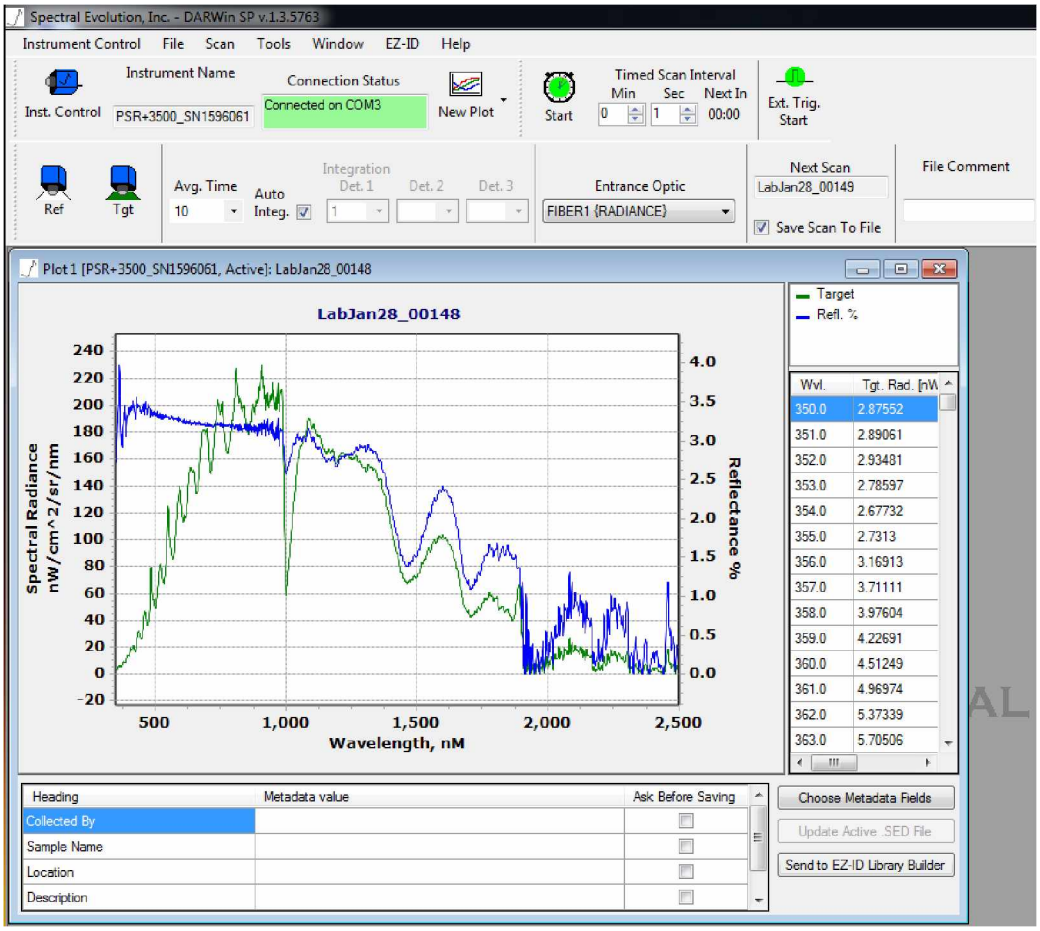

Figure 3.9 DARWin PSR+ Hylab Software

The power of the spectroradiometer must be left to idle for thirty minutes before beginning data collection. The idling procedure ensures that the unit and fiber optics will remain as constant as possible throughout data collection. The unit can now be made to collect reference and target reflectances based on inputs to DARWin. During the lab testing procedure, the pistol grip was mounted to a tripod for stabilization to maximize the repeatability of the testing procedure (Figure 3.10).

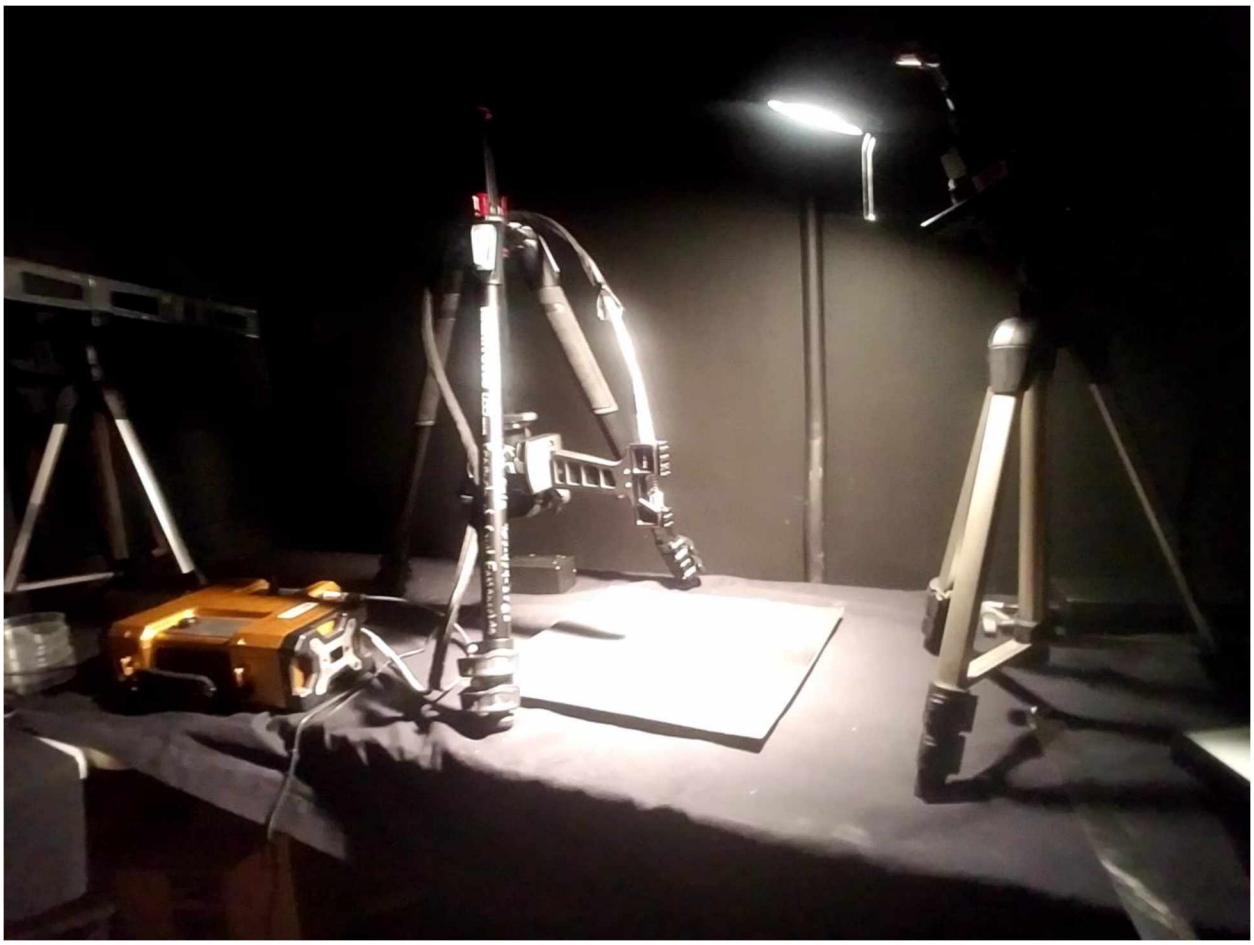

Figure 3.10 Hylab Testing Setup

Before testing a given material with the PSR+ unit, the device must be referenced to a highly reflective white panel (Figure 3.11) which will adjust the recorded spectra in accordance to lighting conditions currently present. The procedure for lab testing was to reference between

every sample material. Ten spectral reflectance curves were obtained for each fabricated lab material used in the relationship analyses presented in CHAPTER 5.

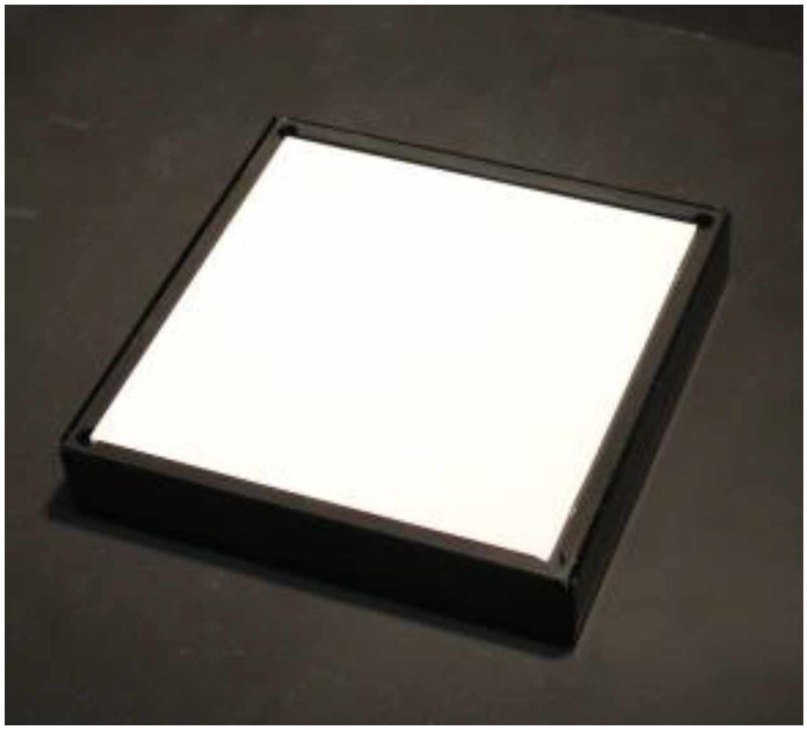

Figure 3.11 Hylab White 99% Reflectance Panel, 5x5 inches

Table 3.2 100 mL Sample Fabrication Checklist

Brine	
Check	Step
	Add solid rock salt to Nalgene container at weight to make predetermined concentration
	For a 100 mL solution add grams of salt equal to desired concentration
	Fill bottle to 100 mL line
	Agitate until no solid salt remains
	For a 100 mL solution add ml of beet to meet desired concentration in sealable plastic container
	Fill bottle to 100 mL line
	Agitate solution
Beet-Brine	
Check	Step
	Add solid rock salt to Nalgene container at weight to make predetermined concentration
	For a 100 mL solution add grams of salt equal to desired concentration
	Fill bottle to 100 mL line
	Agitate until no solid salt remains
	Fill bottle to 100 mL line if volume has decreased
	Add beet juice at a volume such that desired percentage is met
Lab road fabrication	
Check	Step
	Fabricate HMA PG 52-28 in accordance to Alaska standards
	Gyratorally compact specimen, extrude, and cool
	Use coring device to remove core from extruded asphalt pavement
	Use concrete saw to cut core horizontally into lifts of desired thickness
	Begin assembling road by laying stacking empty black pvc end cap, washers as spacers to make asphalt pavement lift slightly below rim at desired height for ice thickness
	Pour desired volume of water on surface and let freeze, ensure short period of time frozen to prevent sublimation of ice content

3.2.2. Field Data

Setting up the hyperspectral unit follows the same steps as data collection in the lab apart from the added steps of securing the hyperspectral unit into a carrying backpack and connecting the included PDA unit to the hyperspectral unit via Bluetooth for remote activation and data storage. Solutions (mixtures of brine and beet-brine deicers) were fabricated in an identical procedure to lab solutions. Details regarding material type, temperature, cloud coverage, time, and artifacts of note are to be recorded by hand by the tester in the field. After data collection was completed all data from the PDA is extracted via USB cable.

3.3. Experimental Design & Data Collection

3.3.1. Lab Data Collection

The black matte board background used by the Hylab has a consistent reflectance of about 4% across all wavelengths. The targeted materials, brine, beet, and beet-brine solutions were placed in petri dishes on top of this constant and non-reflective background. The reflectance of the material was then obtained using the PSR+ unit, which was pointed at the material orthogonal to the orientation of the material surface. Polystyrene, borosilicate, and flint glass dishes were tested to determine which one would have the best efficacy. The polystyrene dish was deemed to be most advantageous because it allowed thinnest film thicknesses to be applied. The polystyrene petri dish had a diameter of 88 mm. The thinnest possible film thickness achieved in the polystyrene dish before the water would stick to itself or the rim of the dish was ~0.8 mm or 5 mL of liquid. Anything below 5 mL would result in incomplete surface coverage therefore the minimum thickness value creatable in the lab under these conditions were 0.8 mm. Several other thicknesses were tested such as 1.6 mm with 10 mL of liquid and 3.6 mm with 22 mL of liquid.

As discussed in Section 3.1.2, a range of solutions were selected that would represent a range of real-world conditions beginning with the initial application concentration of 23.3% down to 0%. This would simulate dilution and migration of chemicals in a real-world environment. Tested concentrations of brine can be seen in Table 3. Water used for dilution was the same as that used by AKDOT&PF northern region. A 40% mixture was created past the total dissolution capacity of salt in water to mimic the application of solid salt and the subsequent melt or liquid application that then begins to dry, however since exact calculation of percentage was not easily

done it was excluded from relationship calculations in later R analysis but still included in the early lab work (Table 3.3).

Table 3.3 Brine Analysis Breakdown

Lab Date	Height		Brine Concentration					
24-Jan 2018	3.6 mm	**(%)**	**0**	**5**	**10**	**15**	**23.3**	**~40**
		(mg/cm^2)	0	18.0	36.0	54.0	83.9	144.0
15-Jun 2018	3.6 mm	**(%)**	**-**	**5**	**10**	**15**	**23.3**	**~40**
		(mg/cm^2)	0	18.0	36.0	54.0	83.9	144.0
27-Jun 2018	1.6 mm	**(%)**	**0**	**5**	**10**	**15**	**23.3**	**~40**
		(mg/cm^2)	0.0	8.0	16.0	24.0	37.3	64.0
9-Jul 2018	1.6 mm	**(%)**	**0**	**5**	**10**	**15**	**23.3**	**~40**
		(mg/cm^2)	0.0	8.0	16.0	24.0	37.3	64.0
6-Sep 2018	0.8 mm	**(%)**	**0**	**5**	**10**	**15**	**23.3**	**~40**
		(mg/cm^2)	0.0	4.0	8.0	12.0	18.6	32.0
17-Sep 2018	0.8 mm	**(%)**	**0**	**5**	**10**	**15**	**23.3**	**~40**
		(mg/cm^2)	0.0	4.0	8.0	12.0	18.6	32.0
28-Jan 2019	0.8 mm	**(%)**	**0**	**5**	**10**	**15**	**23.3**	**~40**
		(mg/cm^2)	0.0	4.0	8.0	12.0	18.6	32.0

Beet-brine mixed deicers are applied as a 23.3% brine mixture mixed with beet juice at an 80:20 ratio by the AKDOT&PF northern region. This is the maximum concentration that could be found on winter roadways, the diluted corresponding values were then iterated down exactly like the brine samples to make a complete curve as shown in in Table 3.4.

Table 3.4 Beet-Brine Analysis Breakdown

Lab Date	Height	Beet-Brine Concentration (%-%)				
16-Feb 2018	3.6 mm	0	4.3-5	8.6-10	12.9-15	20-23.3
31-May 2018	3.6 mm	-	4.3-5	8.6-10	12.9-15	-
9-Jul 2018	1.6 mm	0	4.3-5	8.6-10	12.9-15	20-23.3
21-Sep 2018	0.8 mm	0	4.3-5	8.6-10	12.9-15	20-23.3
28-Jan 2019	0.8 mm	0	4.3-5	8.6-10	12.9-15	20-23.3

Even though AKDOT&PF does not apply beet juice as an anti-icer or deicer on its own, several concentrations of a beet-only solution were analyzed to identify key absorption features

independent of saline concentrations. Spectral signatures of beet-derived solutions do not currently exist and adding new spectral curves is an important contribution to the field of spectral imaging. Fabricated concentrations of the beet solutions are given in Table 3.5.

Table 3.5 Beet Analysis Breakdown

Lab Date	Height	Beet Concentration (%)			
16-Feb 2018	3.6 mm	0	10	20	100
8-Jun 2018	3.6 mm	0	10	20	100
9-Jul 2018	1.6 mm	0	10	20	100
21-Sep 2018	0.8 mm	0	10	20	100
28-Jan 2019	0.8 mm	0	10	20	100

These solutions would then be added to the fabricated ice-covered road samples to mimic field conditions. However, due to limitations discussed in Section 3.1.2 of this report, the road samples proved to be problematic and after some experimentation with brine applications were ultimately discarded from data collection. Each solution was placed in a petri dish and ten shots of wavelength data were obtained using the PSR+, averaged into a single curve, and confidence intervals computed.

3.3.2. Field Data Collection

To ensure that each constituent is being adequately represented, a reference panel is used to calibrate the PSR+ unit and the background. This background reflectance is then used to calibrate the reading based on interference (see Figure 3.12).

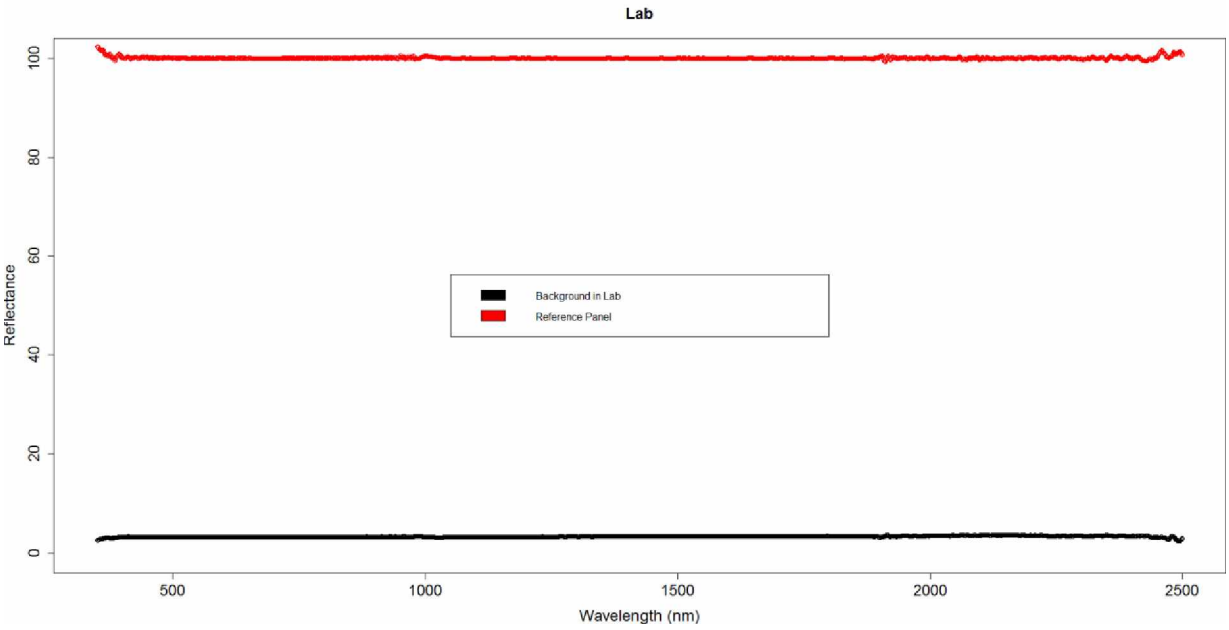

Figure 3.12 Lab Reference Panel and Lab Background

The noise surrounding the reference panel demonstrates the accuracy of the PSR+ spectrometer with near perfect accuracy from the 1000 nm wavelength to the 1900 nm wavelength. Even at the edges of the spectrum recordable by the unit, the PSR+ has a 1% accuracy range except for a few unique points as shown in Figure 3.13 below. The red lines represent standard deviation and shows uncertainty due to either an imperfect machine creating artifacts, ambient changes, or material changes.

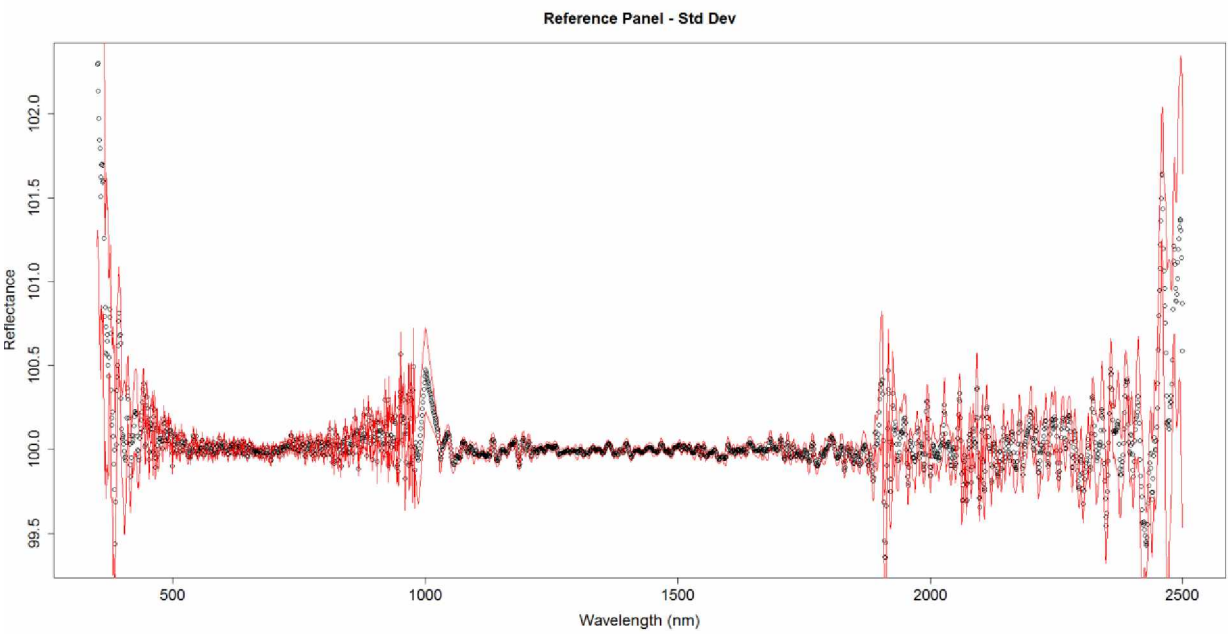

Figure 3.13 Reference Panel Referencing Accuracy

The background material under which the liquid materials are shot in the lab is an extremely muted black matte painted plyboard. The curve itself sits at about 3.2% reflectance as to not interfere with the reflectance given off by the measured targets and produce small standard deviations, typically under 1% (Figure 3.14).

Figure 3.14 Lab Background Reflectance

For delineation of the test area in the field, a metal collar with a 6-inch diameter was utilized to reduce/limit the amount of material spread across the pavement surface. Considering the 30 to 50 gallons per lane mile established by AKDOT&PF in Table 3.1 and assuming 11' lanes, the rates for field applications can be generated. The finalized list of tested application rates and volumes are shown below in Table 3.6.

Table 3.6 Field Volumetrics

Applied (mL)	NaCl (%)	NaCl (mg)	Area (cm^2)	Conc. (mg/cm^2)	Conc. (gal/lane mile)
0.5	5	25	182.41	0.14	8.38
1	5	50	182.41	0.27	16.77
5	5	250	182.41	1.37	83.85
10	5	500	182.41	2.74	167.69
Applied (mL)	NaCl (%)	NaCl (mg)	Area (cm^2)	Conc. (mg/cm^2)	Conc. (gal/lane mile)
0.5	10	50	182.41	0.27	16.77
1	10	100	182.41	0.55	33.54
5	10	500	182.41	2.74	167.69
10	10	1000	182.41	5.48	335.38
Applied (mL)	NaCl (%)	NaCl (mg)	Area (cm^2)	Conc. (mg/cm^2)	Conc. (gal/lane mile)
0.5	15	75	182.41	0.41	25.15
1	15	150	182.41	0.82	50.31
5	15	750	182.41	4.11	251.54
10	15	1500	182.41	8.22	503.08
Applied (mL)	NaCl (%)	NaCl (mg)	Area (cm^2)	Conc. (mg/cm^2)	Conc. (gal/lane mile)
0.5	23.3	116.5	182.41	0.64	39.07
1	23.3	233	182.41	1.28	78.14
5	23.3	1165	182.41	6.39	390.72
10	23.3	2330	182.41	12.77	781.45

Liquid doses at 0.5 mL were applied using a perfume spray bottle to ensure complete coverage. For the remainder of the application rates, testing solutions were applied via 1 mL syringe or 5 mL graduated cylinder and spread mechanically using a rinsed rubber glove to ensure complete surface coverage. A side effect of applications exceeding AKDOT&PF applications was chemical migration off the test site. An attempt to counteract this migration was implementation of a barrier (i.e., a non-hardening rope caulk). This proved to be effective at lower concentration but showed limited success at the highest application volumes tested and at longer times elapsed from initial application. All brine concentrations were repeated with appropriate beet-brine concentrations as if solution was diluted from a 23.3% brine solution that had been mixed 80:20 to beet juice.

3.4. Methods of Data Analysis

The first method attempted in the lab to find new relationships was a simple correlation analysis between increasing brine concentration with the spectral signature of salt, ideally the absorption points unique to NaCl that impact the liquid brine curve would be highlighted and as NaCl concentration increased the correlation to a pure salt signature would also increase. This was ultimately unsuccessful as the absorption points most relevant to salt lay within the NIR and IR range that, the medium, water, absorbed completely or at thinner film thicknesses obfuscated to the point it was undetectable with any form of consistency. Therefore, based on the data collected in this research, correlation between the NaCl reflectance curve and changing concentration of brine is not possible while observing the 350-2500 nm wavelengths utilizing a PSR+ 3500 field unit.

Band math is the main tool for analyzing spectral reflectance. Depending on ratios and changes in a material, band math can quantify the changes in a measured surface. A computation employed to determine soil salinity for crop health named a salinity index calculated as the square root of ETM+ satellite's Band 3 * Band 4 was the closest example of monitoring salinity in a medium that was found before conducting experimentation (Asfaw, Suryabhagavan, & Argaw, 2016). This project enlists a similar method to the salinity index and that of the NDVI (see section 2.6 for more discussion), to test correlation, key absorption points, and curve changes for winter roadway deicing materials.

The average wavelength curves were imported into Excel and RStudio and first visually inspected. If the curves were visually similar when repeatedly imaging the same solution, then the results were deemed to be free of error and external effects and could be further analyzed. If the curves appeared to be translated horizontally, had significant shifts in vertical magnitude, or

some other unexpected change then more scrutiny would be given to results and retesting would follow to check if the results were an aberration due to error or determine what the cause was.

The process by which the spectra were collated and analyzed evolved as the project advanced. Preliminary procedures involved checking for noise, replication, and consistent identification points such as valley and peak wavelength locations. Computational analysis began with the simplest approaches and branched outward with new procedures replacing ineffective ones.

A common spectral analysis approach is to identify the local minima and maxima along a spectral curve, often referred to as "peaks" and "valleys." These peaks and valleys can provide valuable insight on what materials are present or what substances have been added to a material based on shifts and changes in the curve. The reasoning behind this approach is that the local minima and maxima would theoretically be the points most affected by the addition of new materials to an otherwise homogenous materials curve and therefore be the most sensitive points to monitor for sodium chloride concentration changes. This approach generated the first successful relationships in the research with a linear comparison between two reflectance values on a reflectance curve, however most of the relationships only worked if the points were offset by 1 to counteract the proximity to 0 reflectance and normalized to isolate changes due to salt content. For the peak and valley analysis of spectra obtained in this study, the local minima and maxima were first identified by visual inspection. To expedite and automate the process, methods were developed in Excel and RStudio for analysis. These computer-generated methods were refined over several iterations to avoid identifying false peaks and valleys generated by noise in the data.

These peaks and valleys in the reflectance curve can be normalized to highlight changes and the entire curve can be offset to move the lowest reflectance values farther away from 0. The goal of this analysis is to identify a relationship between certain peaks and valleys that will show a trend as salt concentration is increased or decreased. This trend could then ideally be repeated, tested, and extracted if successful, as a reliable identifier or even measurement of salt present.

Concerns were raised with limiting selection of wavelengths to the valleys and peaks of the spectra due to dampened effects of change as demonstrated in Figure 3.15.

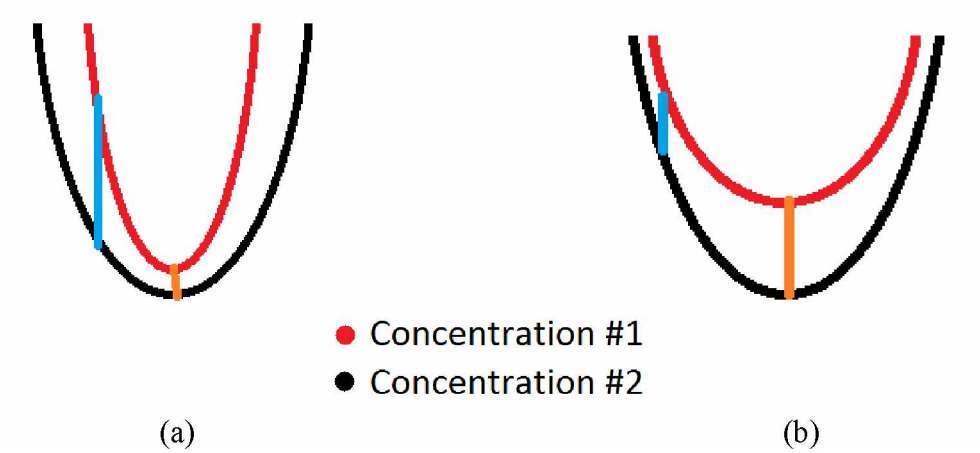

Figure 3.15 Effects of Depression in (a) Spectra 1 and (b) Spectra 2

If these valleys approached zero or were for some other reason resistive to the absorptive capabilities being added by additional materials, the valleys would not be the best sources for measurement of changes in the spectra. In the figure above the red curve has a material added to the surface that changes its shape to that of a black curve in two forms of severity. The point of the curve where the orange line touches represents a point of key significance (e.g., a valley on the curve), however this valley is not located at the point where the greatest change in reflectance occurs. Rather, wavelength associated with the largest change in reflectance is denoted by the blue line, which is some distance away from the key valley location. This point of actual greatest change in reflectance would be the point at which the reflectance curve should be analyzed.

Based on this observation, RStudio was used to divide each wavelength by every other wavelength and then the value was compared to the next iteration of concentration (or film thickness). If the values ascend with each iteration the wavelength pair would be stored by the program. If the wavelength ratio descends throughout all concentrations the wavelength pair will be saved. This program would then collate and organize these wavelengths, x-values, y-values, R squared value, and standard deviations. For each data subset thousands of wavelengths would be paired up.

The last step for the large subsets was to order based on how many times a given wavelength was repeated in a computation. These "most repeated" wavelengths should therefore be the best and most consistent representation of change in the spectra as the concentration is changed because a wavelength will match with more points the better a representation of change it is. These successful relationships can be further culled by comparing to repeated data sets in the lab. The relationships resulting from this research must be repeatable and eliminating relationships that don't repeat will be key in excluding false positives or relationships that only work under specialized or idealized situations.

CHAPTER 4. DATA

4.1. Data Characteristics

This section discusses the characteristics of the spectral curves identified in the lab (Section 4.1.1.) and in the field (Section 4.1.2.). The remainder of the chapter breaks down the comparisons between the salt (Section 4.2), beet (Section 4.3), and beet-brine (Section 4.4) being analyzed.

4.1.1. Lab Data Characteristics

First let us consider the individual components on their own. Figure 4.1 shows the significant differences of each individual element as detected by the PSR+ hyperspectrometer in the HyLab over the wavelengths 350 nm to 2500 nm.

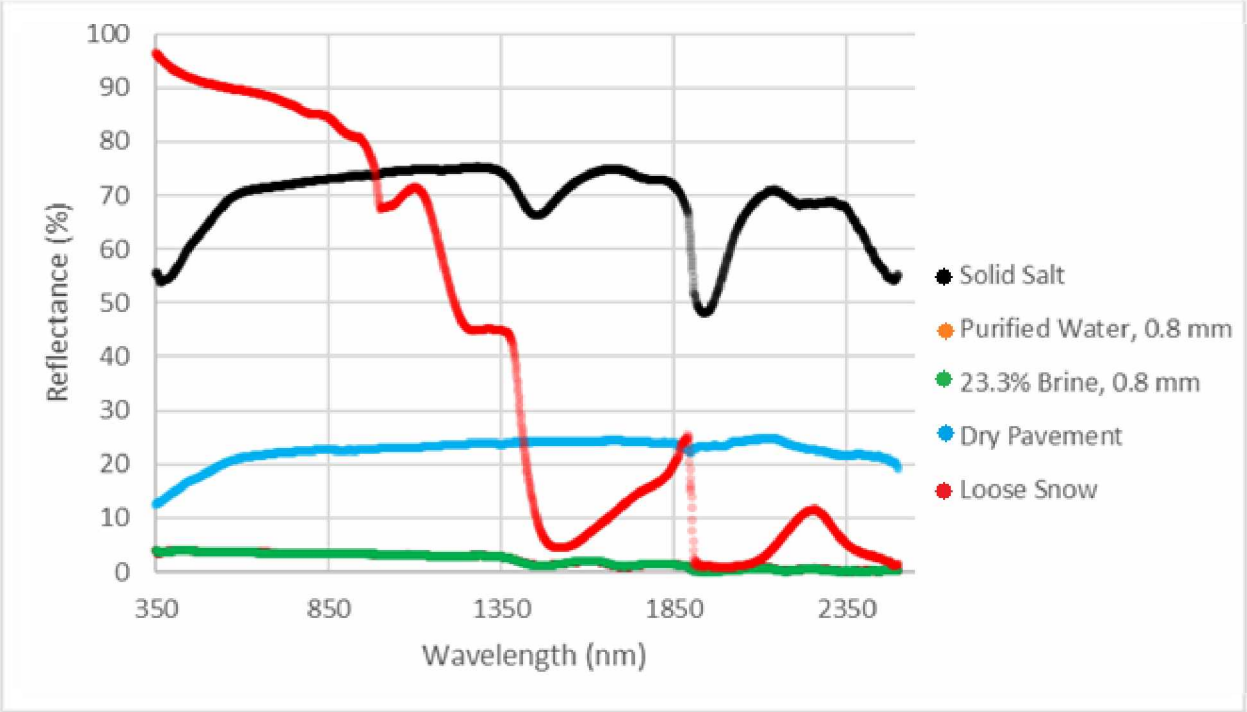

Figure 4.1 Common Winter Roadway Surface Materials

Visual inspection indicates that the differences between select prime constituents of a winter roadway are significant, each having their own unique identifiers (i.e., peaks and valleys at specific wavelengths). Solid salt has a very high reflectance over the entire visible spectrum as compared to asphalt pavement or water. The reflectance properties of water can be so low that, depending on the film thickness, reflectance can reach 0% as shown in the figure below. The low reflectance values indicate more absorption of light.

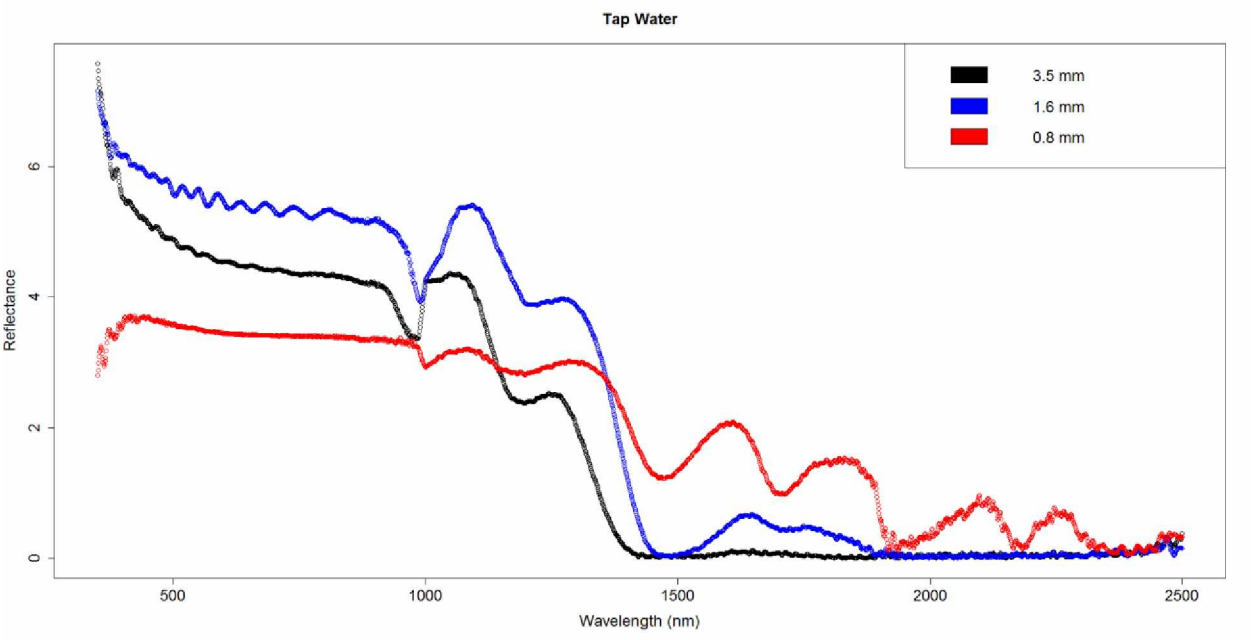

Figure 4.2 Effects on Reflectance Depending on Film Thickness

At a film thickness of 3.5 mm, the reflectance takes on a value of nearly 0% after the 1400 nm wavelength. If a host material or a surface material has a reflectance at or near 0% it can make interpretation of other materials present difficult or impossible. Typically, band math overcomes this issue by identifying the effects of certain key absorption points that signifies a given material. These key signatures points are manifested on a reflectance curve as a valley. However, a problem discovered while analyzing water films in this research is that materials that have near

max absorption (e.g. reflectance near or at 0%, which absorb all light entering) are not capable of representing the absorptive capabilities of added materials accurately. If a material is already highly absorptive of light with reflectance near 0%, adding more absorption will be negligible and not produce a noticeable change as shown back in Figure 3.15. A reflectance that is unable to significantly change value due to a very low initial reflectance is problematic since some of the key signifiers for salt absorption lay within the NIR bounds.

The temperature, shape, and imperfections of a target can also have a great impact on the resulting reflectance spectra. For example, the reflectance curves for water vary greatly depending on the state (liquid, solid, or gas). The impacts of spectra are not limited to only phase changes but may also be influenced by the various physical states that the element may occupy. The grain size of ice and snow, while not necessarily visually significantly different, can produce very different reflectance values depending on crystal size (e.g., fine or coarse snow) to solid ice. The effects are shown below in Figure 4.3 comparing the different types of snow, frost, and ice (ECOSTRESS Spectral Library, 2018).

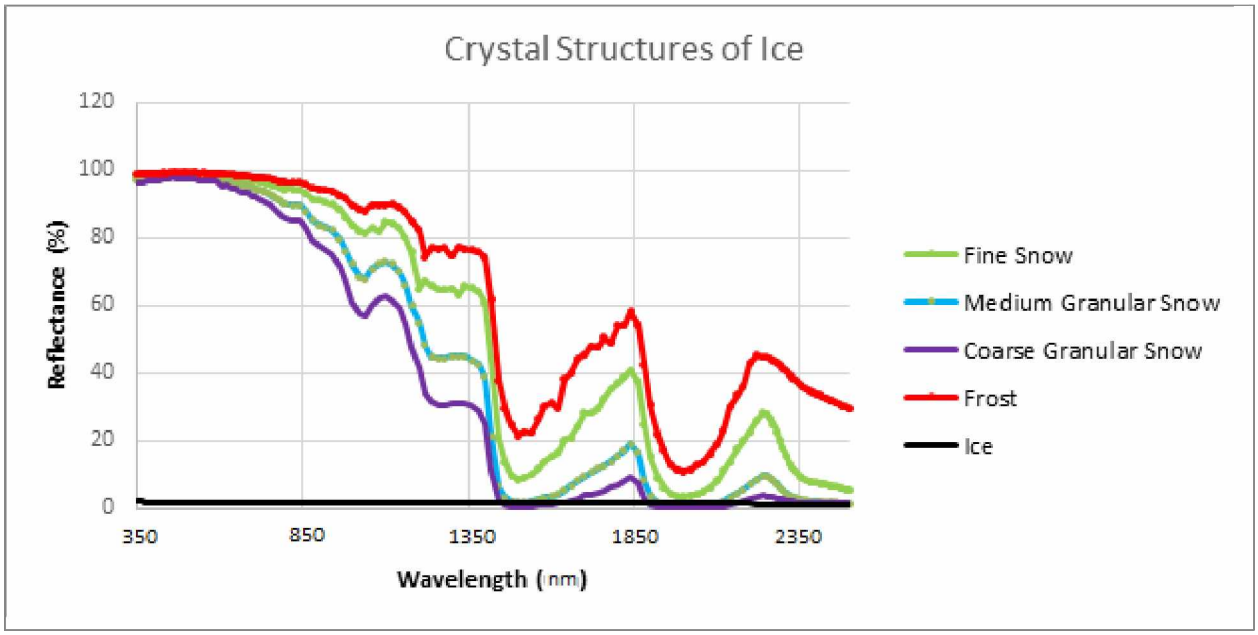

Figure 4.3 Ice Crystal Differences in Reflectance

Since background reflectance can be highly variable due to different coverage percentages (e.g., the ratio of asphalt to ice) and the many differences that variable grain size can cause, this research will focus on the changes caused by the addition and manipulation of deicing and anti-icing materials. It would be unrealistic within the scope and budget of this project to account for all possible permutations of winter roadway coverage but could be addressed with follow-on research.

4.1.2. Field Data Characteristics

Collecting spectral data in the field is more dynamic than that of collecting data in the lab. Spectral imaging is highly dependent on referencing due to atmospheric interference and subtle changes in lighting environment. Slight changes in reflectance percentage may be present in a sampled area due to changes in cloud cover, changes in light angle, changes in equipment, or changes in environment (e.g. extra material or new material that will slightly change way light bounces in an area). However, these slight changes in reflectance value should not alter the

overall shape of the reflectance curve, which, in addition to how reflectance value relate to each other, is what is being analyzed in this research. Comparing a measurement under poor conditions (see Figure 4.4a) to ideal conditions (see Figure 4.4b) confirms that noise is increased as conditions deteriorate, uncertainty and scatter are magnified under cloudy conditions. However, the trend, valleys, peaks, and relative magnitude remain the same, which are the main vectors being used in bandmath analysis.

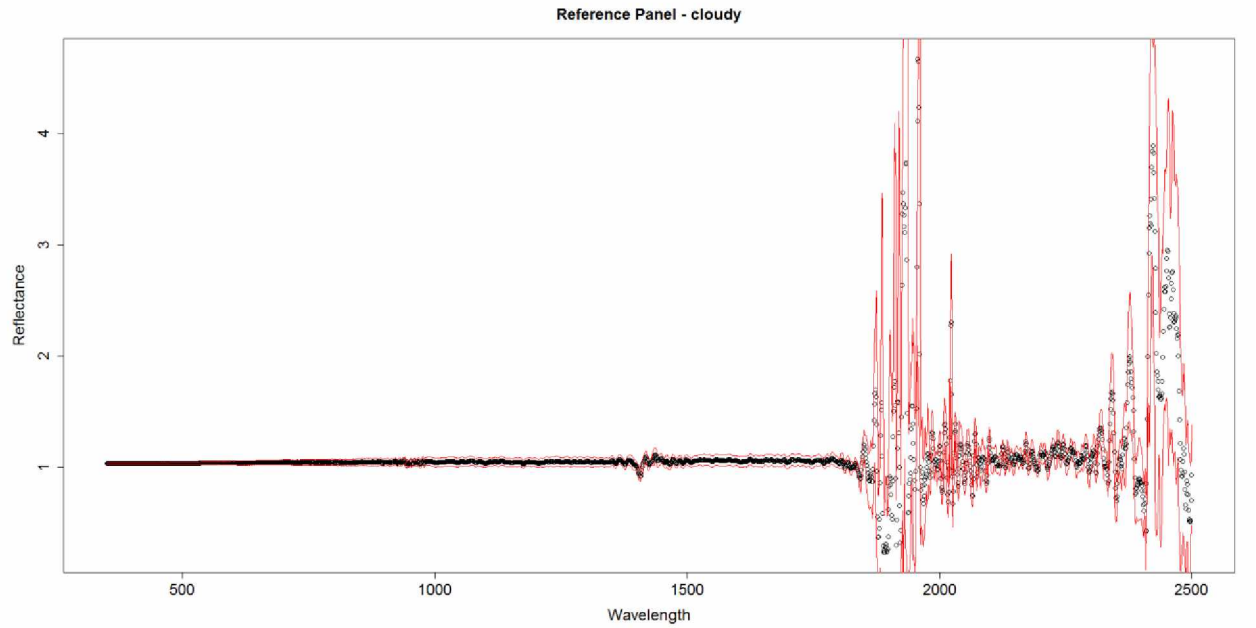

(a)

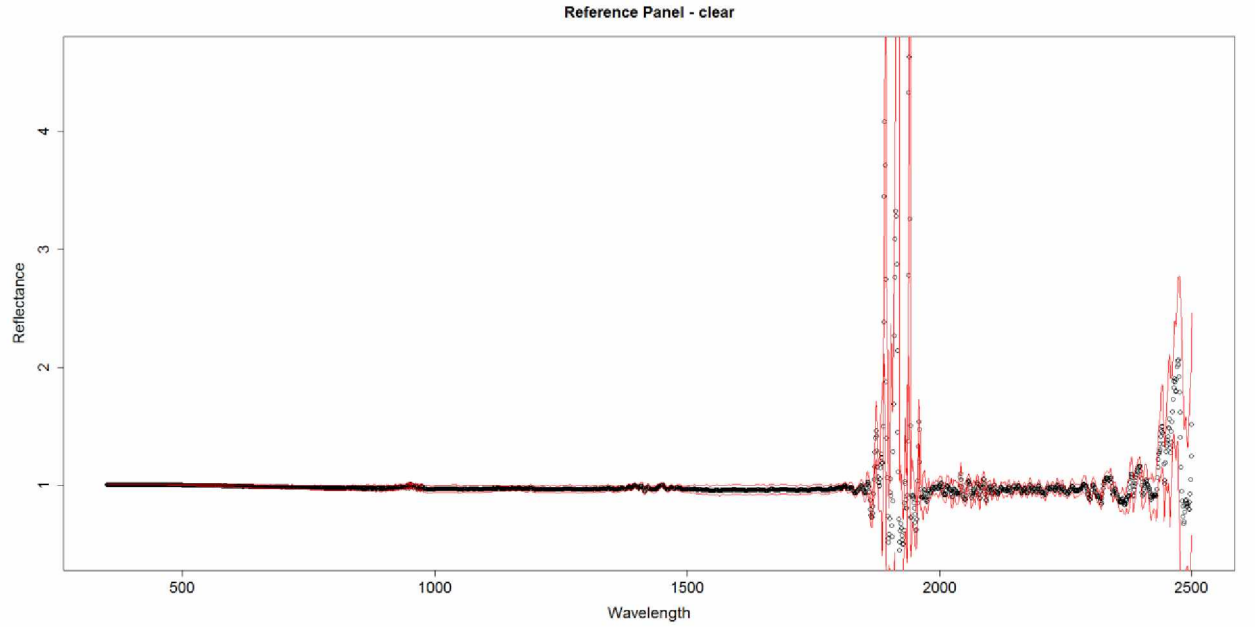

(b)

Figure 4.4 Coverage Effects of (a) Cloudy and (b) Clear Sky

Another change introduced by field conditions is a background that changes based on sample sets, instead of a static matte background, asphalt pavement becomes the dominant background.

These winter roadway backgrounds, while quite uniform to the human eye, are not equivalent to spectral imaging and band math analysis. One sample site utilized for testing is shown below in Figure 4.5 with test sites labeled with numbers corresponding to the order of shot acquisition.

Figure 4.5 Example Testing Site

These backgrounds once analyzed with the hyperspectrometer and compared at values of interest using bandmath relationships established in the lab portion reveals just how different these backgrounds can be utilizing boxplots as shown in Figure 4.6.

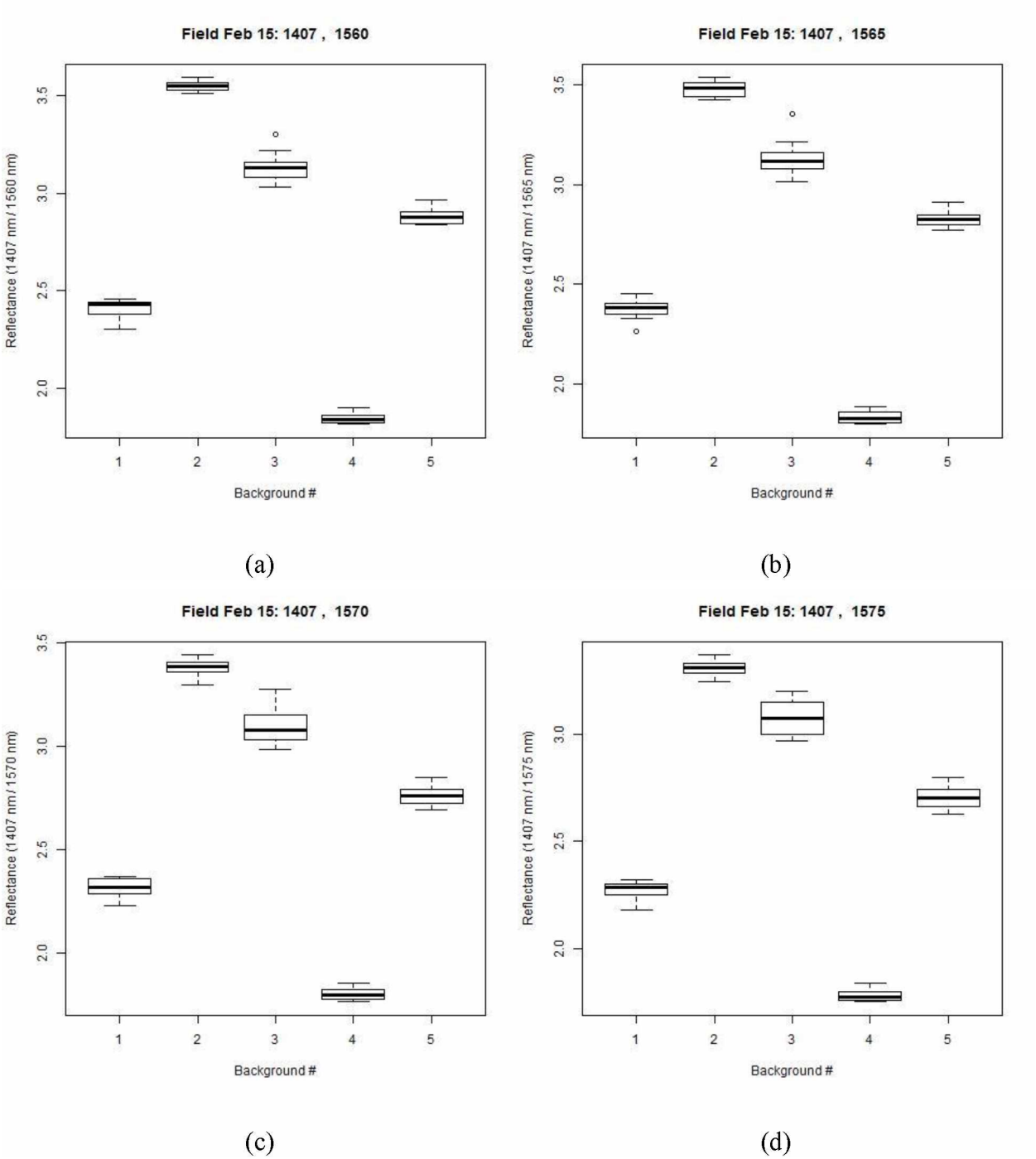

Figure 4.6 Good Condition Asphalt Pavement Background with varied Wavelength Pairs to 1407 nm (a) 1560 nm through (d) 1575 nm

The differences between backgrounds taken inches apart shows the significant effects that changes in road background can make with points being nearly double the value just due to slight changes in ice surface coverage and moving 1 foot horizontally on asphalt pavement. Ideally, a small cluster of shots on well-maintained asphalt pavement would have near equal reflectance value when analyzed. Analysis of variance for a background analysis would ideally indicate no statistically significant difference but testing shown in Figure 4.7 indicates a large difference.

Analysis of Variance

Values	Df	Sum Sq.	Mean Sq.	F value	Pr(>F)
ind	4	12.8843	3.2211	936.08	<2.2e-16 ***
Residuals	45	0.1548	0.0034	-	-

Pairwise Comparisons Using t-Tests with Non-Pooled Standard Deviation

Background #	1	2	3	4
2	<2e-16	-	-	-
3	3.70E-12	7.00E-04	-	-
4	9.40E-14	<2e-16	3.80E-13	-
5	2.30E-13	5.30E-15	7.80E-08	<2e-16

Figure 4.7 ANOVA and Pairwise t-test (1407 nm, 1575 nm)

The ANOVA test shows that there is quite a bit of difference between the testing sites even though the sites had extremely proximity and similar surface features. Pairwise testing confirmed that all points were significantly statistically different from one another and suggests that different concentrations of deicing compounds are identifiable using further analysis.

4.2. Data Comparisons (Salt)

4.2.1. Lab Data Comparisons (Salt)

Analysis for salt began with obtaining ten measurements, which were compared to each other to ensure accuracy and to check for noise and wavelengths that may have uncertainty in analysis (Figure 4.8) before being averaged together for computational analysis (Figure 4.9).

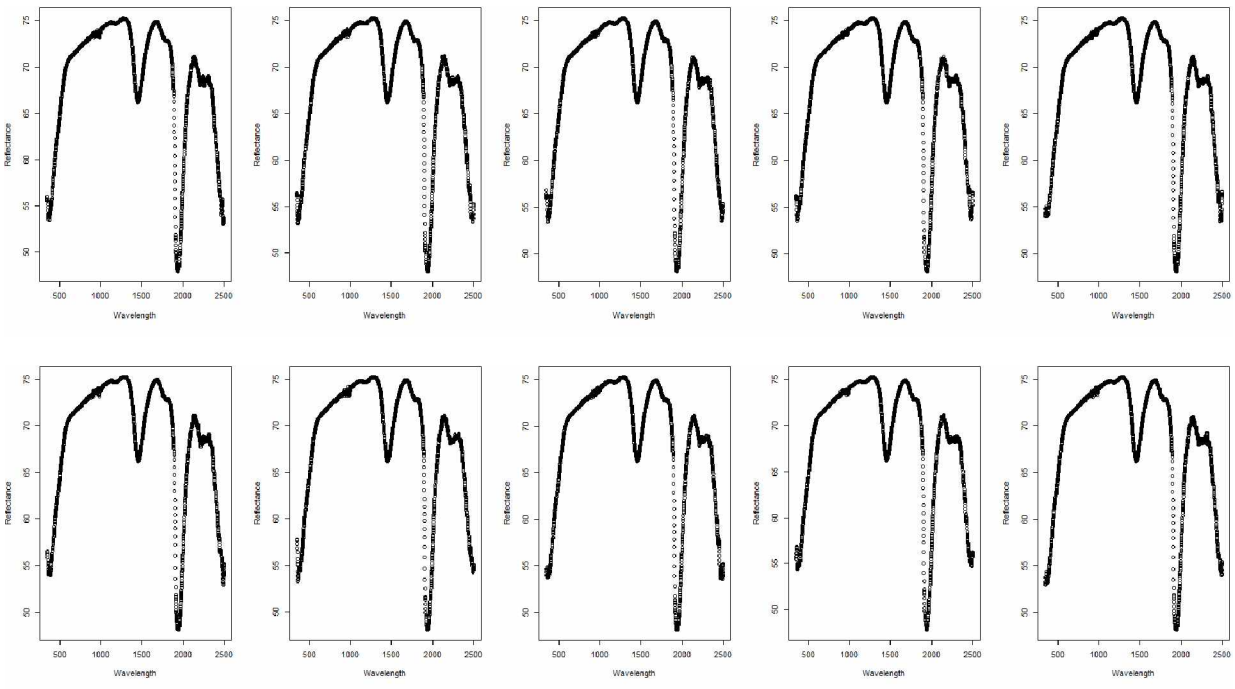

Figure 4.8 Salt Crystals 10 Measurements in Lab Setting (Reflectance % vs. Wavelength nm)

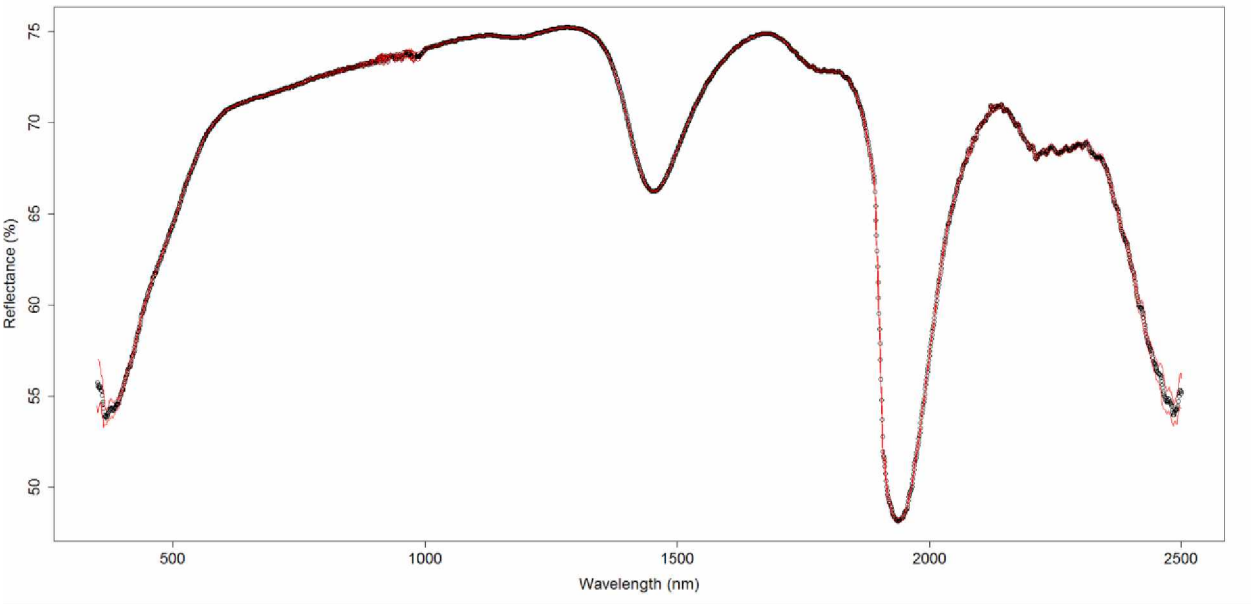

Figure 4.9 Solid Salt Crystals Average of Above 10

These lab-derived measurements of sodium chloride (Figure 4.9) were confirmed with existing spectra from a scientific library hosted by ECOSTRESS and shown in Figure 4.10. No library currently exists for exact concentrations of brine and beet mixtures, which means that validation with previous studies for these curves would not be possible. Spectra identification for these solutions will be a valuable contribution for anyone pursuing reflectance related work with these materials at different concentrations and thicknesses.

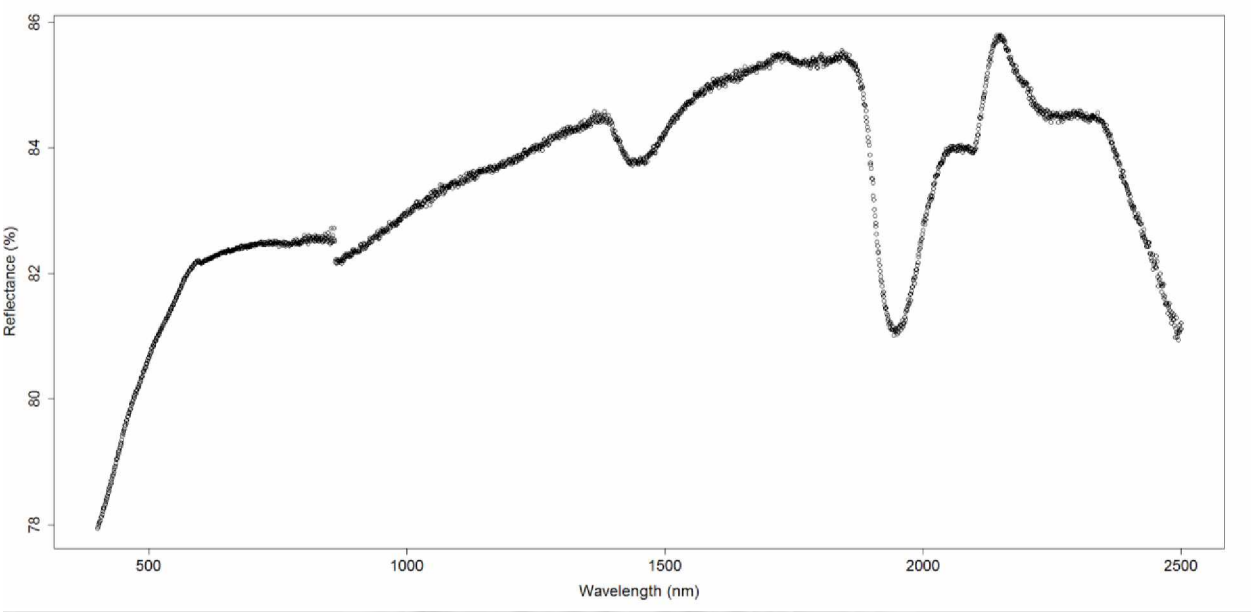

Figure 4.10 Lab Salt Reflectance

Visual inspection of the curves indicates slight differences around the 1450 nm with the USGS spectral library reporting a much less severe valley and a plateau from 600 nm to 850 nm. These differences are possibly explained by different lighting settings, crystal sizes, surface imperfections, and possibly backgrounds used in this analysis as compared to those obtained and cataloged in other studies previously. However, both spectra have significant key absorption points (e.g., points where significant absorption causes a dip or valley on the curve). Both the UAF-generated and established online spectra have the same valley locations at about the 1950 and 1450 nm wavelength, these are key identifiers for salt as these are the locations of large reflectance changes, confirming the accuracy of the UAF Hylab PSR+ hyperspectrometer.

The solid salt from AKDOT&PF northern region was then dissolved in water to create deicing and anti-icing solutions at three different thicknesses, 3.6 mm, 1.6 mm, and 0.8 mm. The 3.6 mm height was selected as an upper bound to test the ability to detect salt as a thicker water layer would have a higher $\frac{mg}{cm^2}$ concentration of salt present. Although a 3.6 mm film thickness does not mimic real world applications of deicing and anti-icing material, it represents an upper

bound that may be experienced under conditions of melt and accumulation without proper runoff or a solid salt application on a particularly icy or snowy road. Similarly, a 1.6 mm thickness application was done and the thinnest application achievable in the lab was 0.8 mm thick, which is still thicker liquid layer than should be found on a well-maintained road. These different thicknesses could then be used to investigate how much water film thickness would affect the efficacy of hyperspectral readings or derived computations. Each individual concentration and liquid height had 10 different reflectance curves recorded. In other words, each day would be about 60 recordings for this phase of the research. Each curve was then be collated and compared to each other as demonstrated in Figure 4.11 below.

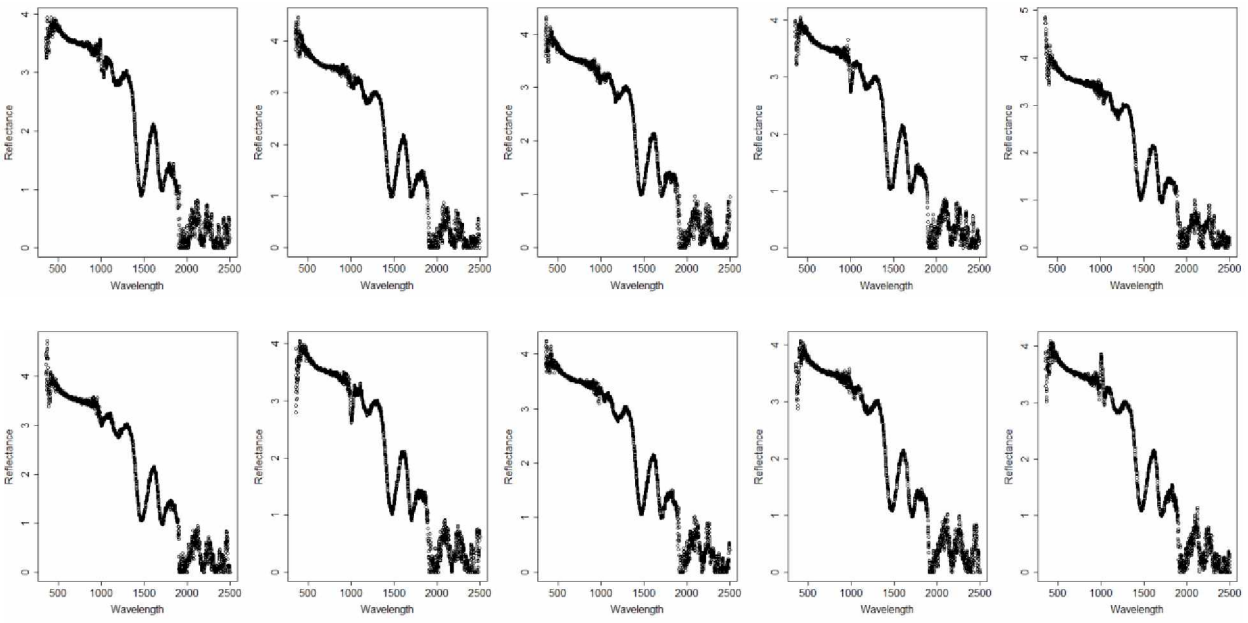

Figure 4.11 Individual 23.3% Brine Reflectances @ 0.8 mm, 5mL, sep 17

The first step, like all spectra gathered in this research, is to take ten measurements, check for reasonable standard deviation values, and average for computational analysis and comparison.

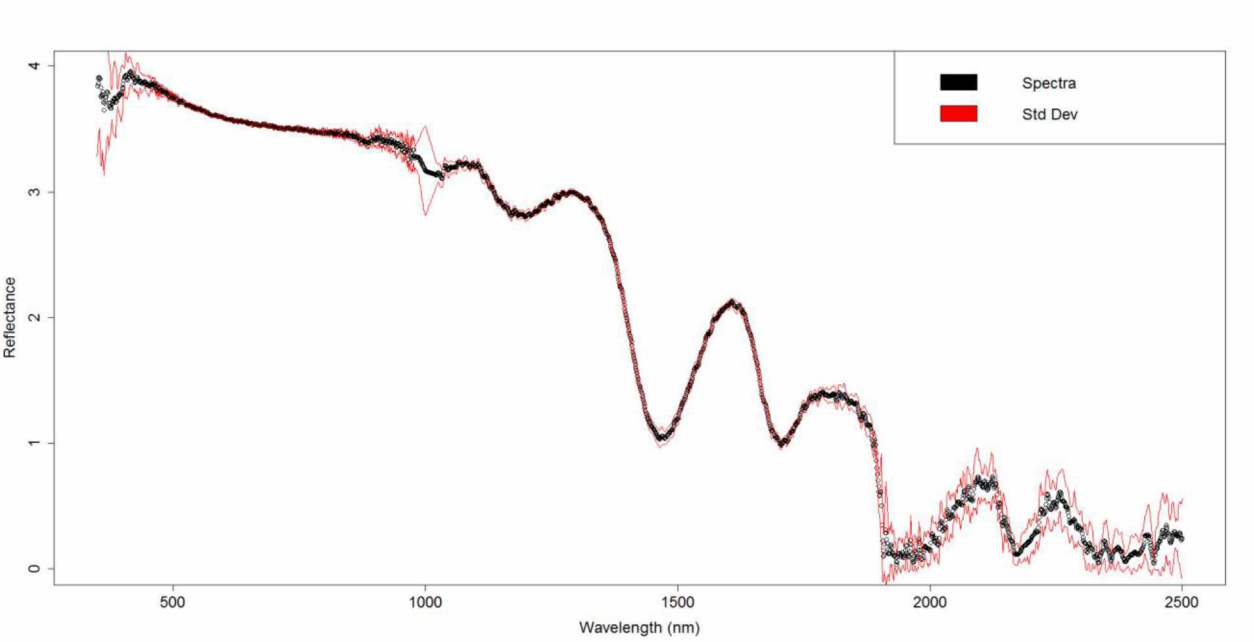

Figure 4.12 Averaged 23.3% Brine @ 0.8 mm, 5mL, sep 17

The averaged spectral curves are used for comparative and analytic purposes (i.e., to compare a brine of 5% concentration to a brine of 10% concentration). The red lines in Figure 4.12 denote the standard deviation and highlight locations where the derived relationships may need more scrutiny or warrant additional data collection. In genreal, the deviations from the mean are relatively small, basically zero, with the exception of wavelengths under 475 nm and a small area in the vicinity of the 1000 nm wavelength. This 1000 nm wavelength uncertainty corresponds exactly with a group of uncertainty inherent to the reference panel (refer back to Figure 3.13) and in the background material as shown in Figure 3.14. This uncertainty may be due to inefficiences of Hylab and lab equipment (i.e. imperfection of reference panel, wear and tear on equipment, or outdated calibration) . Comparing different concentrations and volumes can begin after subsequent spectra are generated below.

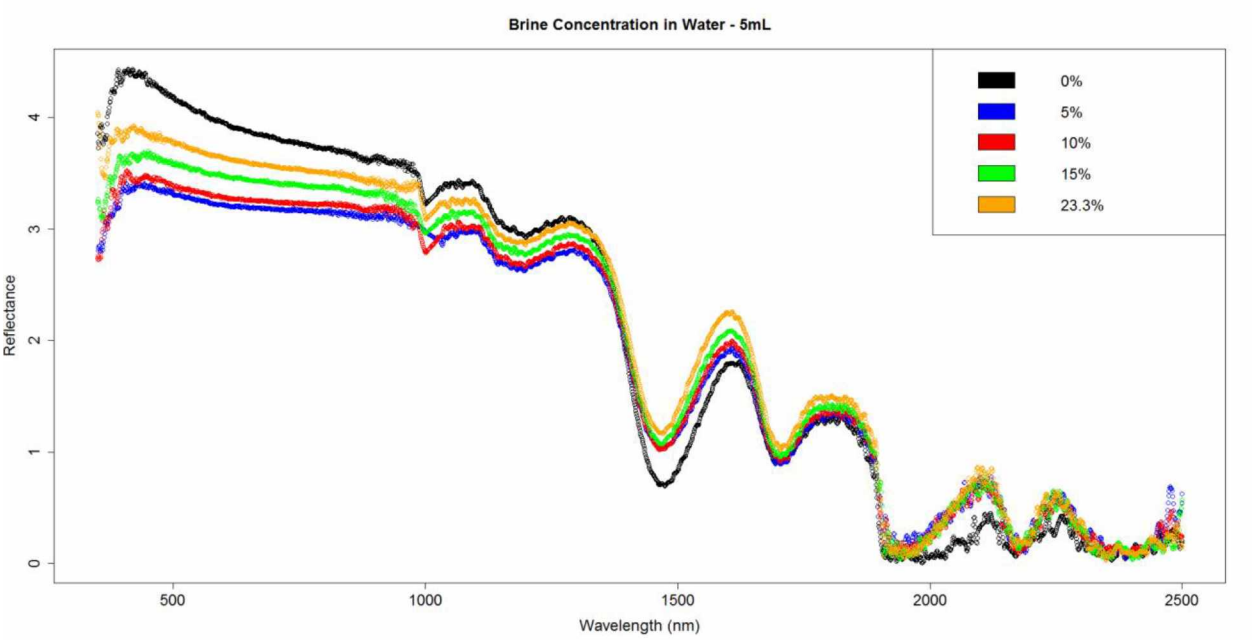

Figure 4.13 Brine Concentrations – 5 mL

Visual comparison between the changes in the reflectance spectra as concentration changes is difficult. The changes appear minor in terms of reflectance with some added noise beyond the 1800 nm wavelength. Mathematical comparisons are then necessary to identify these differences and to obtain relationships to quantify how those change from one concentration or film thickness to the next (see Figure 4.14).

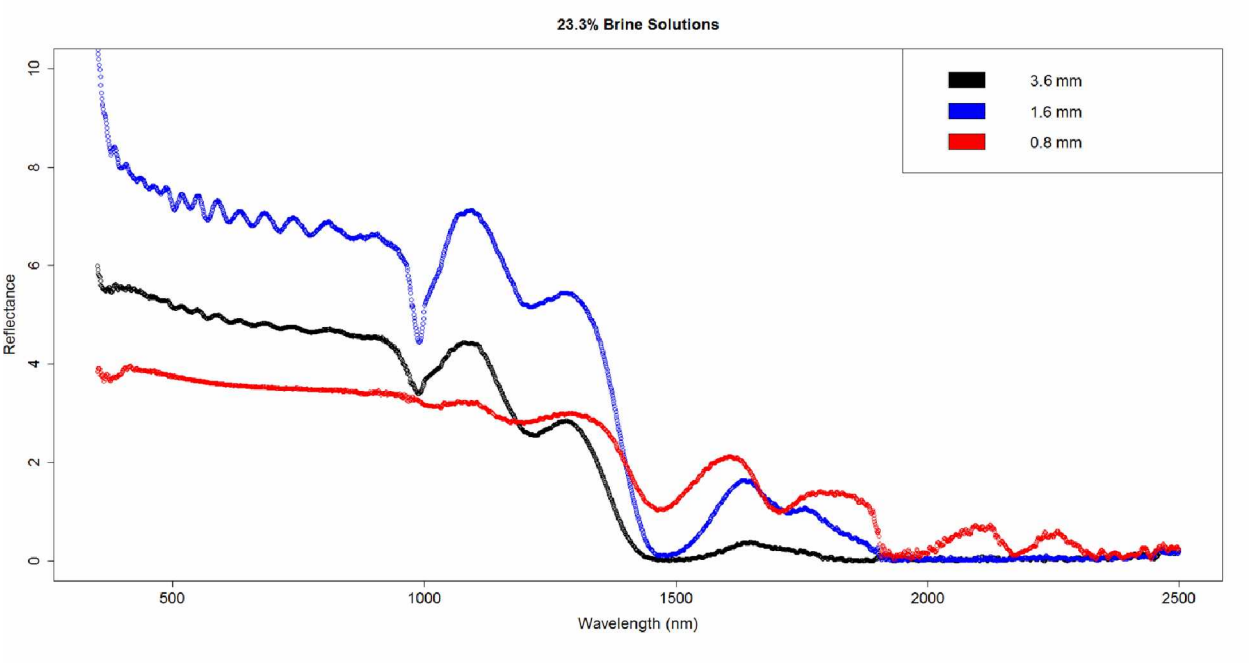

Figure 4.14 Brine Film Thickness Differences

Visually, the differences between film thicknesses are significant (Figure 4.14). At less than 1 mm thicknesses, much more of the near infrared spectra is present and usable with the added benefit of a much smoother curve in the visual spectrum. Peaks, valleys, and natural curvature in the sub-1500 nm wavelength are more pronounced with a thicker film. However, the opposite is true at wavelengths exceeding 1500 wavelength nm. Validation by replication of the 0.8 mm brine films indicated perfectly matching trends and curve features, yet slight deviation in magnitude can be seen (Figure 4.15).

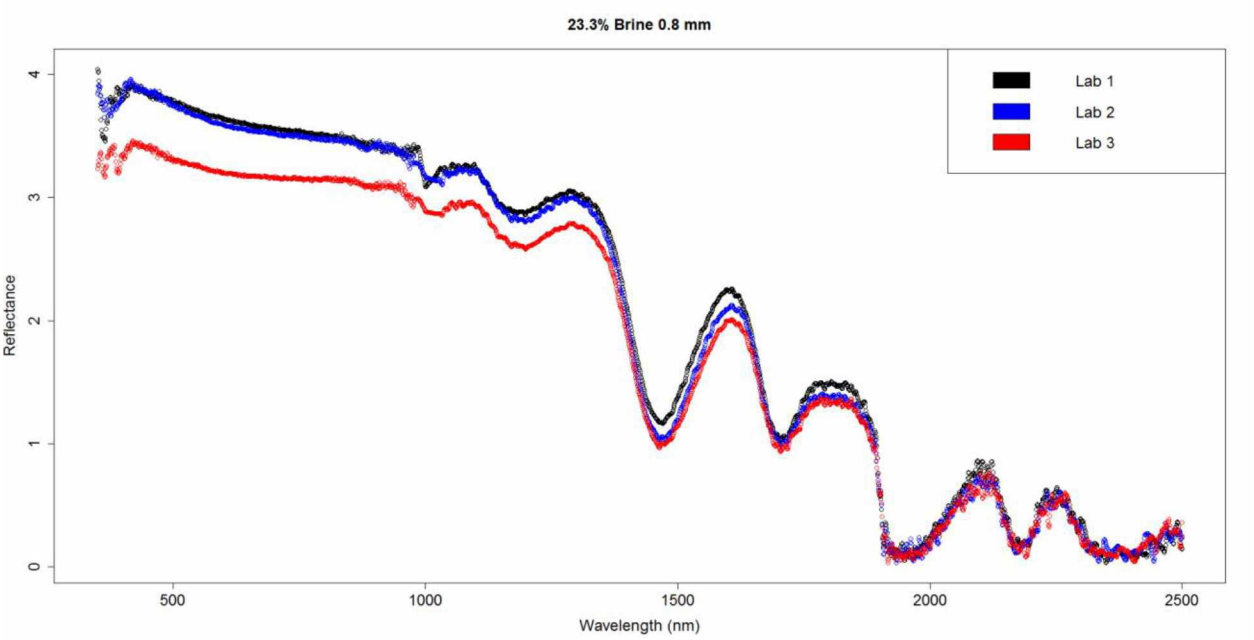

Figure 4.15 Repeatability 0.8 mm 23.3% Brine

Slight shifts in reflectance values are expected due to the nature of the device and the tendency for there to be small changes in the surrounding environment (reflective surfaces such as metals, ice, or snow). However, the magnitude of these variations is relatively small, and the shape of the spectra is expected to remain nearly the same. Normalizing reflectance to a point such as the 700 nm wavelength reveals the graphs are even more accurate in repetition than shown in Figure 4.15 as shown in Figure 4.16.

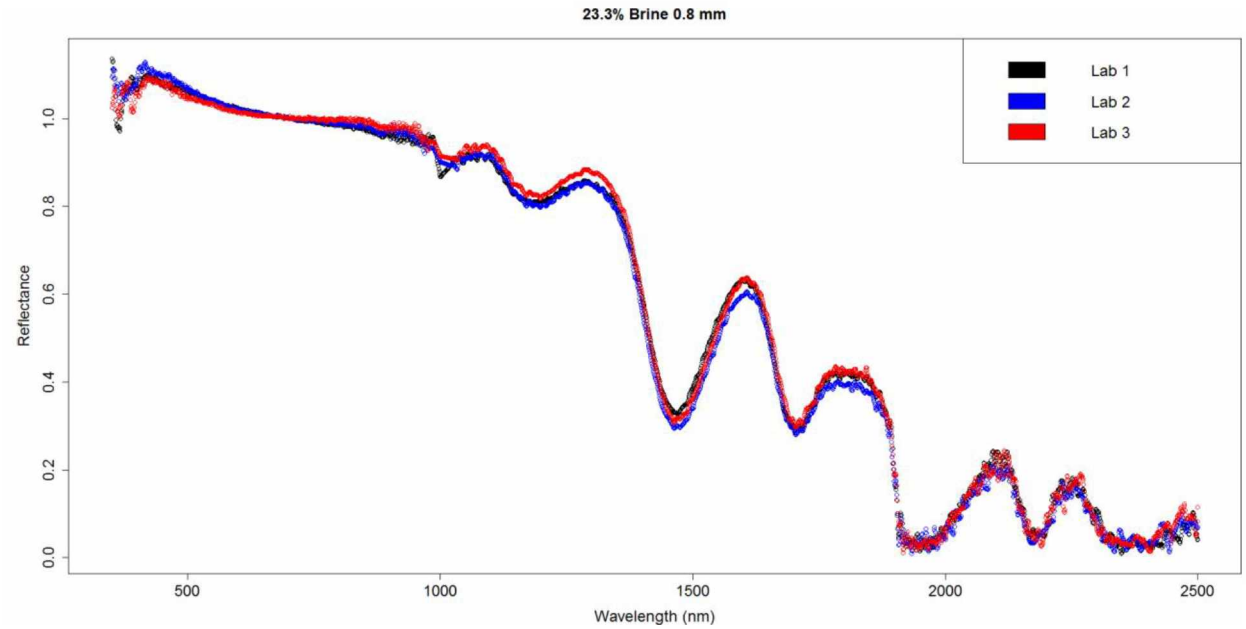

Figure 4.16 Repeatabiling 0.8 mm 23.3% Brine Normalized to 700 nm

4.2.2. Field Data Comparisons (Salt)

The first step of analyzing the field data was recording the backgrounds before the deicing material is applied. The respective reflectance curves of well-maintained asphalt pavement with light icing is shown below in Figure 4.17.

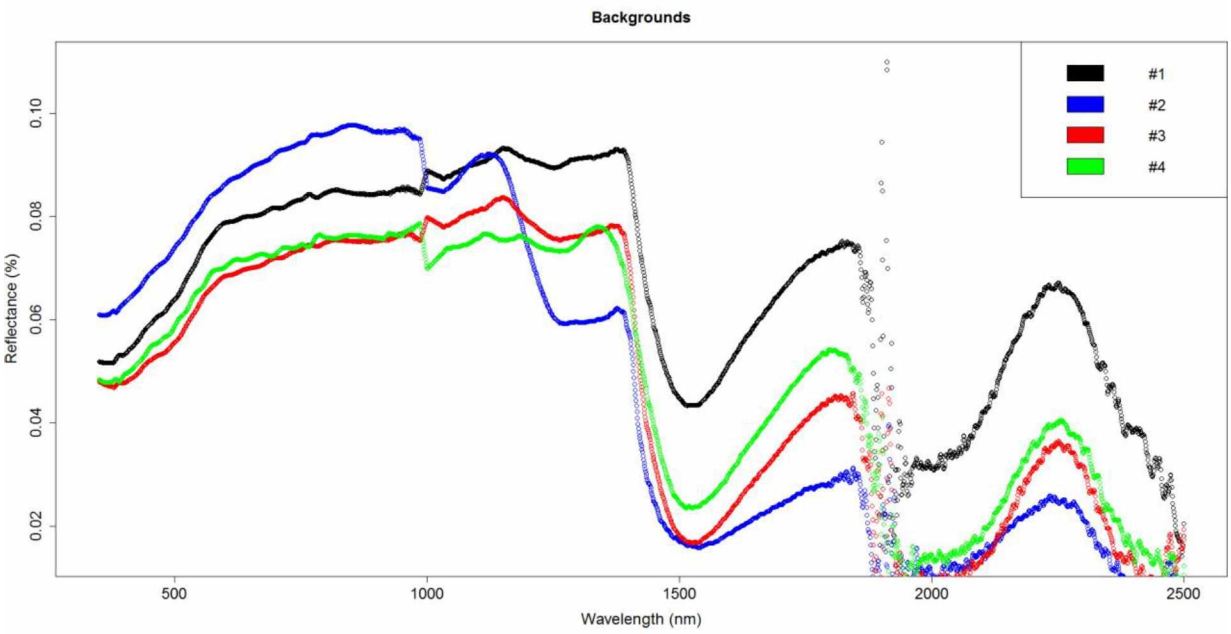

Figure 4.17 Field Background Reflectance Curves

The background curves have significant differences in reflectance magnitudes at certain portions of the curve. The shapes of the background curves are similar; however, there are severe deviances around the 1000 nm wavelength and the 1250 nm wavelength. The differences established in the background material are echoed after deicing compounds are applied as shown in Figure 4.18.

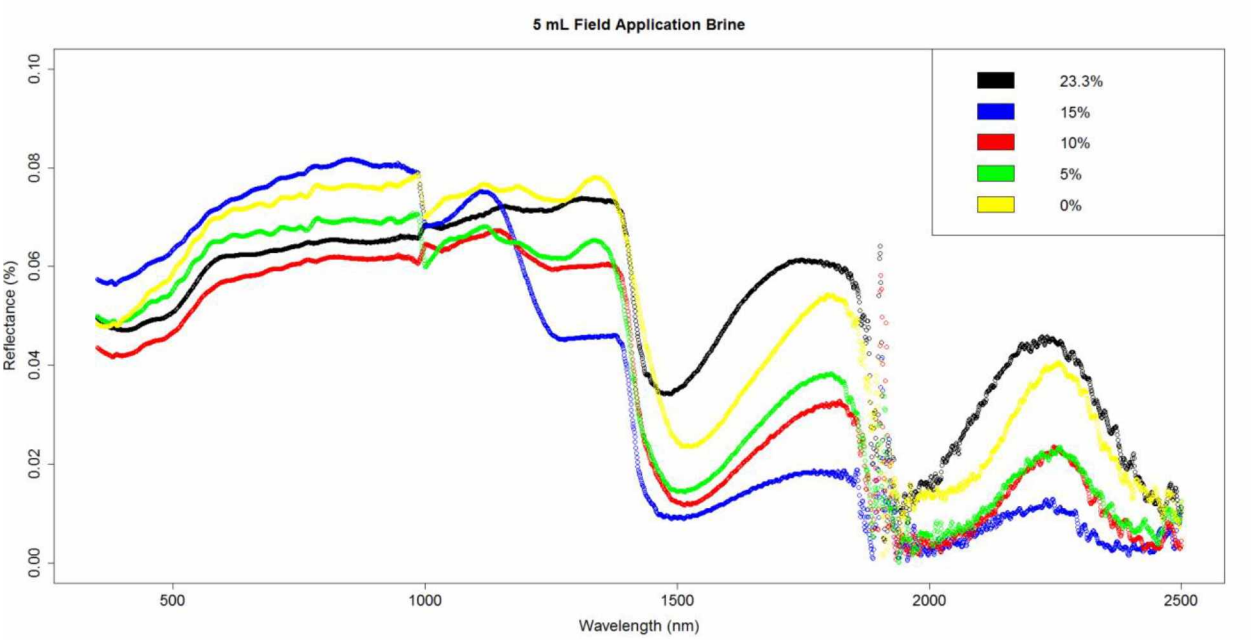

Figure 4.18 Field Changing Salt Concentration

The difference in magnitude makes linear comparison between the curves unhelpful. To rectify the different backgrounds and the backgrounds effect on generated reflectance curves, each compound shot was divided by its respective background before deicing solutions were applied as shown in Figure 4.19.

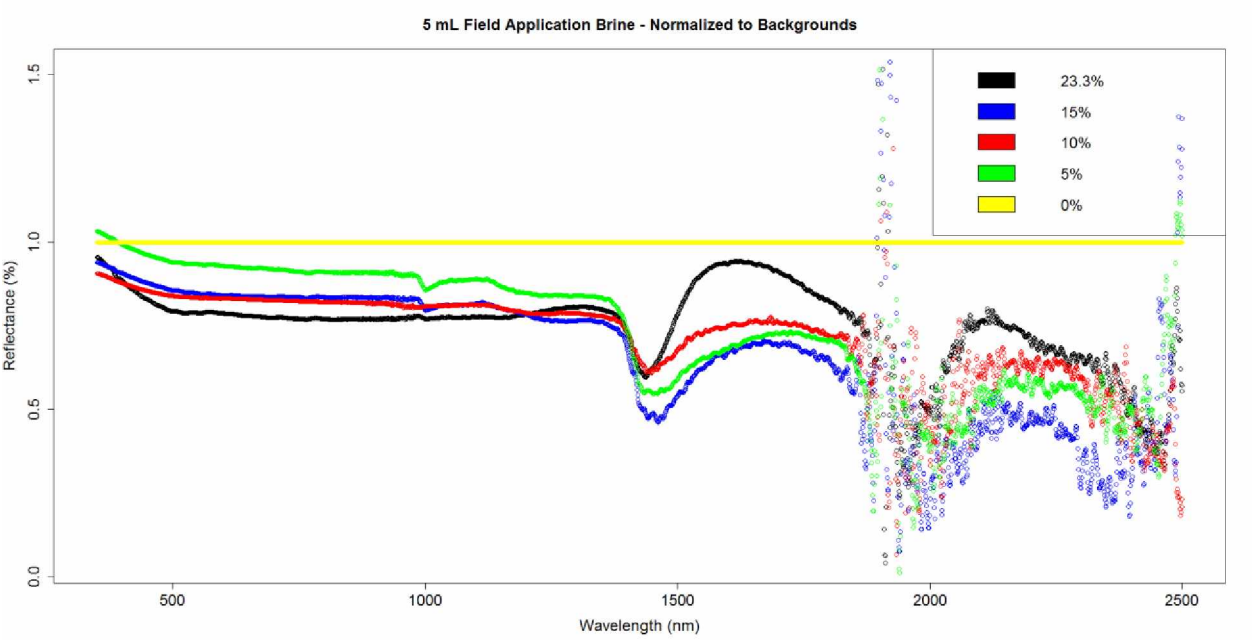

Figure 4.19 Field Changing Salt Concentration - Normalized to Background

Normalizing by the respective backgrounds highlight the degradation due to scatter and uncertainty, exceeding the 1800 nm wavelength the curves become incredibly scattered. Even with normalization, no obvious relationships between concentration and reflectance values can be observed. Since the procedure for each application site was to apply deicing material of a specified concentration at numerous volumetric applications, the final approach to eliminate the variance due to significant changes in background reflectance was to compare the curves of constant concentration as volumetric application rate on surface of test site changed.

Once changing background is completely controlled for, a trend among the curves emerges. The trend for changes is most visually significant ranging from 1450 to 1800 nm wavelength (Figure 4.20) where one can see significant changes in magnitude as volume changes.

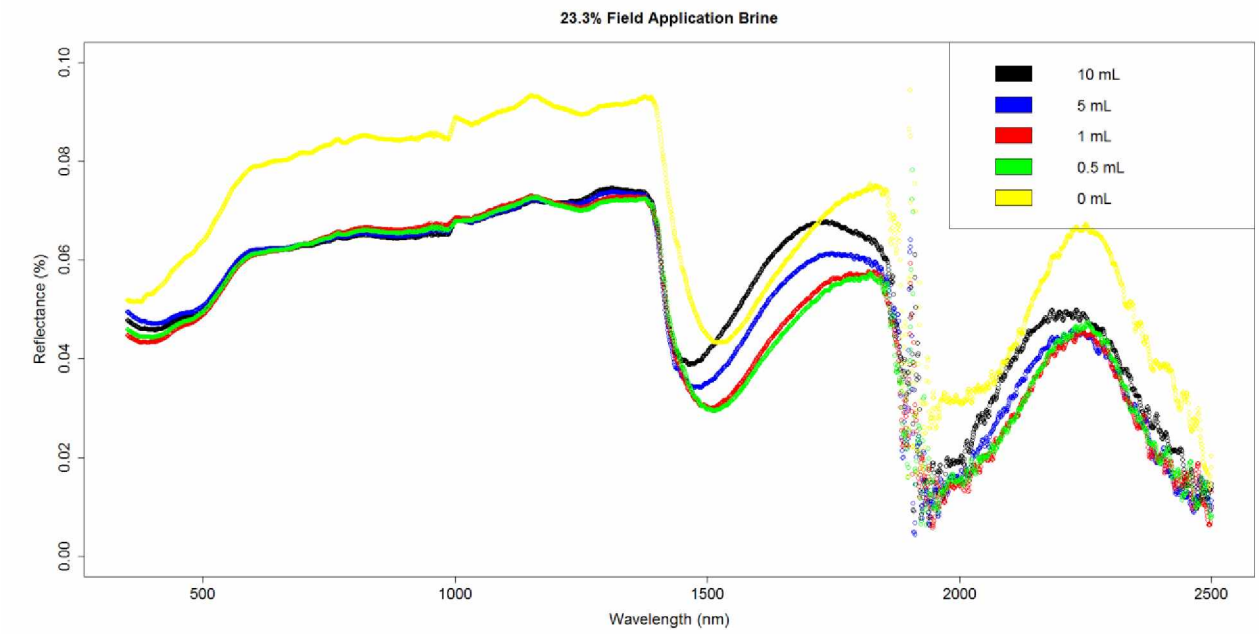

Figure 4.20 Brine - Changing Volume, Constant Concentration

4.3.Data Comparisons (Beet)

Beet extract is a visually striking liquid compared to the clear brine as shown below, which may suggest the visual spectrum will be the key absorption points.

(a) (b)

Figure 4.21 (a) Beet Mixtures After Analysis (b) Individual Petri Dish Filled

Analysis for beet juice solutions (Figure 4.21) mimicked the process for brine solutions. Ten sample of the spectra were obtained and then compared to each other to ensure accuracy, identify areas of noise, and wavelength uncertainty (Figure 4.22).

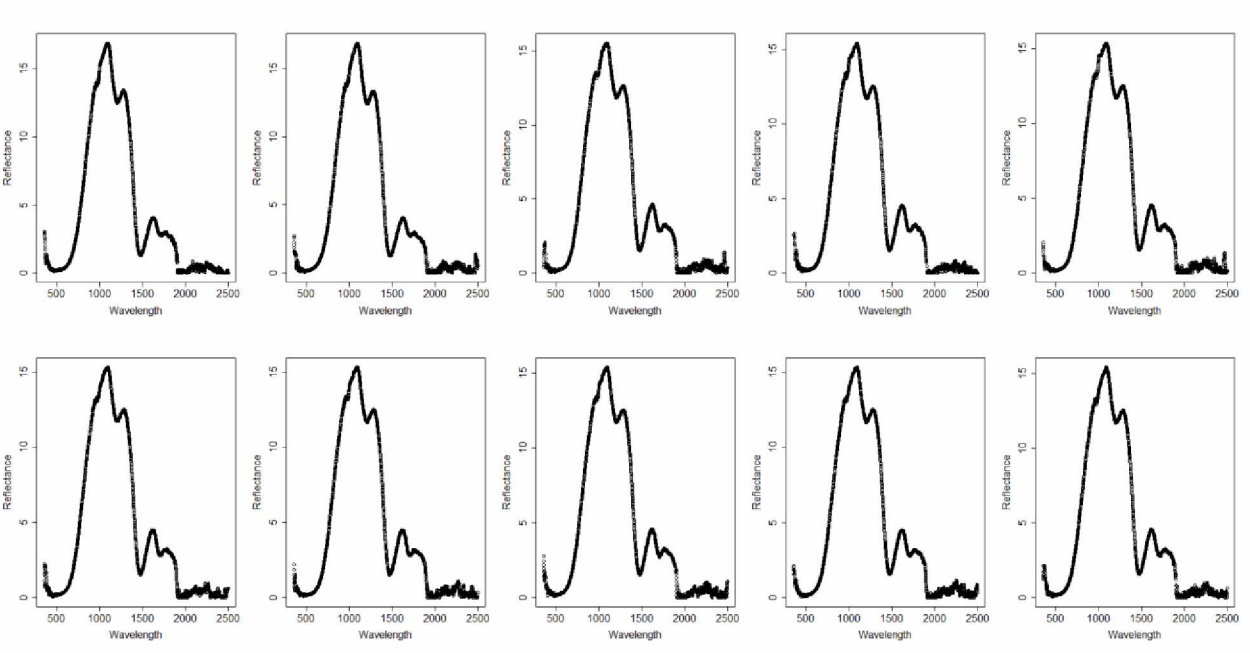

Figure 4.22 100% Beet Juice Initial Measurements @ 0.8 mm, 5mL, sep 21

The lab measurements of the beet extract utilized by the AKDOT&PF Northern Region for deicing and anti-icing purposes could not be validated by a comparison with any existing online-hosted libraries. After confirming the reliability of the PSR+3500 unit with the brine analysis, it is a safe assumption that the spectral curves obtained for the beet solutions will be an accurate representation. The average of the 10 measured spectra and the associated standard deviation is shown below in Figure 4.23.

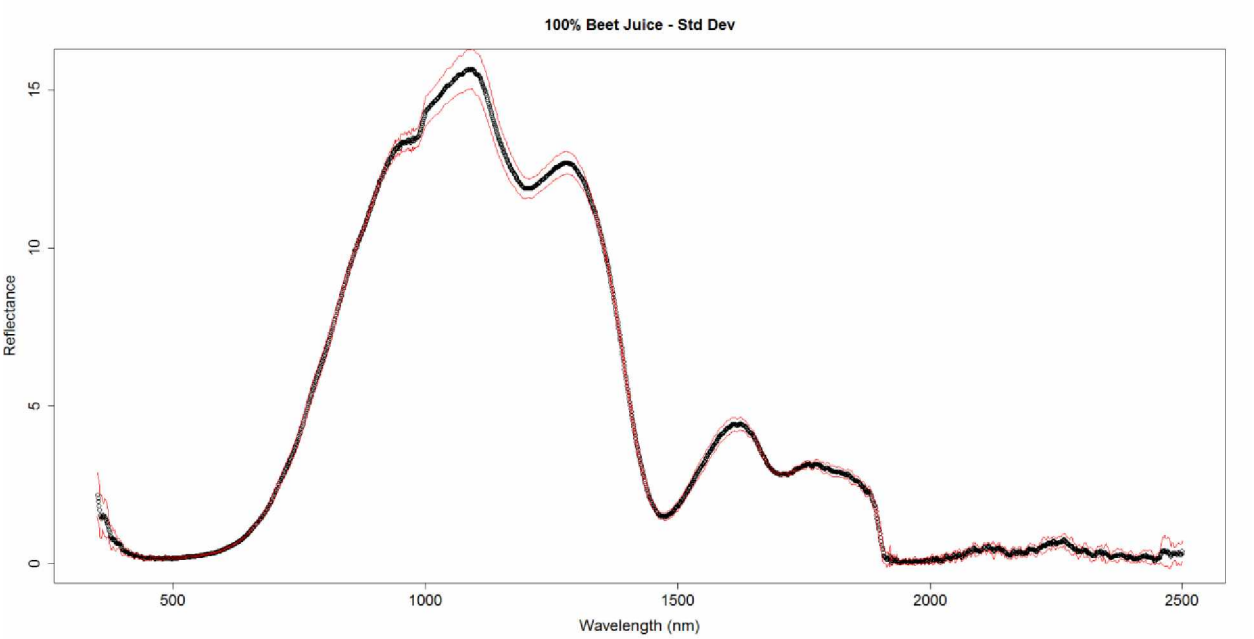

Figure 4.23 Averaged 100% Beet Juice Initial Measurements @ 0.8 mm, 5mL, sep 21

The maximum concentration of beet extract applied by AKDOT&PF is 20% and it is only used in conjunction with a 23.3% brine mixture. A dilution point of 10% beet was also selected for comparison to the full 20% beet and the pure 100% beet spectra.

An increase in beet juice concentration causes significant changes in the reflectance spectra as shown below in Figure 4.24. Adding beet juice has significant impacts on the visual spectrum and the NIR spectrum. The visual spectrum gets absorbed, with higher concentrations of beet juice obliterating the reflectance values over a larger swath of the visual spectrum while simultaneously increasing the reflectance in the NIR. At 100% concentration, the visual spectrum is absorbed nearly completely until the 550 nm wavelength and the inflated reflectance begins to trend toward a reflectance mimicking that of tap water at 1450 nm wavelength. The changes are much more muted beyond this point, even approaching a near-zero value after the 1900 nm wavelength.

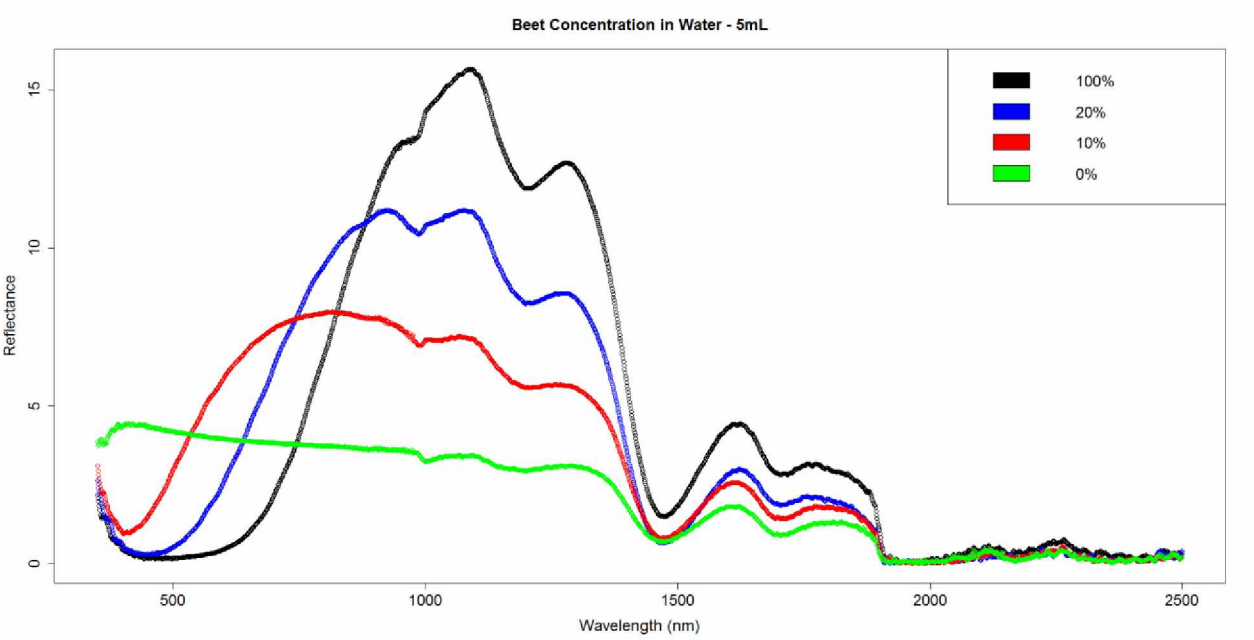

Figure 4.24 Beet Juice Reflectance Differences in Concentration

Differences in the reflectance based on liquid volume are significant, much like the brine differences shown previously in Figure 4.14. The increasing thickness again obliterates the NIR and IR wavelengths as thickness increases, however the beet differences shown in Figure 4.25 show the maximum reflectance to be found at the intermediate point 1.6 mm thickness.

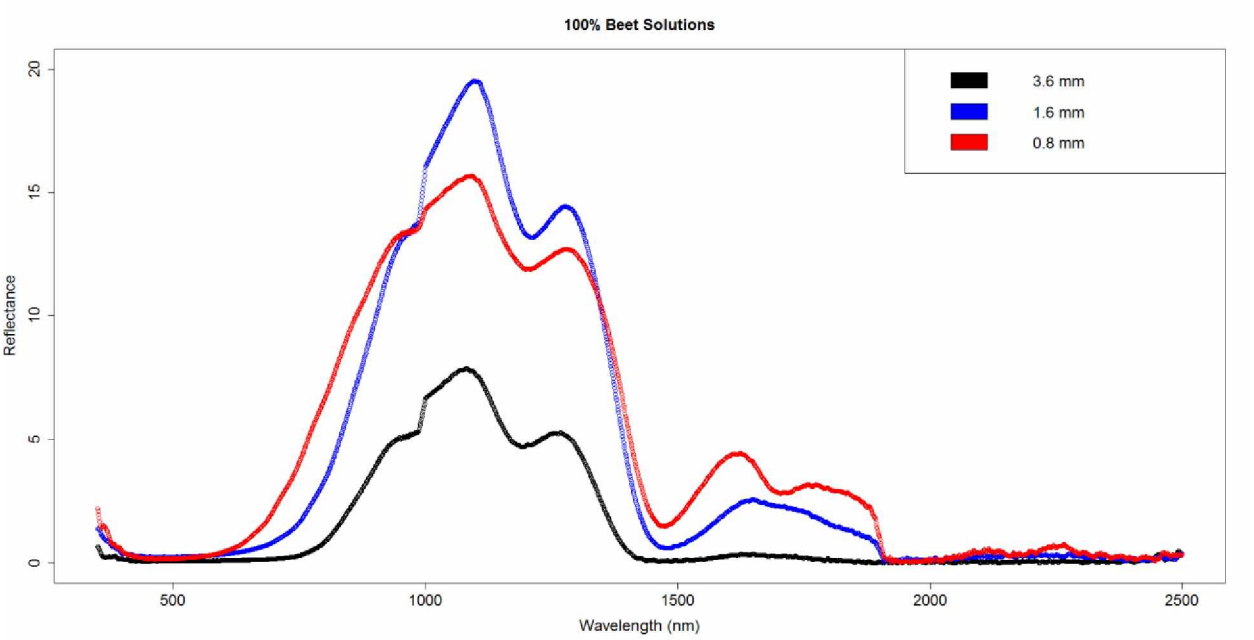

Figure 4.25 100% Beet Film Thickness Differences

Repeatability in the beet solutions is less perfect than the pure brine mixtures with notable visual differences around the 1000 nm wavelength. However, there is reasonable replication along the entirety of the spectrum, except for wavelengths in the vicinity of 1000 nm (Figure 4.26).

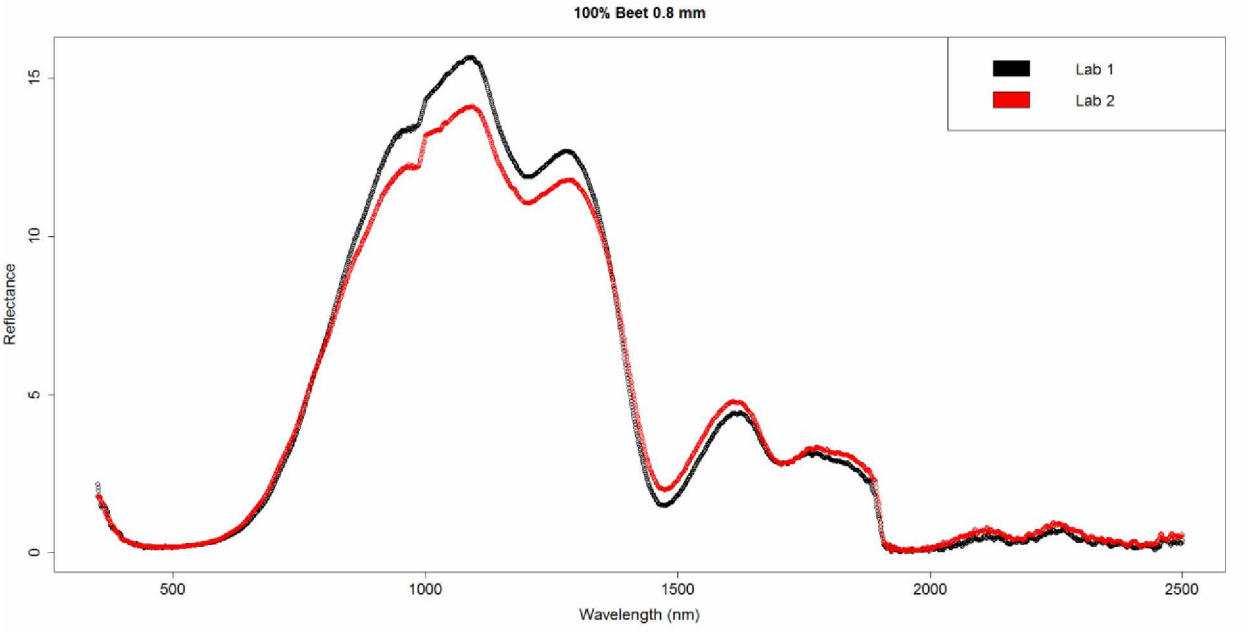

Figure 4.26 Replication 100% Beet 0.8 mm

For actual roadway applications in the AKDOT&PF northern region, beet extract concentrations will not exceed 20% by volume. Comparing these reduced concentrations also reduces the effects of the beet juice showing a dampening of overall reflectance values and a diminishing of the severity of the peak around the 1000 nm wavelength. The differences between the 0.8 mm thickness and the 1.6 mm thickness are reduced as shown in Figure 4.27 when compared to the differences demonstrated in the 100% beet concentration in Figure 4.25.

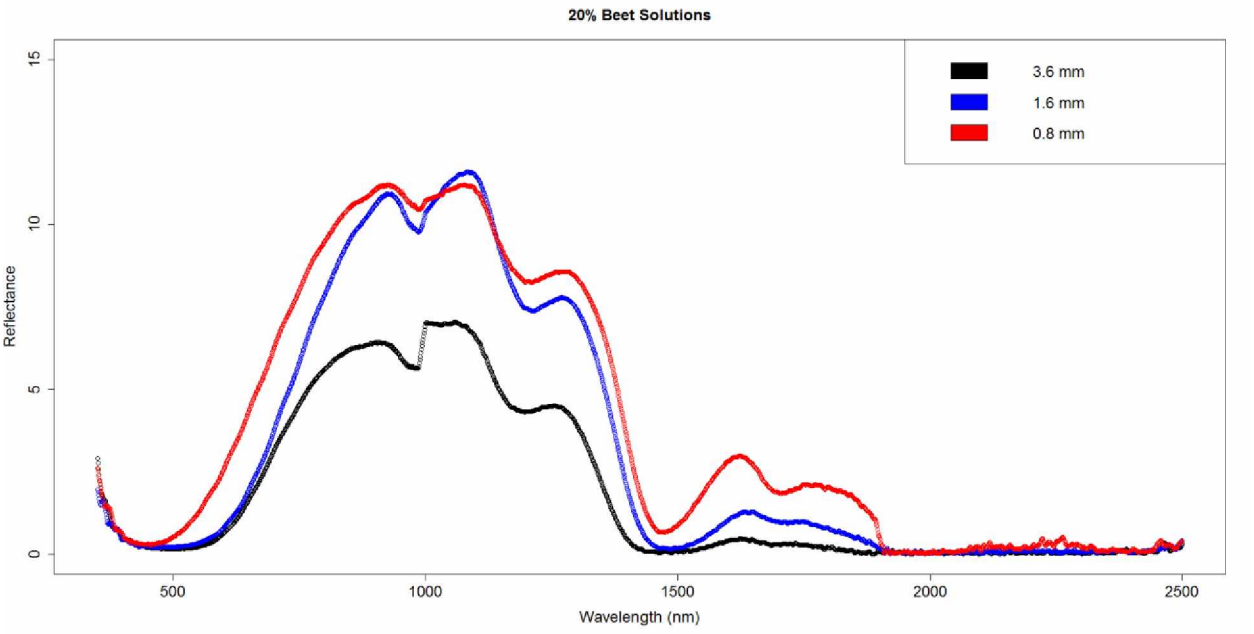

Figure 4.27 20% Beet Film Thickness Differences

The replication of 20% beet (Figure 4.28) shares the same differences as the differences in Figure 4.26. This repeating artifact suggests the possibility of changes to the chemical over time. This could be a result of microbial activity feeding off the high sugar content found in beet extract, or some other unrecorded factor.

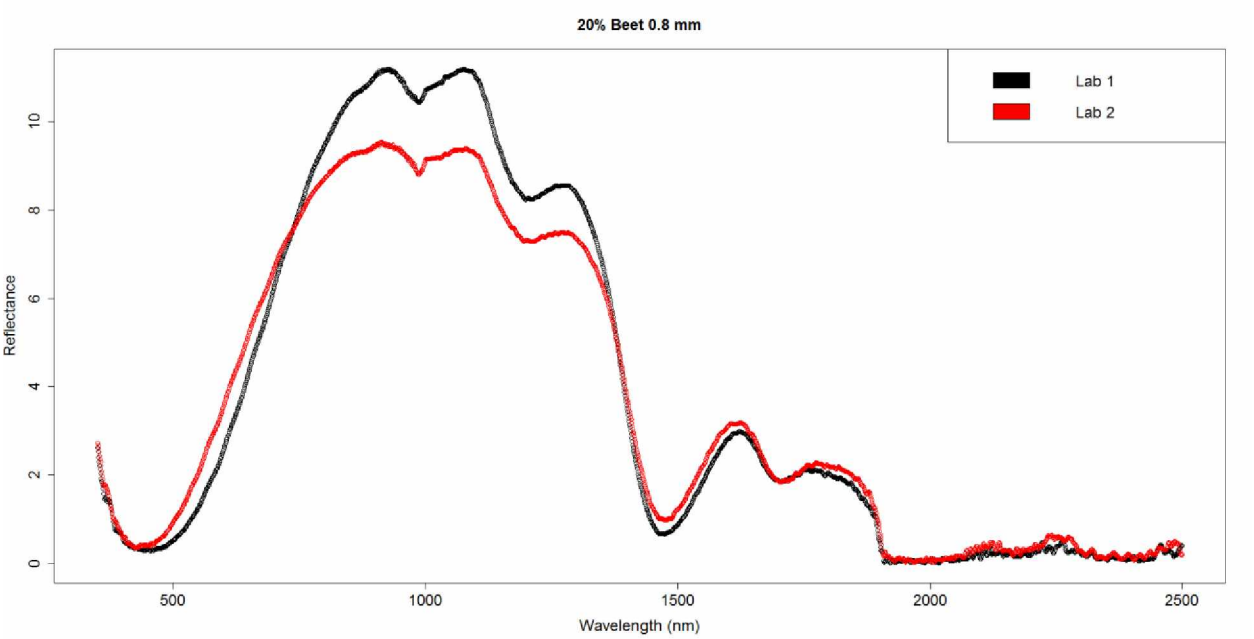

Figure 4.28 Repeatibility 20% Beet 0.8 mm

4.4. Data Comparisons (Beet-Brine mixtures)

4.4.1. Lab Data Comparisons

Analysis for beet-brine anti-icing and deicing mixture began with taking ten measurements over a short period of time of each sampled concentration. These spectra could be compared to each other to ensure accuracy and then averaged together as was done in the previous analyses to identify variations and uncertainty. Figure 4.24 and Figure 4.25 show the first 10 spectra recorded and the subsequent averaged curve in black with red lines denoting standard deviation respectively.

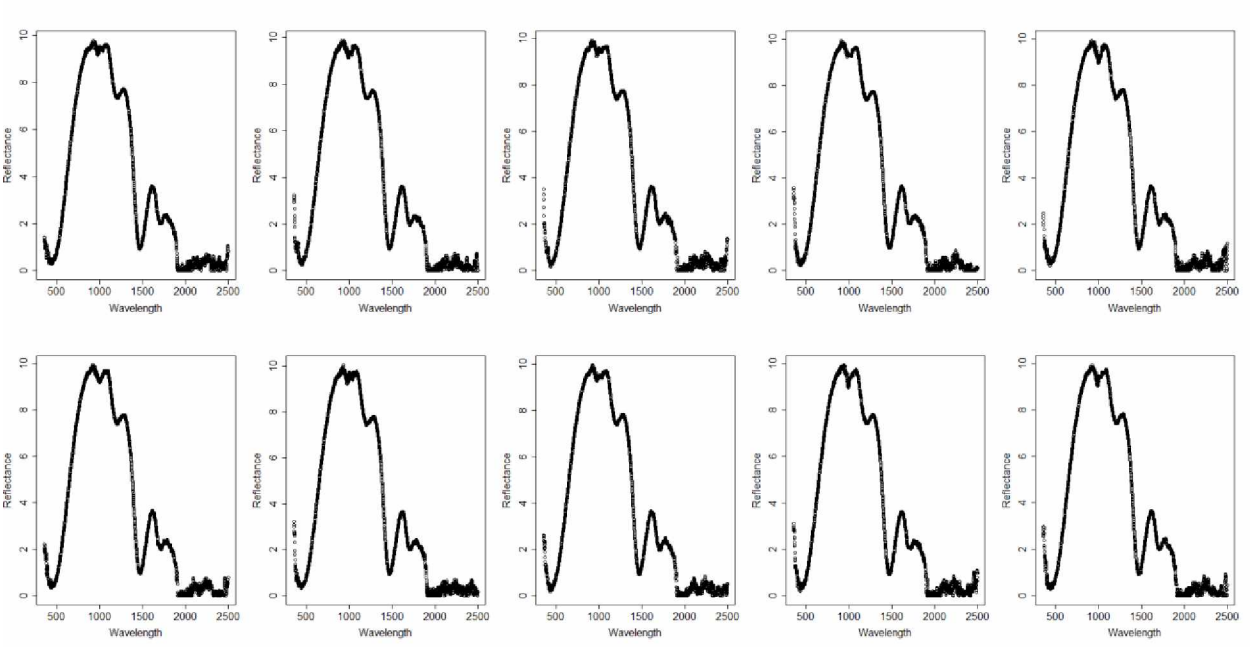

Figure 4.29 23.3% Brine 20% Beet Initial Measurements @ 0.8 mm, 5mL, sep 21

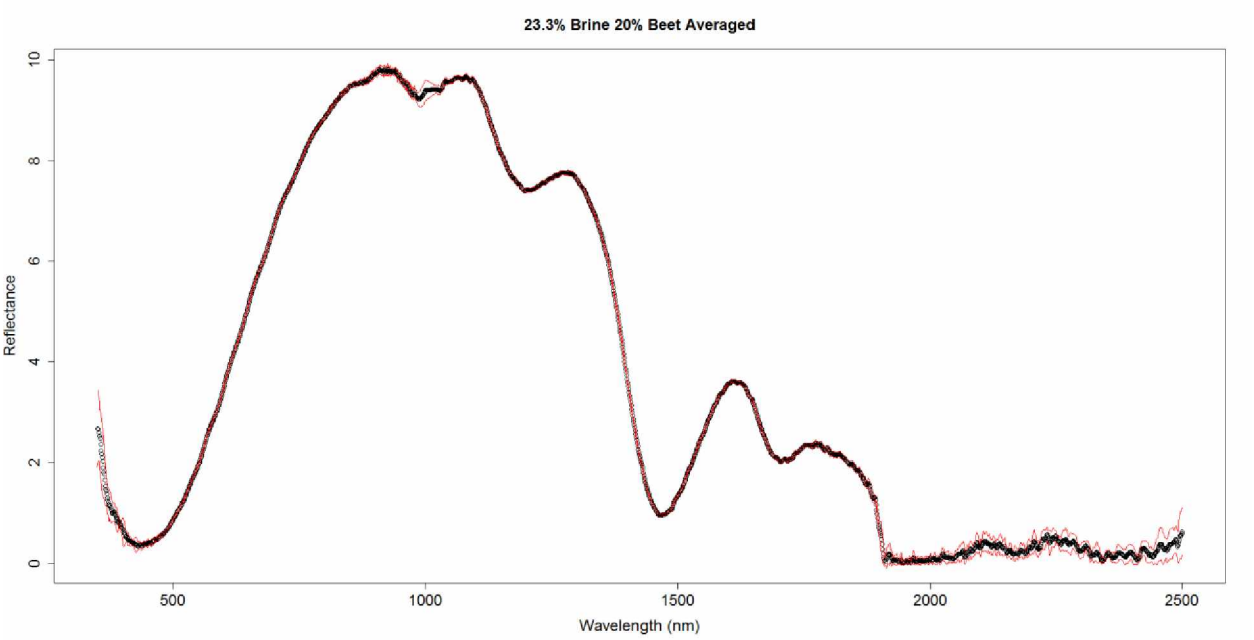

Figure 4.30 Averaged 23.3% Brine 20% Beet Initial Measurements @ 0.8 mm, 5mL, sep 21

The impact of changing solution thickness follows the same trends established by the brine solutions past the 1450 nm wavelength when compared to each other as demonstrated in Figure 4.31.

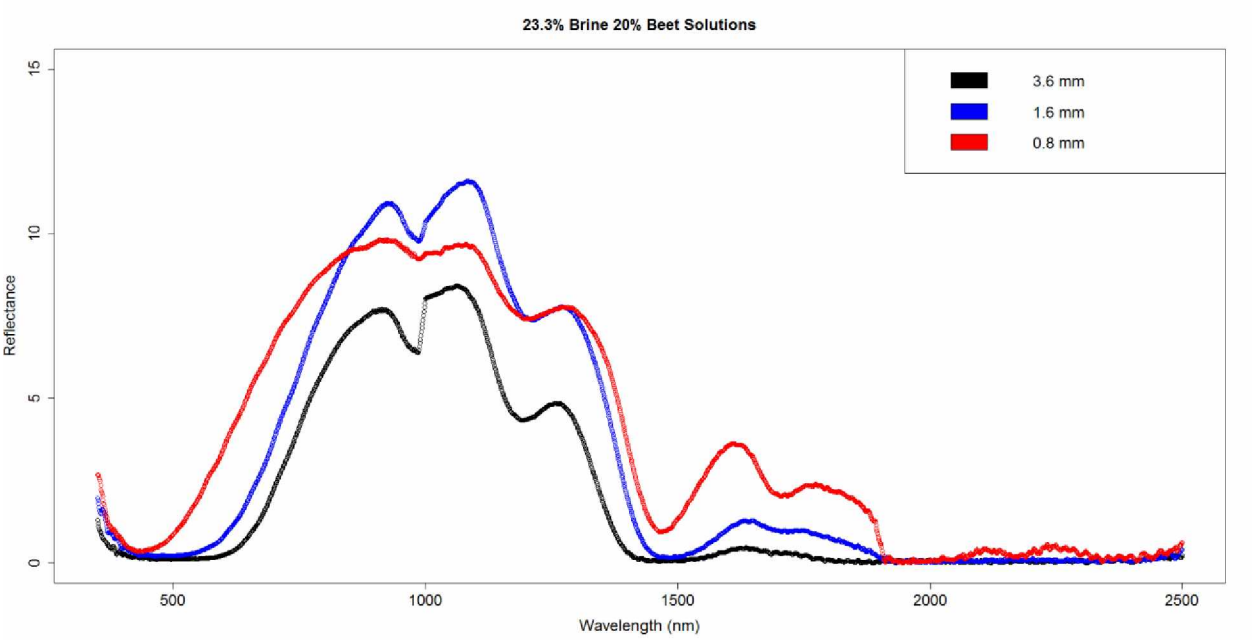

Figure 4.31 23% Brine 20% Beet Film Thickness Differences

Interestingly, the reflectance values do not follow the same trend for brine around the 1000 nm wavelength. Instead, the 1.6 mm thickness has the highest reflectance value. Moving forward with testing replication of results with the 0.8 mm thickness also shows slight changes as shown in Figure 4.32

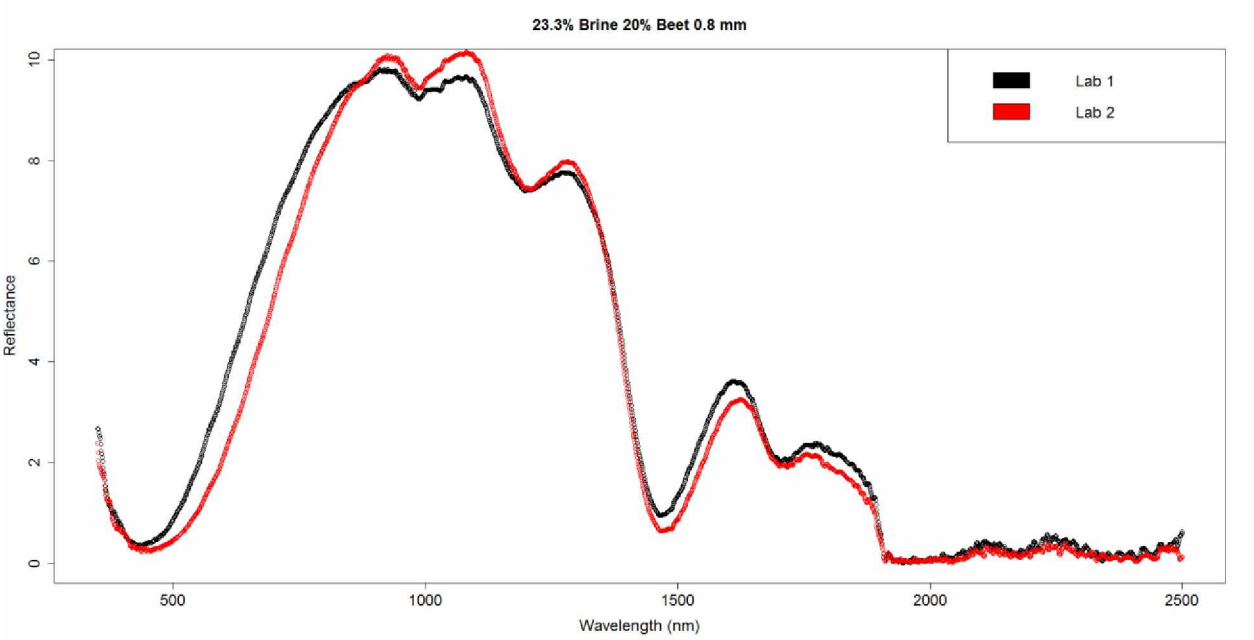

Figure 4.32 Repeatability 23.3% Brine 20% Beet 0.8 mm

Slight shifts in reflectance values are expected due to the nature of the device and the ability for slight shifts in environment, however the shape of the spectra is expected to remain the same. These slight changes could, again, be a result of slight microbial activity between generation of spectra.

4.4.2. Field Data Comparisons

Much like the brine deicing solutions, the varied backgrounds underlying the beet-brine solutions caused offset and other such disruptions as demonstrated by the lack of visual linear trend as deicing concentration changes as demonstrated below in Figure 4.33.

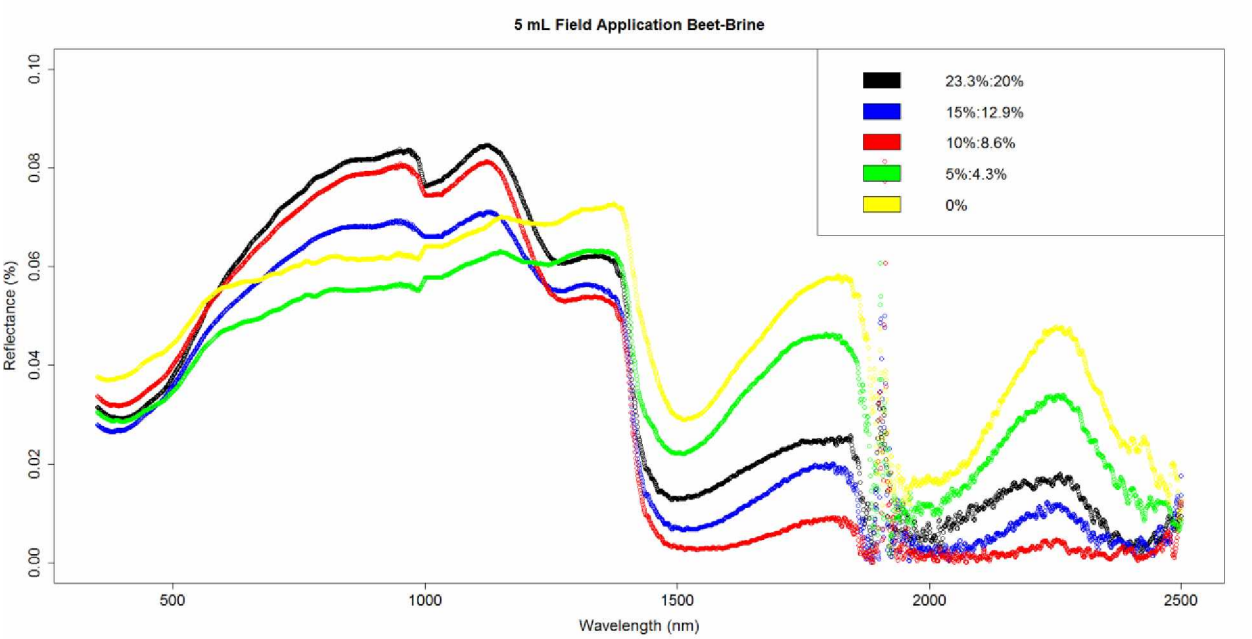

Figure 4.33 Field Changing Beet-Brine Concentration

A possible remedy for the varied backgrounds is normalizing each concentration to the appropriate surface layer underlying the applied deicer as shown in Figure 4.34.

Figure 4.34 Field Changing Beet-Brine Concentration, Normalized to Background

Similar to the brine deicer most data is obliterated past the 1800 nm wavelength, additionally there are strong deviations in expectations around the 1400 nm wavelength. However, the curves

do not appear to be great indicators of changing deicer presence. Identical to the brine deicer testing, the procedure for each application site was to apply deicing material of a specified concentration at numerous volumetric applications. To eliminate the variance due to significant changes in background reflectance, the curves of constant concentration as volumetric application rate on the surface of test site were compared.

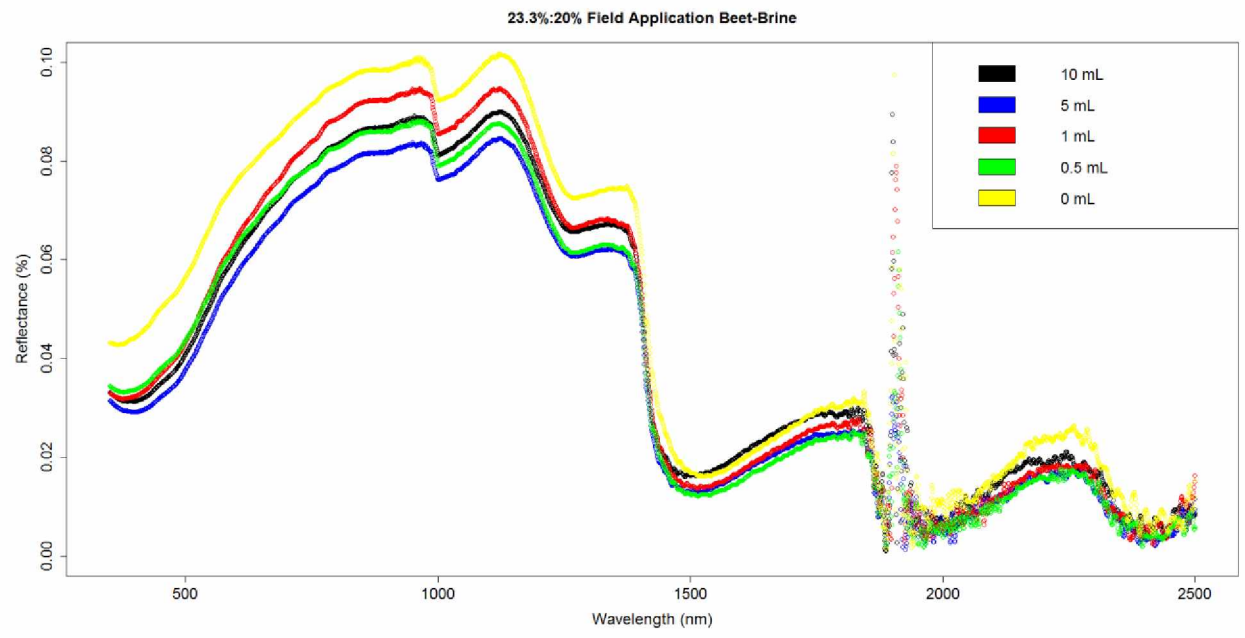

Figure 4.35 Beet-Brine - Changing Volume, Constant Concentration

For most of the curve, there appears to be no visually linear trend as volume increases. However, when looking in isolated segments of the spectral curve such as the visual range, there appears to be a semi-continuous trend from 0 mL application to the 5 mL application. The lack of continuation at the 10 mL application is speculated to have resulted from material migration at the higher volumes. Some migration was also noticed at the 5 mL application and is inherent to the deicing capabilities of the test materials (i.e., the deicer melts some of the native frozen material and then carries a portion of the deicer material away from the test location). Presumably, the lack of continuity in the relative changes in spectra are a result of this migration.

CHAPTER 5. ANALYSIS

5.1. Correlation Analysis

Correlation was one of the first attempted metrics used to analyze the spectra gathered from the different brine concentrations. If a clear correlation could be found from the comparison of the solid salt spectra to brine solutions of different concentrations, a correlation factor could be used to identify presence, or possibly even concentration, of the amount of brine present. For correlation analysis, the statistical package R was used. When correlation factors were checked there was not a relationship between increasing sodium chloride concentration in water and correlation to solid sodium chloride. The correlation was checked comparing: 1) the complete spectral curve; 2) a truncated curve that excluded wavelengths past the 1400 nm wavelength where water cuts obliterates the curve; and 3) smaller areas around key identified valleys of the curve. The procedures used for brine were also tested on the pure beet curves without success. Because of ineffectiveness correlation analysis was abandoned for future use in comparisons.

5.2. Peak and Valley Analysis (Manual)

Peak and valley analysis requires the identification of local minima and maxima of reflectance curves as discussed in Section 3.4. An example of a range of brine concentrations analyzed are shown in Figure 5.1.

Relationship Adjustments

Salt water in petri dish analysis:

23.3% POI		
feature	x	y
Valley 1	986	3.56587
Peak 1	1001	5.11018
Valley 2	1030	4.98235
Peak 2	1058	5.13705
Valley 3	1193	2.50581
Peak 3	1256	2.91556
Valley 4	1457	0.03988
Peak 4	1632	0.23096

* - logged

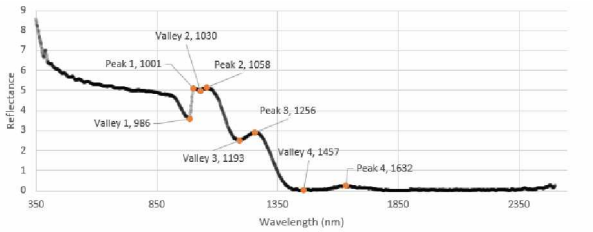

REGULAR	Result						Linear Relationship?			Logged Result*						Logged Linear Relationship?		
Relationship	0	5	10	15	23.3	40	0 to 40	5 to 40	10 to 40	0	5	10	15	23.3	40	0 to 40	5 to 40	10 to 40
V1/P1	0.79328	0.849057	0.78432	0.592232	0.697797	0.763311	0	0	0	0.839543	0.871592	0.838517	0.755799	0.779415	0.885644	0	0	0
V1/P2	0.774537	0.782968	0.759508	0.590003	0.694147	0.752542	0	0	0	0.82586	0.81948	0.820975	0.754473	0.776917	0.880347	0	0	0
V1/P3	1.33666	1.551588	1.360467	1.143071	1.223048	1.135467	0	0	0	1.314895	1.654286	1.322786	1.089888	1.188163	1.064664	0	0	0
V1/P4	31.76435	108.8698	28.38387	21.63712	15.43934	3.348762	0	1	1	-0.53932	-0.31029	-0.60522	-1.1158	-0.86755	2.368504	0	0	0
V1/V2	0.789445	0.808699	0.772493	0.59829	0.7157	0.763263	0	0	0	0.836733	0.839509	0.830133	0.759402	0.79171	0.88562	0	0	0
V1/V3	1.40914	1.696311	1.486179	1.265099	1.423041	1.284032	0	0	0	1.394825	1.907672	1.457896	1.169639	1.384053	1.135744	0	0	0
V1/V4	140.6061	101.8236	169.3367	98.90227	89.41499	5.078972	0	0	1	-0.32447	-0.3162	-0.32593	-0.54539	-0.39462	4.482656	0	0	0
V2/P1	1.004858	1.049905	1.01531	0.989874	0.974985	1.000063	0	0	0	1.003358	1.038217	1.0101	0.995256	0.98447	1.000027	0	0	0
V2/P2	0.981115	0.968182	0.983191	0.986148	0.969885	0.985954	0	0	0	0.987005	0.976142	0.988968	0.993509	0.981315	0.994046	0	0	0
V2/P3	1.693164	1.918623	1.761139	1.910564	1.708883	1.487649	0	0	0	1.571463	1.97054	1.593462	1.435192	1.500756	1.202167	0	0	0
V2/P4	40.23631	134.6235	36.74323	36.16493	21.57235	4.38743	0	1	1	-0.64455	-0.3696	-0.72907	-1.46931	-1.0958	2.674402	0	0	0
V2/V3	1.784976	2.097582	1.923874	2.114525	1.988319	1.682294	0	0	0	1.666989	2.272367	1.756219	1.54021	1.748183	1.282429	0	0	0
V2/V4	178.1076	125.9105	219.2082	165.3082	124.9336	6.654292	0	0	1	-0.38778	-0.37665	-0.39263	-0.71818	-0.49844	5.061602	0	0	0
V3/P1	0.562953	0.500531	0.527743	0.468131	0.490357	0.594464	0	0	0	0.601898	0.456888	0.575156	0.646182	0.563139	0.779791	0	0	0

Figure 5.1 Excel Analysis Example

An example of the visual inspection identification for the brine curve in Figure 5.2 where the valleys and peaks are numbered in order of occurrence from left to right and the point of interest's associated wavelength (nm) recorded.

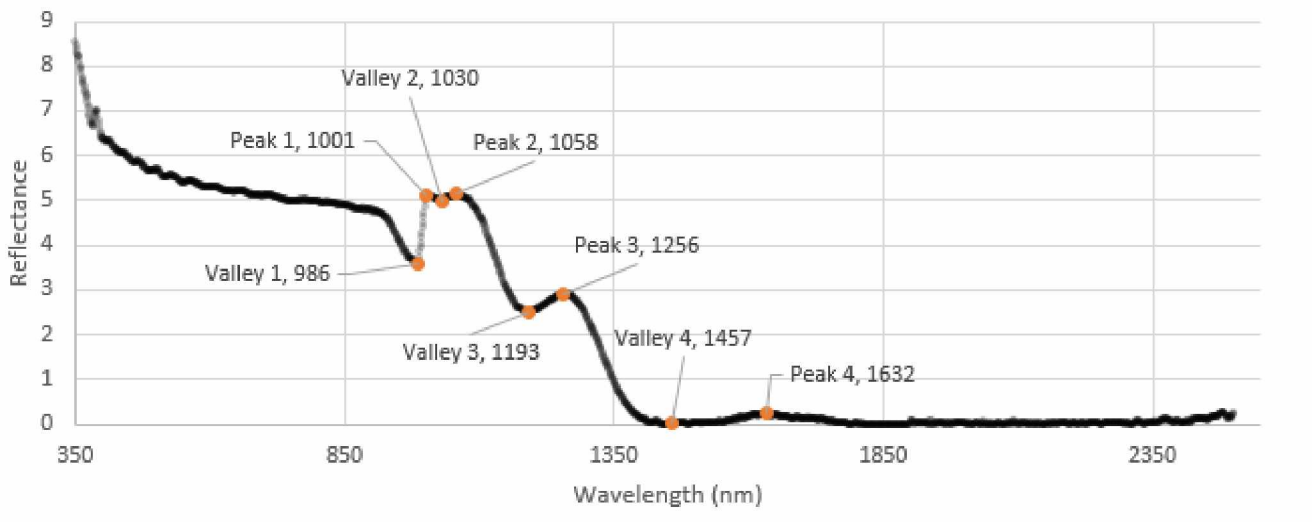

Figure 5.2 23.3% Brine at 3.2 mm with Key Points Marked

For the manual peak and valley analysis, the associated wavelengths and reflectance value for each definitive POI were extracted from the text files that are generated by the PSR+ spectral imaging unit. These were then loaded into a separate Excel Sheet for additional analysis and comparison.

Table 5.1 23.3% Brine at 3.2 mm Example Key Points

3.2 mm 23.3% POI		
feature	**X (nm)**	**Y (% Reflectance)**
Valley 1	986	3.56587
Peak 1	1001	5.11018
Valley 2	1030	4.98235
Peak 2	1058	5.13705
Valley 3	1193	2.50581
Peak 3	1256	2.91556
Valley 4	1457	0.03988
Peak 4	1632	0.23096

Figure 5.3 shows the linear relationship checks from the peaks (P) and valleys (V) extracted from Figure 5.2. Analysis started with comparing the trends in these peaks and valleys as

concentration changed, comparing if the reflectance values were offset by 1, and comparing if offsetting by 1 and normalizing, in order to test which permutations would reveal relationships.

REGULAR	Result						Linear Relationship?		
Relationship	0	5	10	15	23.3	40	0 to 40	5 to 40	10 to 40
V1/P1	0.79328	0.849057	0.78432	0.592232	0.697797	0.763311	0	0	0
V1/P2	0.774537	0.782968	0.759508	0.590003	0.694147	0.752542	0	0	0
V1/P3	1.33666	1.551588	1.360467	1.143071	1.223048	1.135467	0	0	0
V1/P4	31.76435	108.8698	28.38387	21.63712	15.43934	3.348762	0	1	1
V1/V2	0.789445	0.808699	0.772493	0.59829	0.7157	0.763263	0	0	0
V1/V3	1.40914	1.696311	1.486179	1.265099	1.423041	1.284032	0	0	0
V1/V4	140.6061	101.8236	169.3367	98.90227	89.41499	5.078972	0	0	1
V2/P1	1.004858	1.049905	1.01531	0.989874	0.974985	1.000063	0	0	0
V2/P2	0.981115	0.968182	0.983191	0.986148	0.969885	0.985954	0	0	0
V2/P3	1.693164	1.918623	1.761139	1.910564	1.708883	1.487649	0	0	0
V2/P4	40.23631	134.6235	36.74323	36.16493	21.57235	4.38743	0	1	1
V2/V3	1.784976	2.097582	1.923874	2.114525	1.988319	1.682294	0	0	0
V2/V4	178.1076	125.9105	219.2082	165.3082	124.9336	6.654292	0	0	1
V3/P1	0.562953	0.500531	0.527743	0.468131	0.490357	0.594464	0	0	0

Figure 5.3 Brine 3.2 mm Linear Relationship Analysis

These relationships were tested for linearity including all points, excluding tap water as a relationship point, and excluding tap water and 5% brine. Examples of the linear relationship comparisons are shown in Figure 5.4.

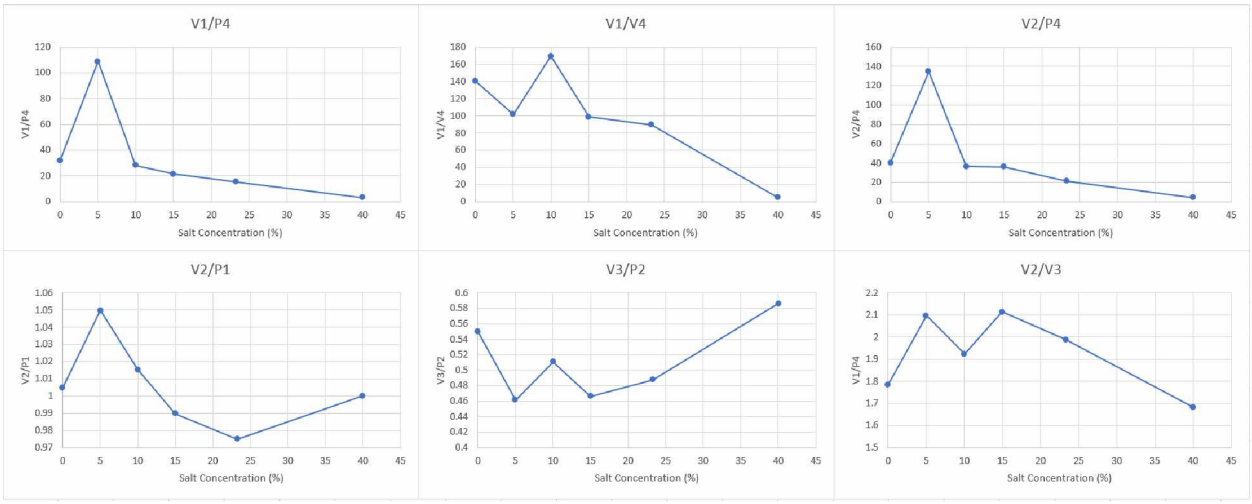

Figure 5.4 Examples of Tested Linear Relationships

The developed linear relationships between peaks and valleys did not generate a relationship that satisfied all "points." The relationships generated, at most, show a linear relationship using 10% to 40% concentration with the 5% and tap water throwing off the curve. In order to generate successful relationships, some possible inadequacies had to be addressed. First, reflectance values near 0 are problematic because shifts in the curve at or near 0 can result in exponential changes in value. Values near zero are addressed by offsetting the curve by a value of one in order to avoid dividing by numbers at or near zero. Second, some vertical reflectance shifts are generated from uncontrolled changes in material and environment. Normalizing the reflectances serves to control for these reflectance shifts that are not associated with adjusting brine concentrations. Offsetting and normalizing the curves generated some of the first relationships that showed a linear trend with increasing or decreasing salt concentration and changes in the reflectance values of a curve as shown below.

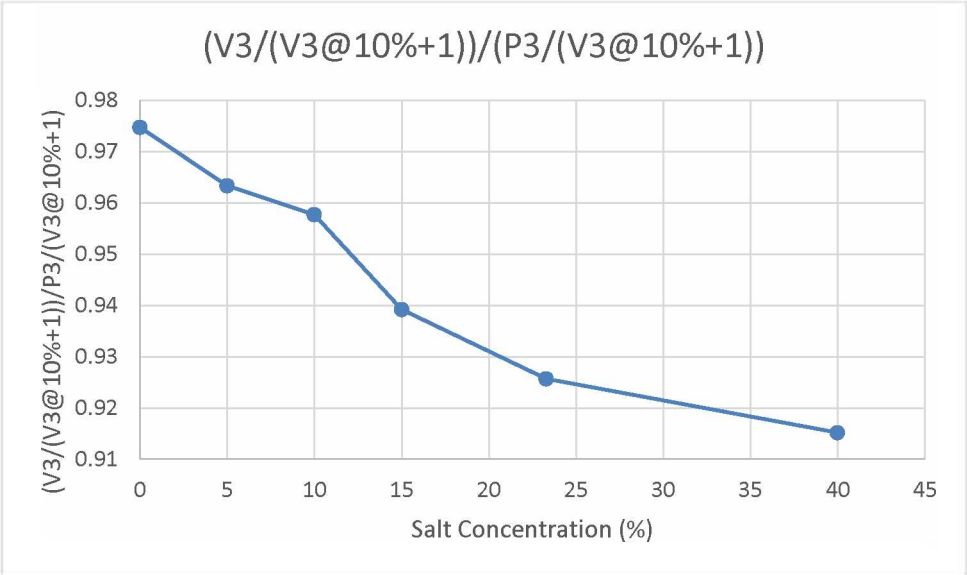

Figure 5.5 Example of Successful Discovered Linear Relationship

For the relationship shown in Figure 5.5 the band math equation is (B1193/B1193@10% +1)/(B1256/B1193@10%+ 1) where B1256 is the third peak located at wavelength 1256 nm and B1193 is the third valley located at wavelength 1193 nm. The values were then normalized to the third valley of a 10% saline solution that was offset by 1. This produced a linear relationship between salt concentration and reflectance recorded in the lab and shows promise for this method at least in a laboratory setting.

While working relationships were derived from local minima and maxima of the brine, beet, and beet-brine solution spectra, these are not necessarily the best or most consistent relationships for identifying concentration or presence of material. The valleys and peaks in a combined spectrum do not necessarily denote the peak and valleys of an added substance such as the addition of salt to water. Due to this fact and the few relationships gathered from testing just the peaks and valleys, a more rigorous testing method for all possible sources of spectra changes from modification of materials present needed to be developed.

5.3.Rstudio Analysis

In order to test all possible permutations of wavelength combinations and account for the larger changes occurring away from the peaks and valleys (see discussion in Section 3.4), the statistical package R was used. Using RStudio code could analyze every single point from 350 nm wavelength to 2500 nm wavelength in order to find relationships as concentrations and film thickness increased or decreased. Figure 5.6 shows an example of the code derived for this purpose. The code starts by selecting a point *j* and comparing it to the same point *i*, then the code iterates *i*+1 until *i* reaches the final wavelength available. The point *j* then iterates by 1 and repeats the process until all point combinations are exhausted.

```
#in the loops i and j had 349 added to them to change it from channel # to wavelength #
for (j in seq(from=1, to=2151, by=1)){
  message(j+349)
  for(i in seq(from=1, to=2151,by=1)){

    if ( ((entity1[i,2]))/((entity1[j,2])) > ((entity2[i,2]))/((entity2[j,2]))
        &((entity2[i,2]))/((entity2[j,2])) > ((entity3[i,2]))/((entity3[j,2]))
        &((entity3[i,2]))/((entity3[j,2])) > ((entity4[i,2]))/((entity4[j,2]))
        &((entity4[i,2]))/((entity4[j,2])) > ((entity5[i,2]))/((entity5[j,2]))
    )
    {
      xvalues=c(xentity1,xentity2,xentity3,xentity4,xentity5)
      yvalues=c(((entity1[i,2]))/((entity1[j,2])),((entity2[i,2]))/((entity2[j,2])),((enti
      lm=lm(yvalues~xvalues)
      entity=(cbind(i+349,j+349,summary(lm)$coefficients[2,1],summary(lm)$r.squared,summar
      entitysuccess=rbind(entitysuccess,entity)
    }


    if ( ((entity1[i,2]))/((entity1[j,2])) < ((entity2[i,2]))/((entity2[j,2]))
      &((entity2[i,2]))/((entity2[j,2])) < ((entity3[i,2]))/((entity3[j,2]))
```

Figure 5.6 Example of RStudio Code for Iterative Linear Relationship Checking

The resulting tables (see Table 5.2) were then analyzed based on which outcome was being tested, (e.g., cut offs for slope, regression coefficient, margin of error, and number of times a given wavelength is found in a data set).

Table 5.2 Example of Beginning Paired Wavelengths from 0.8 mm Brine

Sep6 5 mL Lab	Wvl1	Wvl2	slope	R2	Sigma
1	2347	352	-0.00051	0.699229	0.003458
2	354	353	-0.00088	0.981875	0.001244
3	2303	353	0.001727	0.521017	0.017231
4	353	354	0.000895	0.981824	0.001266
5	2303	354	0.001809	0.546578	0.017138
6	2304	354	0.001699	0.552789	0.015894
7	2347	355	-0.00047	0.653186	0.003568
8	2297	357	0.00236	0.485806	0.025257
9	2155	358	0.002369	0.80095	0.012288
10	2156	358	0.002387	0.756787	0.014075
11	2297	358	0.002477	0.553549	0.023144
12	2395	358	0.000259	0.887472	0.000958
13	2154	359	0.002192	0.748242	0.01323
14	2155	359	0.002408	0.828588	0.011395
15	2156	359	0.002424	0.790307	0.01299
16	2395	359	0.000268	0.910297	0.000874
17	2155	360	0.002404	0.82306	0.011595
18	2156	360	0.002421	0.79145	0.012927
19	2296	360	0.002175	0.52231	0.021641
20	2155	361	0.002461	0.846946	0.010883

Comparison of matching points for the 22 mL application, equivalently a 3.6 mm film thickness) are shown in Table 5.3.

Table 5.3 3.6 mm Highest Freq Wvl (nm) for (a) Test 1 (June 15th), (b) Test 2 (January 24th), and (c) the resulting matched values

15-Jun	22 mL
Wvl (nm)	Freq
1923	1137
2036	1101
2058	1098
2120	1074
2037	1057
2161	1056
2162	1032
2160	938
2119	924
2035	884
2118	873
2445	632
1024	539
1023	538
1025	537
1026	534
1028	532
1029	532
1027	531
1030	530

(a)

+

24-Jan	22 mL
Wvl (nm)	Freq
1861	1374
2146	1347
1860	1326
2145	1283
2335	1223
2334	1182
2120	1124
1897	1060
2057	955
2333	931
1938	813
1544	752
1909	702
1898	687
1937	673
1859	653
2447	629
2446	596
2495	555
2210	528

(b)

=

Repeated	22 mL
Wvl (nm)	Freq
2120	871
2446	279
2118	173
2445	161
2119	122
1282	50
1283	48
1281	47
1280	46
1284	45
1273	43
1279	42
1272	41
1278	41
1285	41
1277	40
1286	40
1274	39
1275	39
1276	39

(c)

Analyzing the 22 mL solutions from Table 5.3a (June) and Table 5.3b (January), the most common points to have relationships with increasing or decreasing salt concentration were found in the NIR wavelengths (approximately 2000 nm and greater), dominated the top 20 repeated wavelengths. Wavelengths in the NIR are surprising considering how close to 0 the reflectance values for the brine spectra were beyond the 1400 nm wavelength. Repeated values were checked by sequentially testing wavelengths and resulted in frequently occurring paired values including several in the region of 2120 nm and 2446 nm. Strong relationships were also observed in the 1275 nm region. These points would have to be checked against points discovered in the

1.6 mm and 0.8 mm heights to see if indeed this relationship for brine works for all film thicknesses or just the 3.6 mm.

Similarly, Table 5.4 shows the results from the thinner 10 mL liquid application, which is equivalent to 1.6 mm thickness.

Table 5.4 1.6 mm Highest Freq Wvl (nm) for (a) Test 1 (June 27th), (b) Test 2 (July 9th), and (c) the resulting matched values

27-Jun	10 mL
Wvl (nm)	Freq
2083	1677
2084	1656
2041	1593
2363	1571
2145	1521
1995	1514
2364	1459
2035	1374
2287	1374
2163	1230
1484	1160
1534	1133
1533	1124
1668	1116
1892	1116
2342	1109
1667	1105
1891	1102
2445	1100
1450	1099

(a)

+

9-Jul	10 mL
Wvl (nm)	Freq
1535	1426
1534	1422
1533	1404
1536	1393
1588	1389
1559	1383
1393	1381
1589	1380
1558	1379
1560	1379
1587	1379
1392	1374
1394	1374
1391	1371
1402	1371
1538	1371
1561	1371
1390	1370
1423	1369
1430	1369

(b)

=

Repeated	10 mL
Wvl (nm)	Freq
1484	1073
1534	1070
1668	1064
1533	1063
1667	1051
1680	1045
1679	1038
1678	1036
1669	1030
1483	1029
1677	1007
1507	1001
1508	997
1482	993
1666	975
1532	973
1500	953
1535	944
1681	936
1691	888

(c)

Comparing the successful relationships from the first lab group of 5 mL (a) to the second (b) and third group (c) of 5 mL showed that the derived relationships are not consistent, many

relationships that were derived in the first lab iteration did not show up in the second or third lab testing (see Table 5.5).

Table 5.5 0.8 mm Highest Freq Wvl (nm) for (a) Test 1 (September 6th), (b) Test 2 (September 17th), and (c) Test 3 (January 28th)

6-Sep	5 mL
Wvl (nm)	Freq
2466	1541
2155	1410
2154	1349
2156	1336
1897	1322
1539	1280
1540	1270
1538	1201
1541	1198
1512	1180
1535	1178
1513	1159
1537	1156
1511	1147
1536	1145
1542	1145
1514	1106
1592	1105
1534	1103
1591	1102

(a)

17-Sep	5 mL
Wvl (nm)	Freq
1912	1797
1913	1788
1911	1595
2426	1482
2425	1480
2427	1394
2428	1091
2355	1026
2370	739
468	619
454	614
2301	585
498	574
467	569
497	532
504	511
475	505
471	495
502	490
455	481

(b)

28-Jan	5 mL
Wvl (nm)	Freq
1935	1743
1930	1596
2159	1581
2495	1356
2009	1273
2010	1193
2235	998
2237	998
388	884
389	773
2236	686
387	663
2234	630
390	558
2158	440
485	393
2374	377
486	369
405	345
406	331

(c)

A more consistent array of wavelengths is achieved by matching the linear relationships between concentration and reflectance ratios. If the matching points from each data set are extracted, nearly 90% of wavelength relationships are eliminated as shown in the first extraction (a) and second extraction (b) in Table 5.6.

.

Table 5.6 0.8 mm Highest Freq Wvl Duplicates (nm) for (a) the resulting matched values (Jan 28th and Sep 17th) and (b) the resulting matched values (Jan 28th, Sep 17th and Sep 6th)

Extracted Once	5 mL
Wvl (nm)	Freq
1930	273
507	154
1407	137
1406	135
1408	132
1409	122
1405	119
1398	115
1400	112
1397	111
1399	111
1410	109
506	108
1401	108
1396	103
1402	100
508	99
1404	99
1403	94
1411	94

(a)

Extracted Twice	5 mL
Wvl (nm)	Freq
1407	111
1408	109
1406	107
1409	101
1398	95
1410	95
507	94
1397	93
1405	92
1399	89
1400	88
1411	86
1396	85
1401	84
1402	79
1412	79
1404	78
1403	74
1395	73
1413	68

(b)

The extraction of points makes a significant difference in the array of wavelengths shown to have the highest successful relationship frequency. The third extraction also shows that there are sharp diminishing returns in impact repeated duplicate comparisons produce. The top 20 frequency for 0.8 mm brine liquid shows an overwhelming impact by wavelength region from 1395 nm to 1415 nm.

Of the three highest frequency wavelengths identified (first three rows of Table 5.6), the top three (1407, 1408, and 1406 respectively) repeated at a frequency of 111, 109, and 107. In total, 97 wavelengths were shared between the three groups. These repeated values are likely to

hold constant when changing salt concentration. Conversely, the points 1407, 1408, and 1406 experience the greatest change in the curve once normalized to themselves. The wavelengths are drawn (vertically) on a curve of 23.3% brine 0.8 mm liquid film thick spectral curve shown below in Figure 5.7.

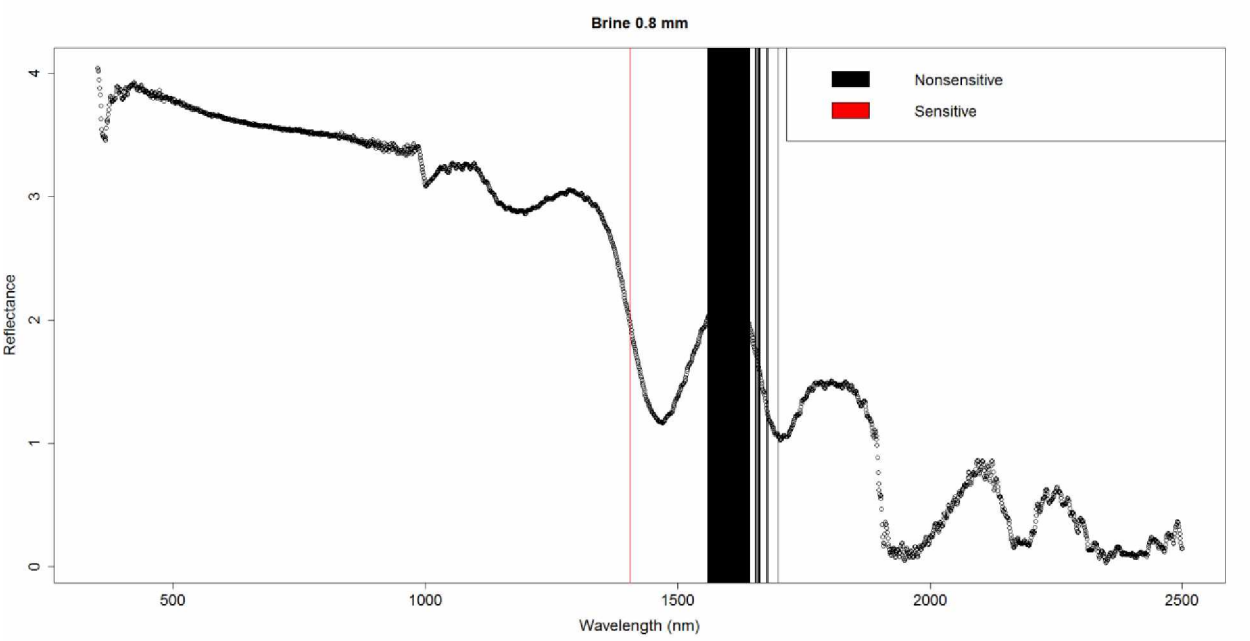

Figure 5.7 Points of Greatest Repitition Brine 0.8 mm

The red line in Figure 5.7 that, theoretically, represents a wavelength that is most sensitive to changes in the brine concentration while the wavelengths identified in black should be the opposite, the portion of the curve least sensitive to the effects of brine concentration (i.e., the peak remains relatively constant).

The relationships established by analyzing each film thickness did not seem to be very similar, a signifier of the dominating effect of changing water volume thicknesses on spectral reflectance interpretation. The selected wavelengths for the 0.8 mm, 1.6 mm, and 3.6 mm brine solutions are slightly different when tested for replication after extraction of matching points of

similar material thicknesses. The resultant data frames of successfully repeated wavelengths were around 1400 for the 0.8 mm film, 1500 for the 1.6 mm film, and 2100 for the 3.6 mm film. These different successful wavelengths suggest the possibility of multiple volumetric dependent correlations for concentration analysis.

When considering that the minimum application thicknesses recordable in the lab with the established equipment was only 0.8 mm, a thickness greater than the estimated maximum for a well-maintained winter roadway. Therefore, the 0.8 mm relationships were of most concern during the field-testing phase. For consistency, other film thicknesses were still tested since to determine if the relationships held valid at all volumetric analysis points.

Table 5.7 Brine Wavelength Pairs Successful Regardless of Film Thickness

Wvl1	Wvl2	slope	R2	y0	y1	y2	y3	y4
1821	1552	-0.00412	0.914939	0.902327	0.881069	0.859307	0.817814	0.813776
1820	1554	-0.00379	0.875204	0.879718	0.862394	0.851986	0.800835	0.800114
1820	1555	-0.00362	0.873141	0.870093	0.851597	0.845217	0.794945	0.793284
1820	1556	-0.00351	0.864103	0.863125	0.843528	0.840255	0.789643	0.788113

The matched pairs for film thickness revealed significant pairing of the 1820 nm wavelength with wavelengths at 1554 nm, 1555 nm, and 1556 nm. These points will be some of the points that will face extra scrutiny during field testing to see if the relationship holds true for film thicknesses less than 0.8 mm and a continuation of a film thickness independent identifier of brine presence.

Analysis of varied beet-only solutions were conducted to isolate the indicators solely from changing beet concentration. Visually, the addition of beet juice makes a stark visual difference (e.g., the solution becomes darker, redder in color, and less transparent) as seen in Figure 4.21. A significant change in the visual spectrum was expected to be produced as red beet carbohydrate is added due to suppression of the green and blue visual wavelengths. The most repeated wavelength values are shown in the table below.

Table 5.8 3.6 mm Beet Highest Freq Wvl (nm) for Test 1 (January 24th)

16-Feb	22 mL
Wvl (nm)	Freq
1920	1706
2069	1672
592	1646
608	1646
602	1643
622	1642
593	1641
607	1641
619	1641
620	1641
598	1640
609	1640
618	1640
603	1639
606	1639
617	1639
610	1638
615	1638
616	1638
621	1638

The 3.6 mm sample of beet extract resulted in the most repeated points occurring at the 1920 nm and 2069 nm wavelengths. However, the majority of the top 20 repeated wavelengths lie in the "orange" visual spectrum (590-625 nm), directly between the yellow and red spectrum. The

domination of red reflectance was expected since the carbohydrate beet juice is a reddish-black in coloring. Repeating procedure for 1.6 mm produced the table shown below.

Table 5.9 1.6 mm Beet Highest Freq Wvl (nm) for Test 1 (July 9th)

9-Jul	10 mL
Wvl (nm)	Freq
2218	1803
2217	1750
2303	1749
643	1728
648	1727
634	1726
647	1726
650	1726
633	1725
635	1725
637	1725
646	1725
632	1724
638	1724
641	1724
642	1724
644	1724
649	1724
672	1724

The 1.6 mm sample of beet continues the trend of being highly reflective in the early red spectrum (625-740 nm) with 17 out of 20 of the most common wavelengths and some slight inclusion in the lower end of the NIR around 2000 nm. The similar amount of frequency also suggests the relationships are drawing from the same points, which is a good sign for field analysis. Moving on to the thinnest application and therefore most realistic the 0.8 mm application is shown below.

Table 5.10 0.8 mm Beet Highest Freq Wvl (nm) for (a) Test 1 (September 21st), (b) Test 2 (January 28th), and (c) the resulting matched values

21-Sep	5 mL
Wvl (nm)	Freq
413	1887
412	1886
424	1883
425	1882
426	1880
414	1875
427	1875
411	1874
423	1874
415	1868
428	1867
431	1866
432	1866
404	1865
420	1863
433	1863
410	1862
417	1862
421	1862
403	1861

(a)

+

28-Jan	5 mL
Wvl (nm)	Freq
432	1714
431	1713
433	1710
430	1709
441	1708
440	1706
442	1705
434	1703
439	1700
435	1699
438	1698
429	1697
437	1696
443	1696
436	1693
414	1687
458	1686
444	1685
454	1681
457	1680

(b)

=

Repeated	5 mL
Wvl (nm)	Freq
403	1553
404	1550
402	1548
414	1541
405	1539
432	1538
431	1536
413	1535
401	1534
433	1532
430	1531
406	1530
415	1530
412	1525
399	1524
429	1524
400	1520
417	1517
425	1516
426	1516

(c)

The 0.8 mm thicknesses are dominated by the violet spectrum unlike the 1.6 mm thickness beet solutions. Analyzing the two 0.8 mm solutions of September (a) and January (b) the comparative third data set was generated (Table 5.10). The resulting top 20 of each data frame is dominated by the violet reflectance wavelengths (380-450 nm) which is a notable difference from the thicker solutions tested. All solutions that included beet juice had their relationships dominated by the visual spectrum. While this is a valuable insight in terms of ice, snow, and liquid backgrounds the impact on already dark or black background may be more muted and may not

provide such a pronounced change in the field. A final check for the beet solutions is a comparison of wavelengths regardless of fluid thickness shown in Table 5.11.

Table 5.11 Beet Wavelength Pairs Successful Regardless of Film Thickness

Extracted	all volumes beet
Wvl (nm)	Freq
403	1211
401	1208
400	1207
399	1205
402	1204
404	1203
396	1200
398	1192
397	1190
426	1188
405	1187
408	1187
395	1186
409	1186
406	1184
407	1182
427	1180
394	1178
425	1176
424	1175

The resulting table showcases the low 400 nm wavelengths nearly identical to the wavelengths highlighted by the 0.8 mm comparison, quite different from the 1.6 mm and 3.6 mm recommended wavelengths. Further field testing will be required to see if the relationships dependent on film thickness or independent of film thickness are best suited for analysis. Or perhaps more importantly if the same wavelengths identified for solely beet concentrations are similar for beet-brine solutions starting with the 3.6 mm application calculated in Table 5.12.

Table 5.12 Beet-Brine 3.6 mm Highest Freq Wvl (nm) for Test 1 (February 16th)

16-Feb	22 mL
Wvl (nm)	Freq
560	1724
559	1723
561	1719
563	1718
562	1715
550	1714
569	1714
566	1712
567	1712
558	1711
564	1710
553	1709
556	1709
565	1709
557	1708
568	1708
570	1708
548	1705
554	1705
547	1703

The addition of salt to the beet juice relationships is not evidenced when analyzing the 20 most common points. The effects of the beet juice still dominate the visual spectrum and continue to be the greatest representation in change of concentration. At a solution thickness of 3.6 mm, the beet-brine relationships with increasing concentration seem to be most predominant in the yellow spectrum (565 – 590 nm), however following beyond the top 20 frequencies reveals it continues its coverage of the visual spectrum. Reducing the application thickness creates surprisingly little difference between the repeated wavelengths as shown in Table 5.13.

Table 5.13 Beet-Brine 1.6 mm Highest Freq Wvl (nm) for Test 1 (July 9th)

9-Jul	10 mL
Wvl (nm)	Freq
561	1776
547	1767
550	1766
548	1765
551	1765
560	1765
566	1765
552	1762
565	1762
564	1761
567	1761
568	1761
563	1760
553	1759
569	1759
562	1758
544	1755
545	1755
557	1755
556	1754

The frequency of the points has slightly increased, but the increase is less than 5%. Capturing the reflectance of the same material twice can generate differences greater than what is seen comparing 3.6 mm beet-brine to 1.6 mm. The wavelength range of prominent pairs however does not continue as reducing the thickness even further to 0.8 mm drastically changes which values dominate the top 20 repeated wavelengths as shown in Table 5.14.

.

Table 5.14 0.8 mm Highest Freq Wvl (nm) for (a) Test 1 (September 21st), (b) Test 2 (January 28th), and (c) the resulting matched values

21-Sep	5 mL
Wvl (nm)	Freq
429	1784
419	1781
430	1780
426	1774
427	1774
418	1773
428	1772
420	1769
425	1766
431	1765
421	1763
432	1763
437	1761
433	1759
438	1759
422	1757
424	1755
436	1754
417	1753
423	1749

(a)

+

28-Jan	5 mL
Wvl (nm)	Freq
418	1518
419	1518
417	1510
416	1493
420	1493
415	1483
2043	1480
427	1473
421	1472
426	1469
429	1466
435	1462
436	1462
428	1461
430	1456
423	1455
424	1455
414	1447
425	1446
422	1445

(b)

=

Repeated	5 mL
Wvl (nm)	Freq
419	1471
418	1470
417	1462
420	1451
416	1449
415	1440
421	1431
427	1430
426	1427
429	1421
428	1417
435	1416
423	1414
424	1414
430	1414
436	1414
414	1407
425	1406
422	1404
434	1398

(c)

The final comparison of 0.8 mm shows two sets of lab testing on different days. Again, the red text in the first column and the red outline in the second column can be used to show how much of the top 20 changed with repetition. The beet-brine relationships were by far the most consistent and therefore show the most promise moving forward into field testing. Of course, this presumes that, at least operationally, a beet solution is always used in the winter maintenance efforts.

The final test for beet-brine solution is a comparison regardless of film thickness in Table 5.15.

Table 5.15 Beet-Brine Wavelength Pairs Successful Regardless of Film Thickness

Extracted	all volumes beet-brine
Wvl (nm)	Freq
417	1053
416	1041
424	1031
418	1027
423	1026
422	1014
421	1012
420	1005
419	1000
382	998
425	986
415	985
426	958
381	936
432	935
431	930
438	925
389	923
466	903
427	899

Much like the pure beet solution, the beet-brine solution (Table 5.15) is dominated not only by similarities to 5 mL beet-brine solution (Table 5.14) but also very similar wavelengths to the extracted 5 mL beet solution (Table 5.10) and extraction of wavelengths regardless of film thickness (Table 5.11). Conversely no wavelengths in the top 20 wavelengths are shared by any of the brine solutions. Additionally, the four surviving wavelength pairs found in Table 5.7 from brine regardless of film thickness are nowhere to be found in the full data frame of Table 5.15.

.

5.4. Considerations for Field Testing

Ultimately, the goal of the lab portion of the project is to prepare for field validation and testing of the relationships, techniques, and understanding gathered in a lab setting. Of the two prime constituents, beet juice and sodium chloride, several different wavelengths were identified as important signifiers of material presence. However, the number of points and frequency and reliability of occurrence for the beet signifiers far outweighed the brine signifiers. The beet signifiers even have the possibility of overwhelming or drowning out some of the brine signifiers deeper in the NIR reflectance range.

For brine solutions, the wavelengths that experienced the most changes as thickness was changed were in the NIR wavelength range. This is problematic due to the distortion in the NIR caused by absorption of NIR wavelengths by water. Regardless, several sets of wavelengths were found to be accurate trackers of changes in salt concentration the lab setting. With temperature, lighting, and concentrations controlled, trends were found for 3.6 mm thick brine solutions heavily in the 2000s with dominating 871 repetitions of the 2120 nm wavelength and scattered linear relationships in the late 1200 wavelengths. For 1.6 mm thick brine solutions there was no longer a strong outlier, however there was very strong coverage scattered throughout the 1400-1600s with repetitions exceeding 1000. For 0.8 mm thick brine solutions the best signifiers of changing salt concentration zeroed in on the low 1400 nm wavelengths with a maximum repetition of 111. The identification of points for salt concentration as film thickness decreases is a fantastic indicator that will be carried over into the field phase of this study. Of the 111 repetitions tested, the majority are adjacent to each other, creating a large portion of a curve that could be sampled and compared to the low 1400 nm wavelengths for more thorough and precise testing. Since the 0.8 mm thickness is the thinnest application creatable in the lab, its

wavelengths have the greatest likelihood of being the wavelengths that will be found in the field. A final analysis compared all points and extracted only the duplicated wavelength pairs that successfully demonstrated a linear change in salt concentration and reflectance values. This analysis only produced four wavelength pairs centering around the 1820 nm wavelength and the 1555 nm wavelength. These points will also be of interest for identifying salt presence in the field.

For beet carbohydrate the changes that were maximized were quite different from the colorless brine solutions. Red beet carbohydrate is visually distinct. Adding beet juice greatly changes the color of the liquid film and as such the greatest changes denoted in the spectral imaging results are in the visual spectrum. For 3.6 mm thick beet solutions, the most common points denoted to have a linear relationship with concentration changes were in the 600 and 1600 nm wavelength. When compared to about 75% of the recorded spectra, the 600 nm wavelength successfully identified changes in concentration. The results of the 3.6 mm beet film thicknesses were mimicked by the 1.6 mm thickness with the key difference of most common wavelengths shifted to mid-600s nm wavelengths instead of low 600 nm wavelengths. However, when looking at the low 600 nm directly, the data reveals the number of repetitions for the wavelengths in the 3.6 mm film slightly increased rather than decreasing as expected. For the 0.8 mm beet thickness the most repeated wavelengths again shifts inside the visual spectrum down to the 400 nm wavelengths. This shift is much more significant and since the 0.8 mm thickness is closest to what will be experienced in actual winter roadways the wavelengths gathered from it will be the ones most anticipated to be reliable field indicators. As a final comparison, the differences regardless of film thickness are tested, the resulting values again showcase the low

400 nm wavelengths with very little loss in repetition, a decrease from maximum of 1400 repetitions to 1200 repetitions which is promising for field applications.

For beet-brine mixtures the visually significant beet signature far outweighs the much less significant brine signatures. In addition, the spectral signatures for beet-brine mixtures is extremely similar to the beet solutions without the salt. The main difference for this mixture is seen in the 3.6 mm and 1.6 mm beet-brine solutions where the wavelengths that experienced greatest change with respect to concentration were located in the mid-500 nm wavelengths. Very little difference is seen between the 3.6 mm and 1.6 mm thickness beet-brine wavelength with most pairs around the mid 500 nm wavelengths. Analyzing the 0.8 mm thicknesses shows nearly identical relationships as the beet solutions with a small range in the low 400 nm wavelengths but a slightly smaller number of repetitions close to about 100 repetion smaller on average. The similarities continue with the final comparison of all beet brine regardless of film thickness repeating most of the values found in the 0.8 mm beet brine thickness, thereby also being very similar to the beets 0.8 mm film thickness and the comparison regardless of film thicknesses. A key section of wavelengths to consider will be the 400 nm wavelengths for any concentration involving beet juice. In conclusion, many of the signifiers for beet were present in beet brine but some of the brine signifiers actaully dissappeared suggesting that brine monitoring and identification will be much harder in the field than beet identification.

5.5. Boxplot and ANOVA Testing

5.5.1. Brine Relationships

Using the brine relationships established in the lab setting, where the 1406-1408 nm wavelengths compared with the 1560-1640 nm wavelengths produced usable relationships to demonstrate changing sodium chloride concentration. Additionally, the pairs surrounding 1820 nm and 1855 nm were generated as usable points regardless of deicer amount applied in the lab, however with the thinner applications done in the field, these pairs indicated that the statistical differences were too small for analysis in field use. Of the available brine points, 1560-1640 nm wavelengths were broken down from 1560 to 1590 iterated by 1 and the graphs are spaced out in gaps of 5 nm to show how the relationship is either maintained or changes at the corresponding pairs. Sets of four different pairs and a corresponding ANOVA is conducted for the different types of comparison shown in this section. For the lab setting, four sets of boxplots were produced to show changes in reflectance (see Figure 5.8 below).

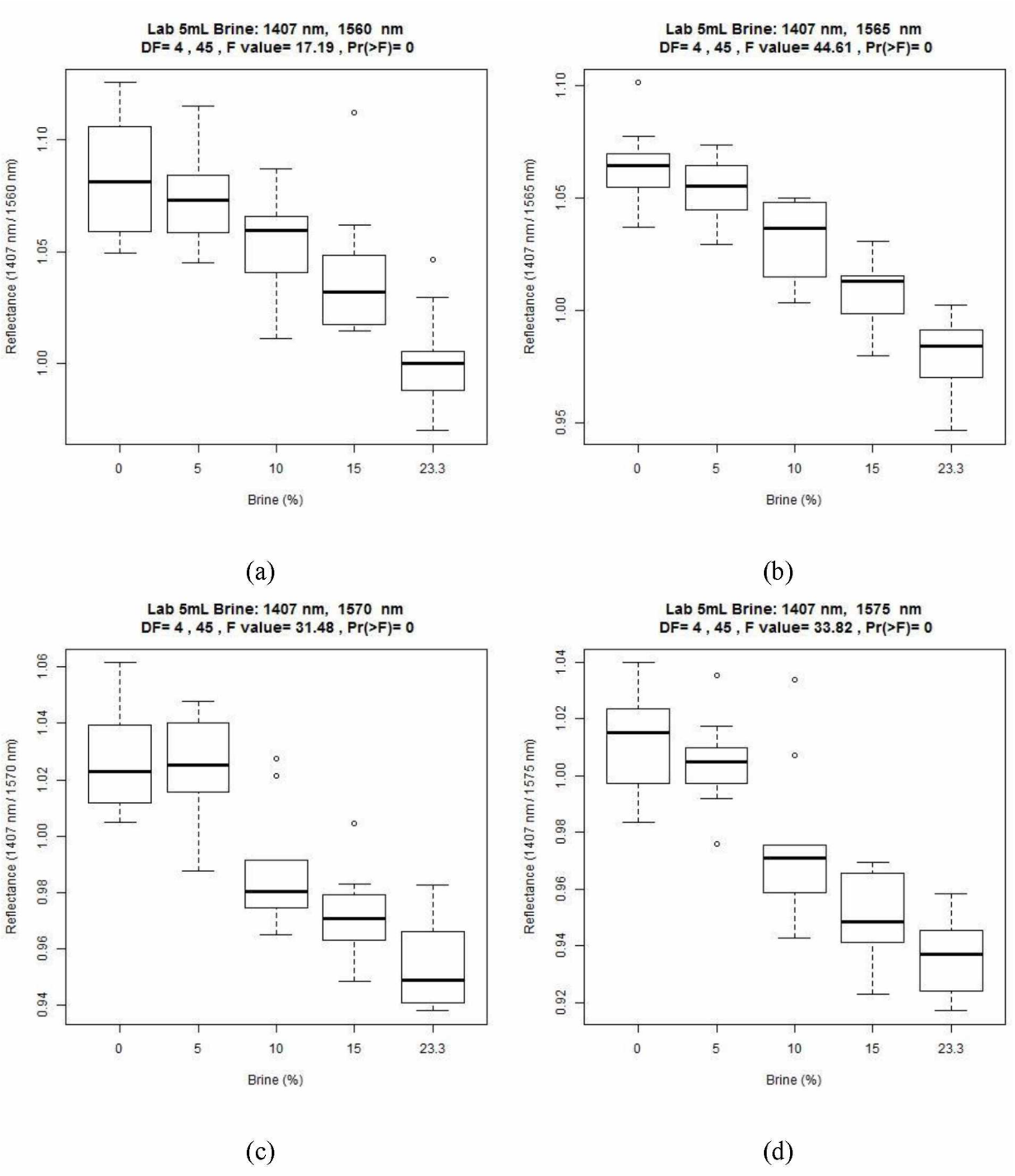

Figure 5.8 Lab Generated Brine Boxplots (a) through (d)

The largest divergence in bandmath values seemed to occur at the transition from 5% saline to 10% saline as seen in Figure 5.8c and Figure 5.8d.

To account for the effects of the dynamic backgrounds on reflectance ratio values, the recorded concentrations and volumetric brine applications were normalized by their respective backgrounds obtained before application. The 0.5 mL application, equivalent to 8.4 – 39.1 gallons per lane mile and most representative of DOT&PF application rates, is depicted below in Figure 5.9.

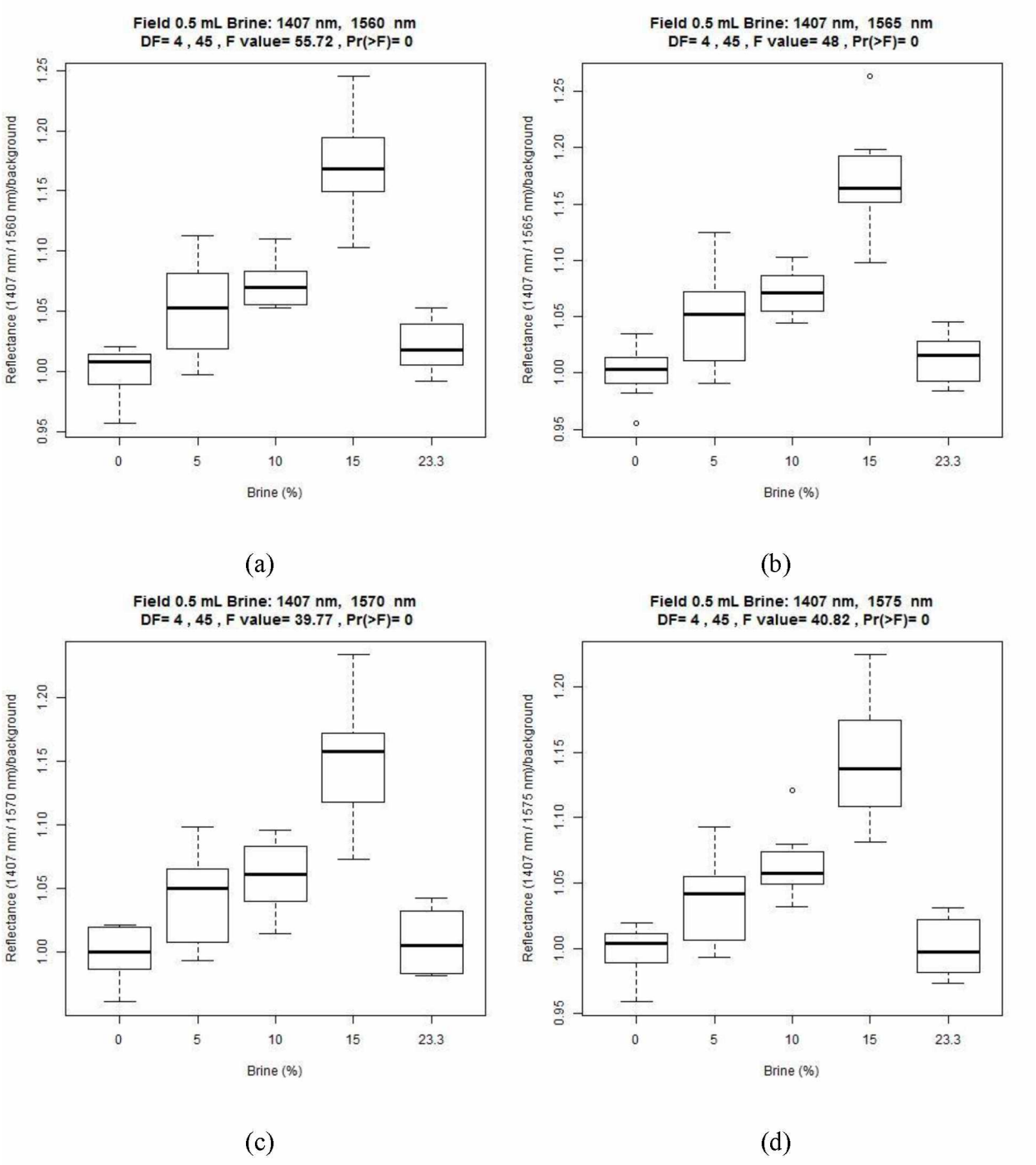

Figure 5.9 0.5 mL Application Field Well-Maintained Pavement

The ANOVA test for 1407 nm compared to 1560 nm showed there was a statistically significant effect of changing concentration of deicing compound at the $p<0.05$ level for the five concentrations [$F(4,45) = 55.72$, $p < 0.001$]. Conducting a pairwise comparison using t-tests

shows that all the different concentrations were statistically significantly different except for 5% brine and 10% brine which had p=0.11. The next set of values are the 1 mL applications which are equivalent to 16.8 – 78.1 gal/ln mile in terms of DOT&PF liquid brine application.

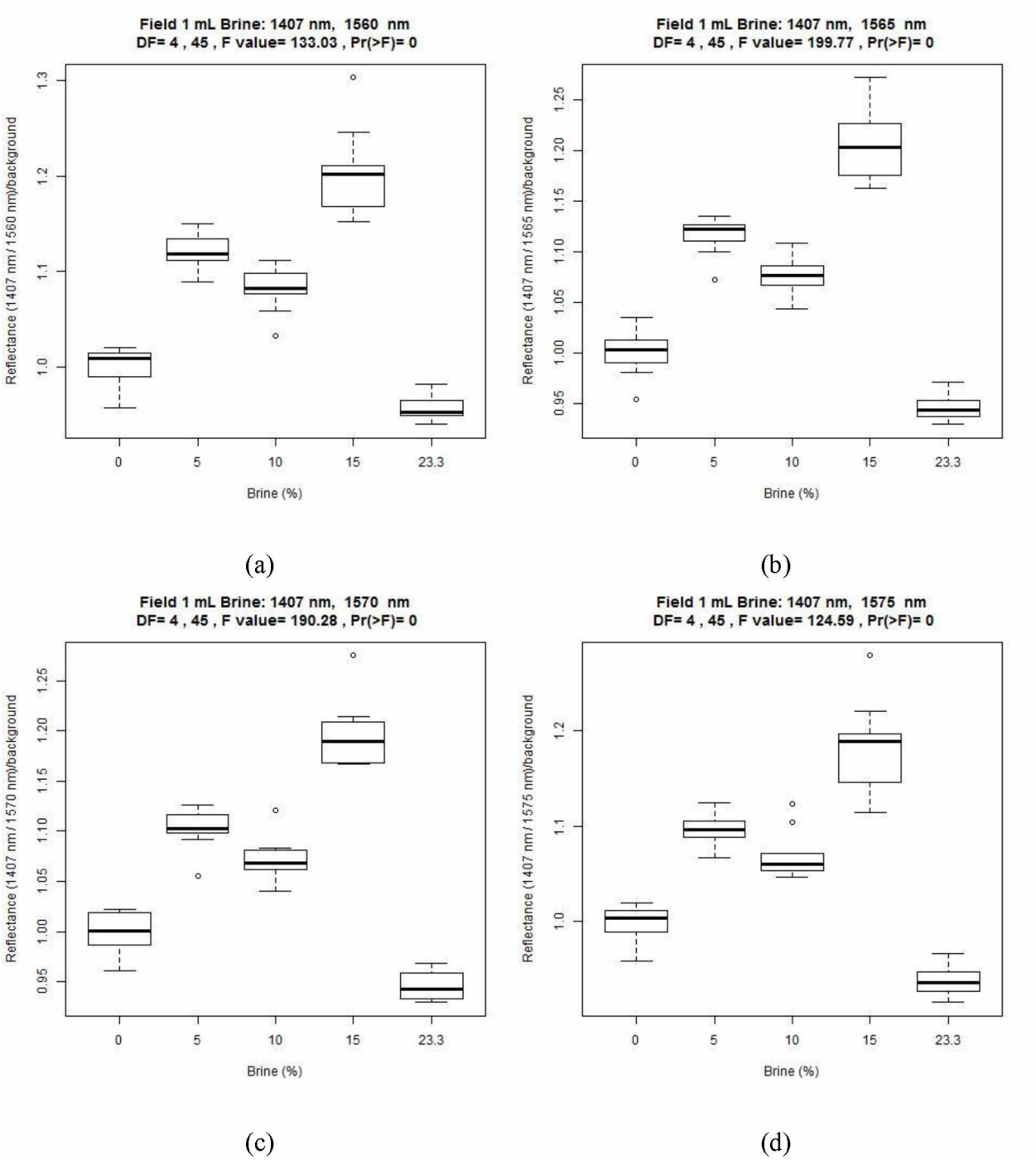

Figure 5.10 1 mL Application Field Well-Maintained Pavement (a) through (d)

The ANOVA test for 1407 nm compared to 1560 nm showed there was a statistically significant effect of changing concentration of deicing compound at the $p<0.05$ level for the five concentrations [$F(4,45) = 133.03$, $p < 0.001$]. Conducting a pairwise comparison using t-tests shows that all the different concentrations were statistically significantly different. There appears to be no valid trend beyond the 23.3% application having a lower band math total than the original value. The next set of figures correspond to 1.37 – 6.39 mg/cm^2.

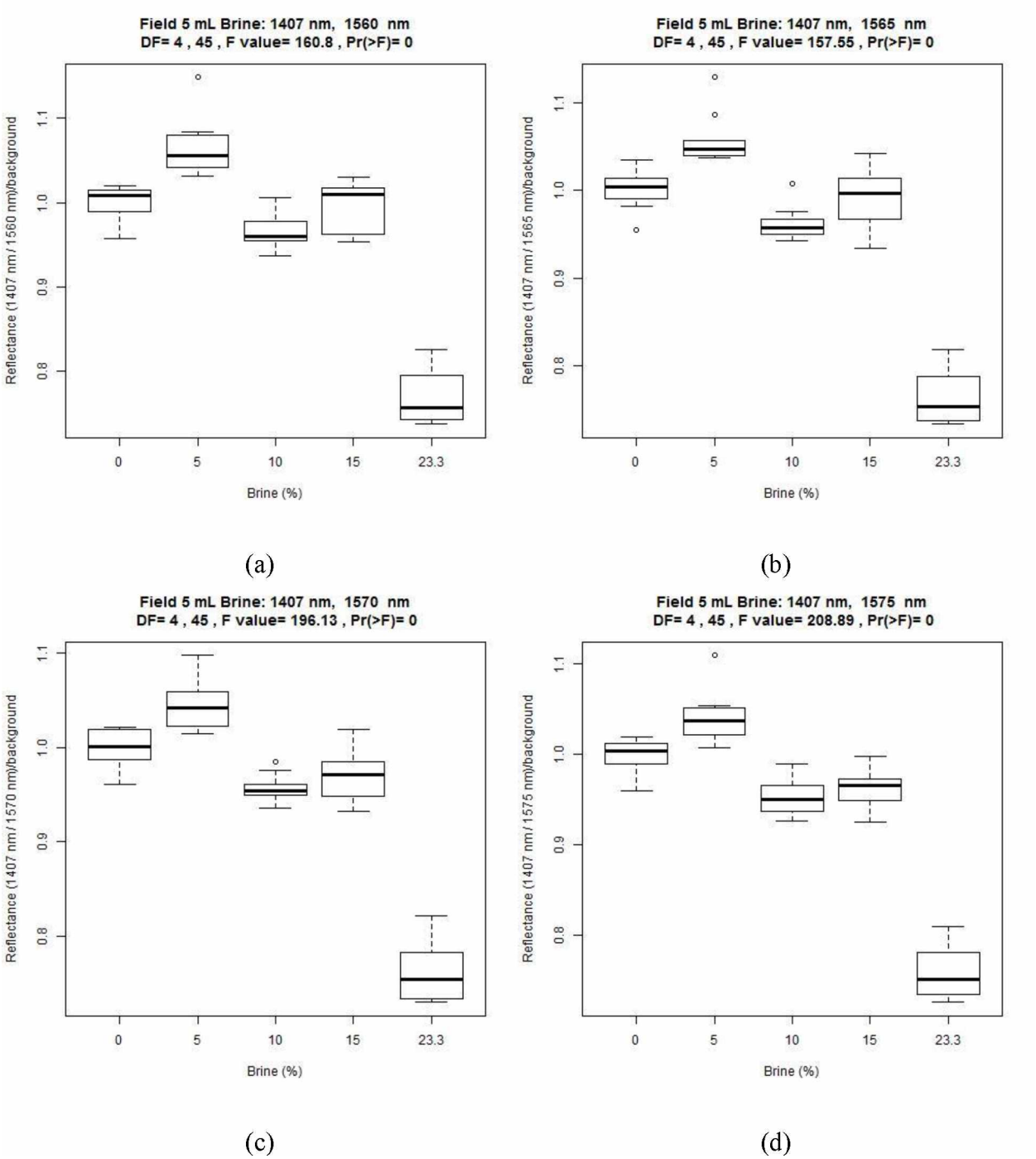

Figure 5.11 5 mL Application Field Well-Maintained Pavement (a) through (d)

The ANOVA test for 1407 nm compared to 1560 nm showed there was a statistically significant effect of changing concentration of deicing compound at the $p<0.05$ level for the five concentrations [$F(4,45) = 160.8$, $p < 0.001$]. Conducting a pairwise comparison using t-tests shows that all the different concentrations were statistically significantly different except for the

0% brine compared to the 15% brine compound with a p=0.65. The trend is starting to approach what was recorded in the lab, there appears to be a noticeable drop in bandmath value transitioning from 5% to 10% and a much more significant drop transitioning from 15% to 23.3%. The next set of figures correspond to 2.74 – 12.77 mg/cm^2.

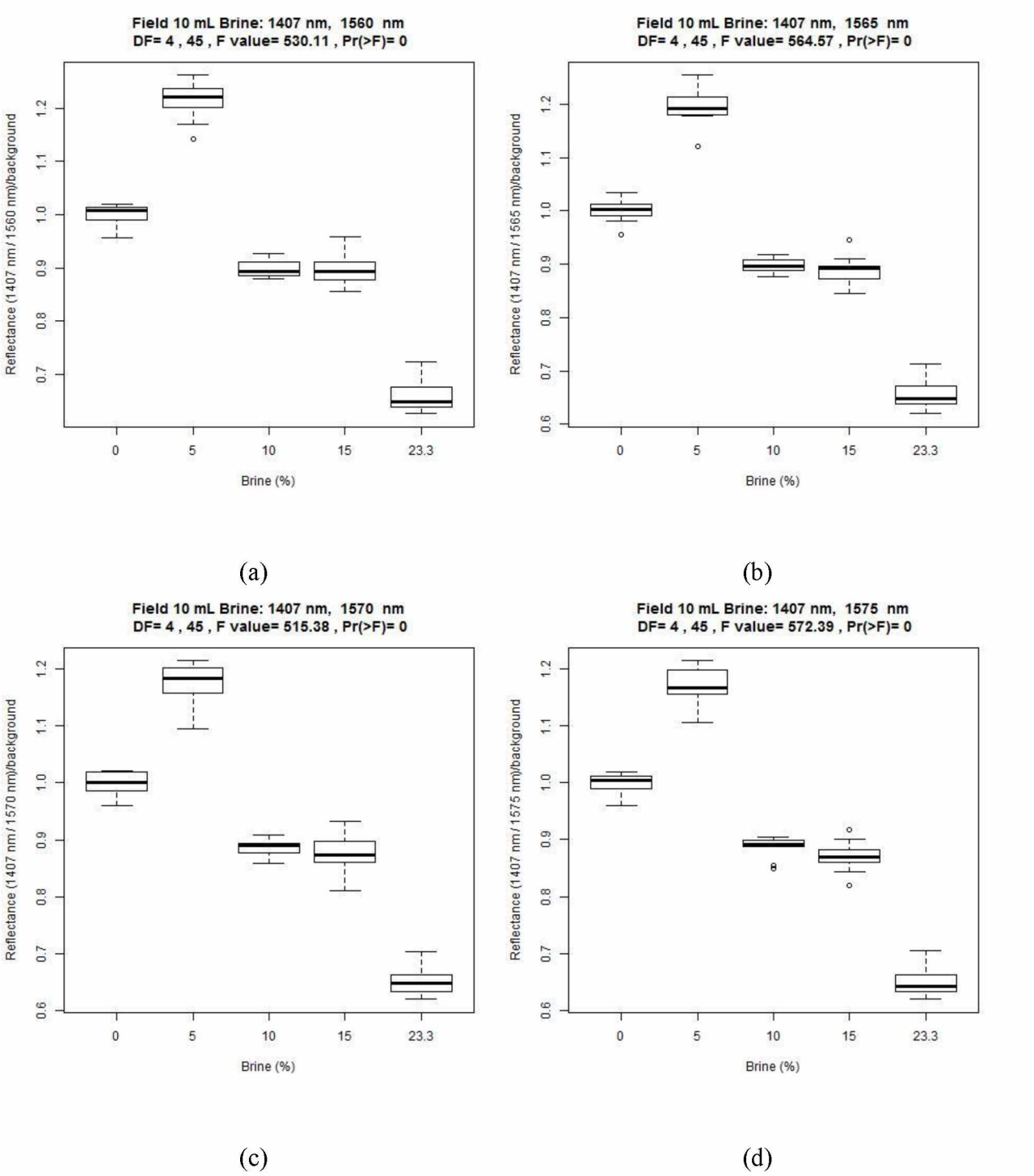

Figure 5.12 10 mL Application Field Well-Maintained Pavement (a) through (d)

The ANOVA test for 1407 nm compared to 1560 nm showed there was a statistically significant effect of changing concentration of deicing compound at the $p<0.05$ level for the five concentrations [$F(4,45) = 530.11$, $p < 0.001$]. Conducting a pairwise comparison using t-tests

shows that all the different concentrations were statistically significantly different except for the 10% brine compared to the 15% brine compound with a p=0.96. Now in Figure 5.12 there is a significant change transitioning from 5% to 10%, practically no change from 10% to 15% and another equally significant change from 15% to 23.3% brine. Comparing concentrations at different volumes will eliminate the need for normalizing to separate backgrounds as all applications will have the same background. Ideally these trends will follow changing salt amounts as demonstrated in the lab trials and eliminate the dynamic backgrounds found in the field.

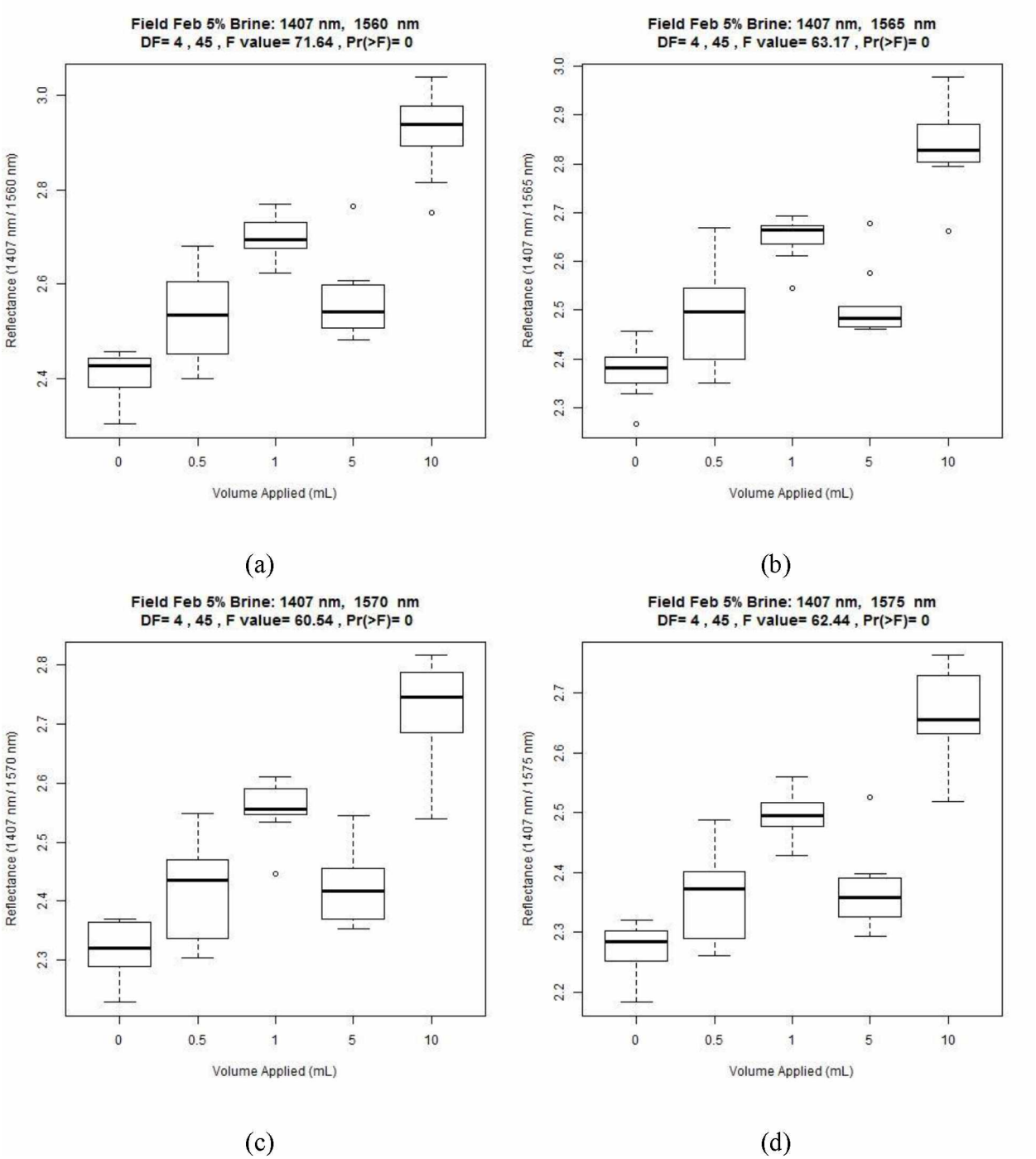

Figure 5.13 5% Concentration Application Field Well-Maintained Pavement (a) through (d)

The ANOVA test for 1407 nm compared to 1560 nm showed there was a statistically significant effect of changing concentration of deicing compound at the $p<0.05$ level for the five concentrations [$F(4,45) = 71.64$, $p < 0.001$]. Conducting a pairwise comparison using t-tests shows that all the different concentrations were statistically significantly different apart from the

0.5 mL 5% brine compared to the 5 mL 5% brine compound with a p=0.48. The 5% comparison shown in Figure 5.13 shows a much more promising relationship between changing salt presence and reflectance value. However, the trend line has a positive slope rather than a negative slope as demonstrated in the lab data and therefore expected in the field data. One might intuit that increasing the concentration should increase the intensity of the relationship, but at concentrations as low as 5% brine the highest concentration no longer depicts the lowest product of band math. The trend returned to negative when comparing concentrations greater than 5% as shown below in Figure 5.14.

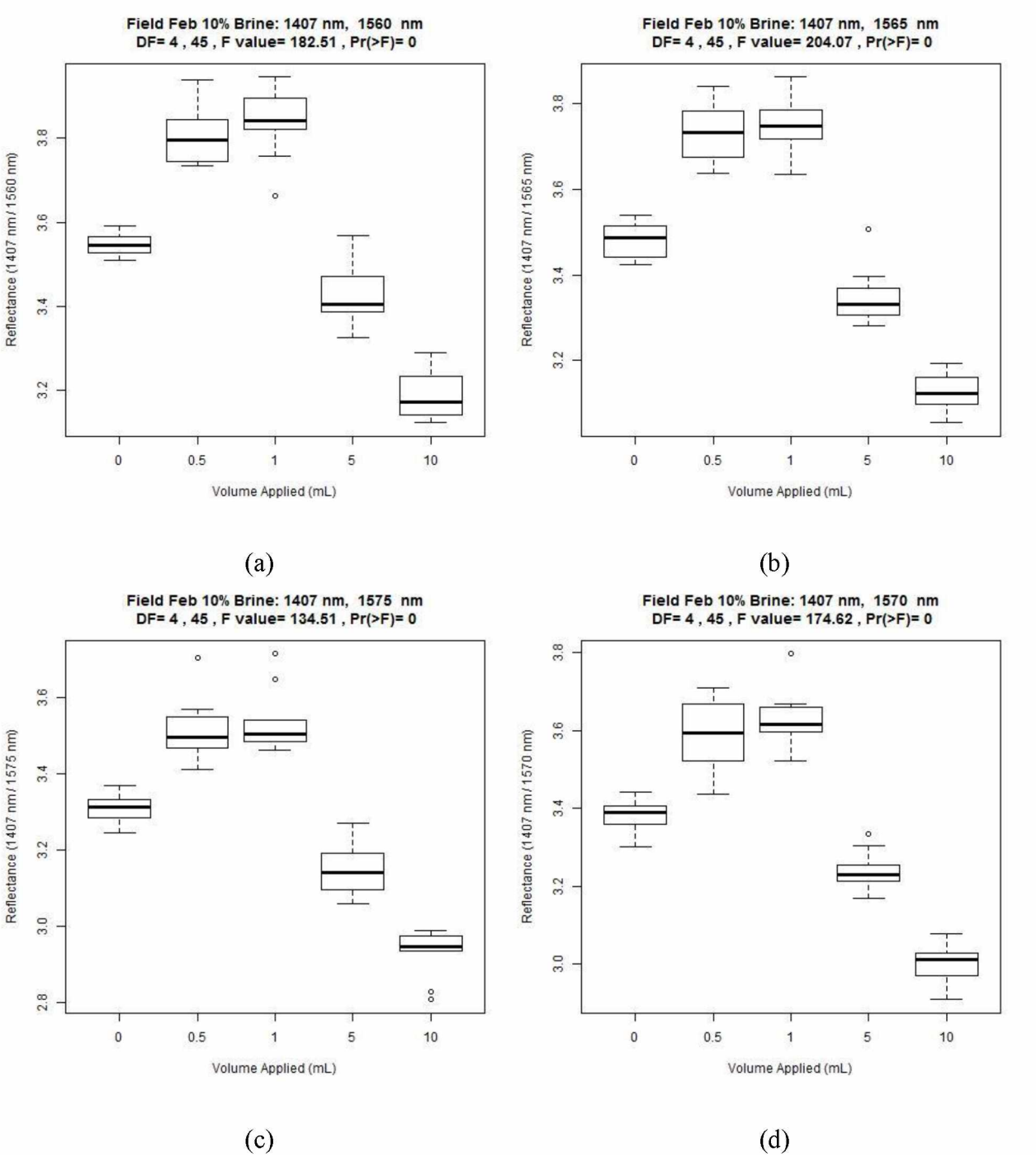

Figure 5.14 10% Concentration Application Field Well-Maintained Pavement (a) through (d)

The ANOVA test for 1407 nm compared to 1560 nm showed there was a statistically significant difference between concentrations of deicing compound [$F(4,45) = 182.51$, $p < 0.001$]. Conducting a pairwise comparison using t-tests shows that all the different concentrations were

statistically significantly different except for the 0.5 mL 10% brine compared to the 1 mL 10% brine compound with a p=0.39. The bandmath product increased from 0 to 1 mL applications, but after 5 mL the trend began to sharply decrease much like the lab generated data. Further increasing the concentration of deicer applied should theoretically magnify this trend further as demonstrated by Figure 5.15.

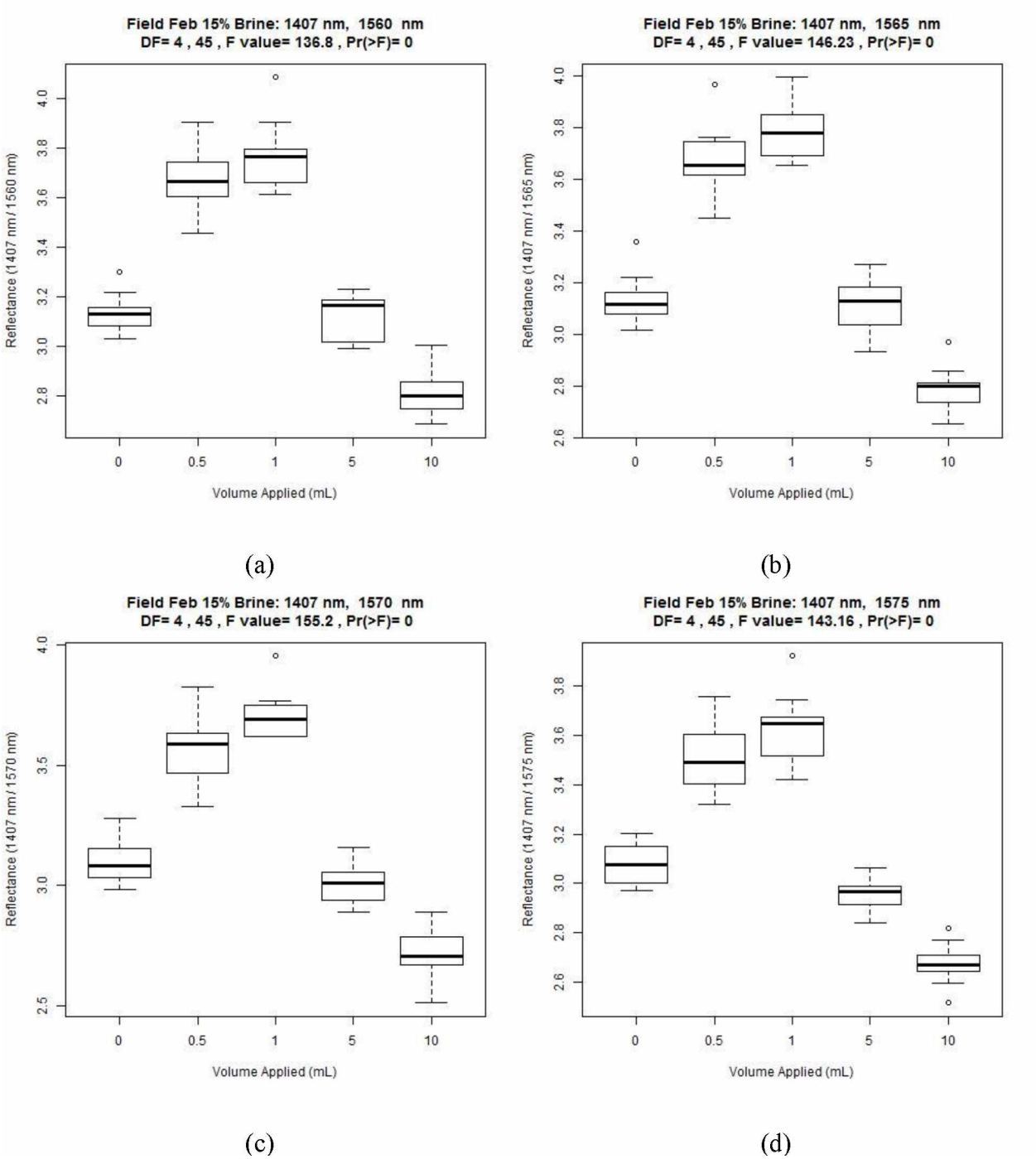

Figure 5.15 15% Concentration Application Field Well-Maintained Pavement (a) through (d)

The ANOVA test for 1407 nm compared to 1560 nm showed there was a statistically significant difference between concentrations of deicing compound [$F(4,45) = 136.8$, $p < 0.001$]. Conducting a pairwise comparison using t-tests shows that most concentrations were statistically

significantly different except for the 0.5 mL 15% brine compared to the 1 mL 15% brine compound with a p=0.15 and the 0 mL 15% brine compared to the 5 mL 15% brine compound with a p=0.69. On top of having more than one comparison being not significantly different the trend did not improve by increasing from 10% brine to 15% brine. Now, at 15% brine, the curve slants upward until a significant amount of brine is applied (5 mL) and the 5 mL itself is not statistically different from no application.

The highest concentration tested in the field setting is the 23.3% brine application shown below in Figure 5.16.

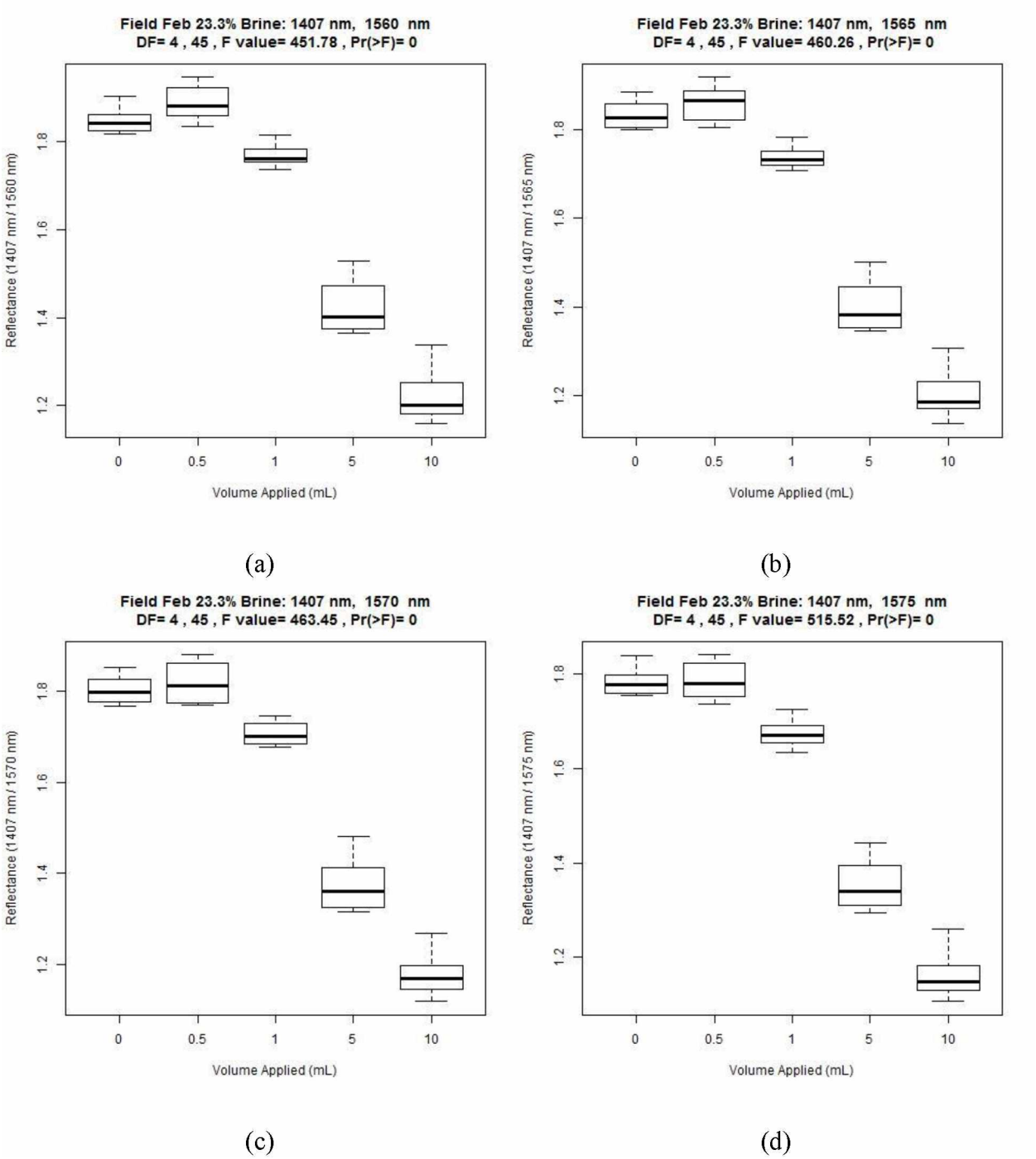

Figure 5.16 23.3% Concentration Application Field Well-Maintained Pavement (a) through (d)

The ANOVA test for 1407 nm compared to 1560 nm showed there was a statistically significant difference between concentrations of deicing compound [$F(4,45) = 451.78$, $p < 0.001$]. Conducting a pairwise comparison using t-tests shows that all concentrations were statistically significantly. The relationships indeed strengthen as amount applied is increased, now with 0 and

0.5 mL being the only volumes which are almost statistically similar and a strong trend going for 0 and 0.5 to 1, to 5, to 10 mL.

5.5.2. Beet-Brine Relationships

Identification of beet-brine relationships in the lab revealed a litany of relationships mainly due to the visual impact that changing beet-brine concentration. The changes in the visual spectrum made the range of working relationships vast with approximately 1700 matching pairs for each wavelength located in the visual spectrum as established by lab generated data. Of the analyzed relationships, the graphs presented here utilize the most commonly found wavelength of 418 nm which was then compared to the rest of the wavelengths from 350 to 2500 iterating by 25 nm. The section of best working relationship, boxplots which had most statistically significant difference as found by ANOVA, showcases very strong relationships between the 525 to 1350 and an assortment of four spread out by 100 nm are shown below in Figure 5.17.

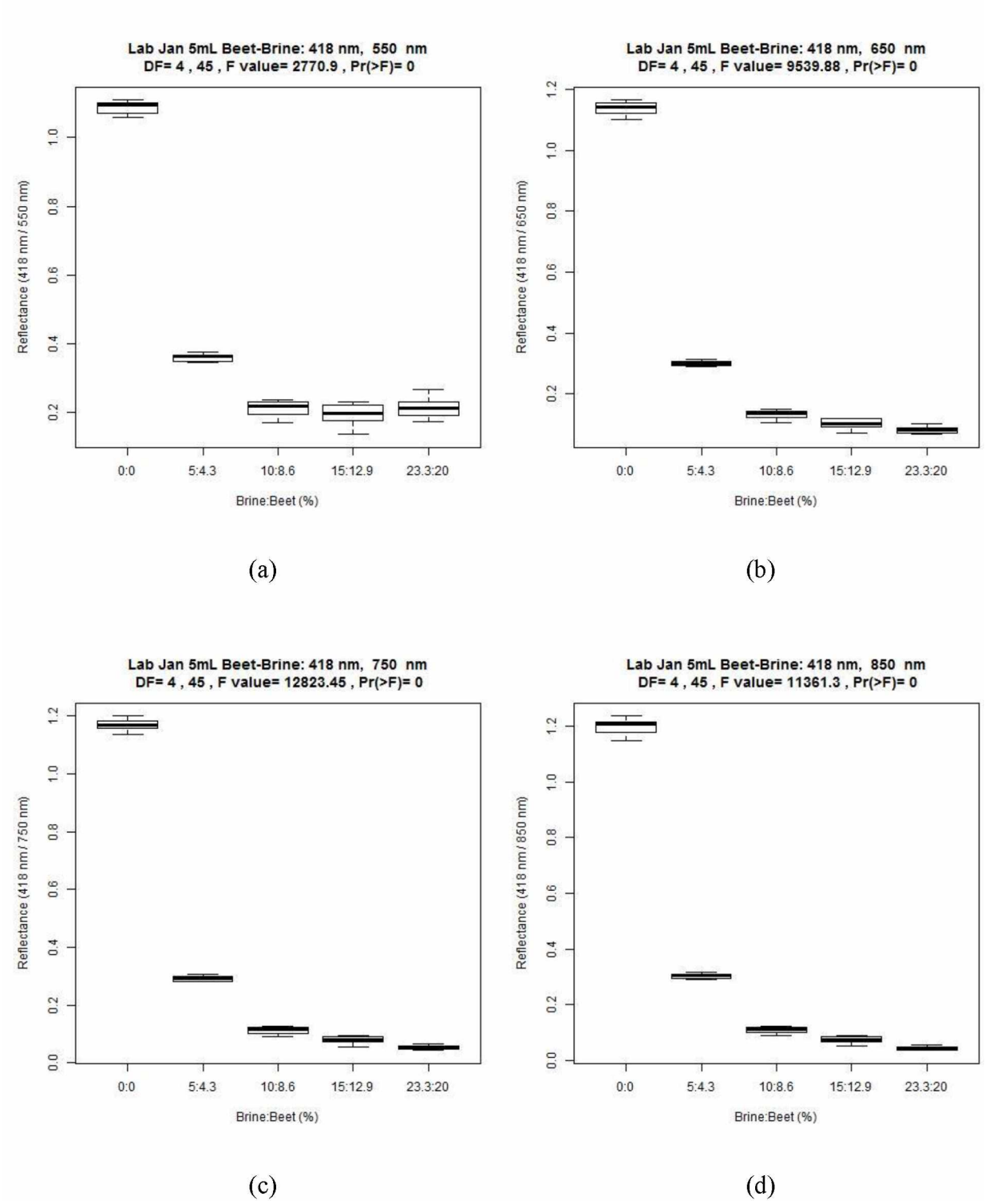

Figure 5.17 Lab Generated Beet-Brine Boxplots (a) through (d)

The ANOVA test for 418 nm compared to 850 nm showed there was a statistically significant difference between concentrations of deicing compound [$F(4,45) = 11361$, $p < 0.001$] in the lab

setting. Conducting a pairwise comparison using t-tests exhibited that all concentrations were statistically significantly different.

The backgrounds for the beet-brine applications, much like the brine applications, are a source for inconsistency in reflectance values for relationship comparisons. Since this uncertainty could possibly be from ice formations, surface striations, or other inconsistencies the backgrounds will be normalized out to solidify trends. Background comparisons are shown in the figures below.

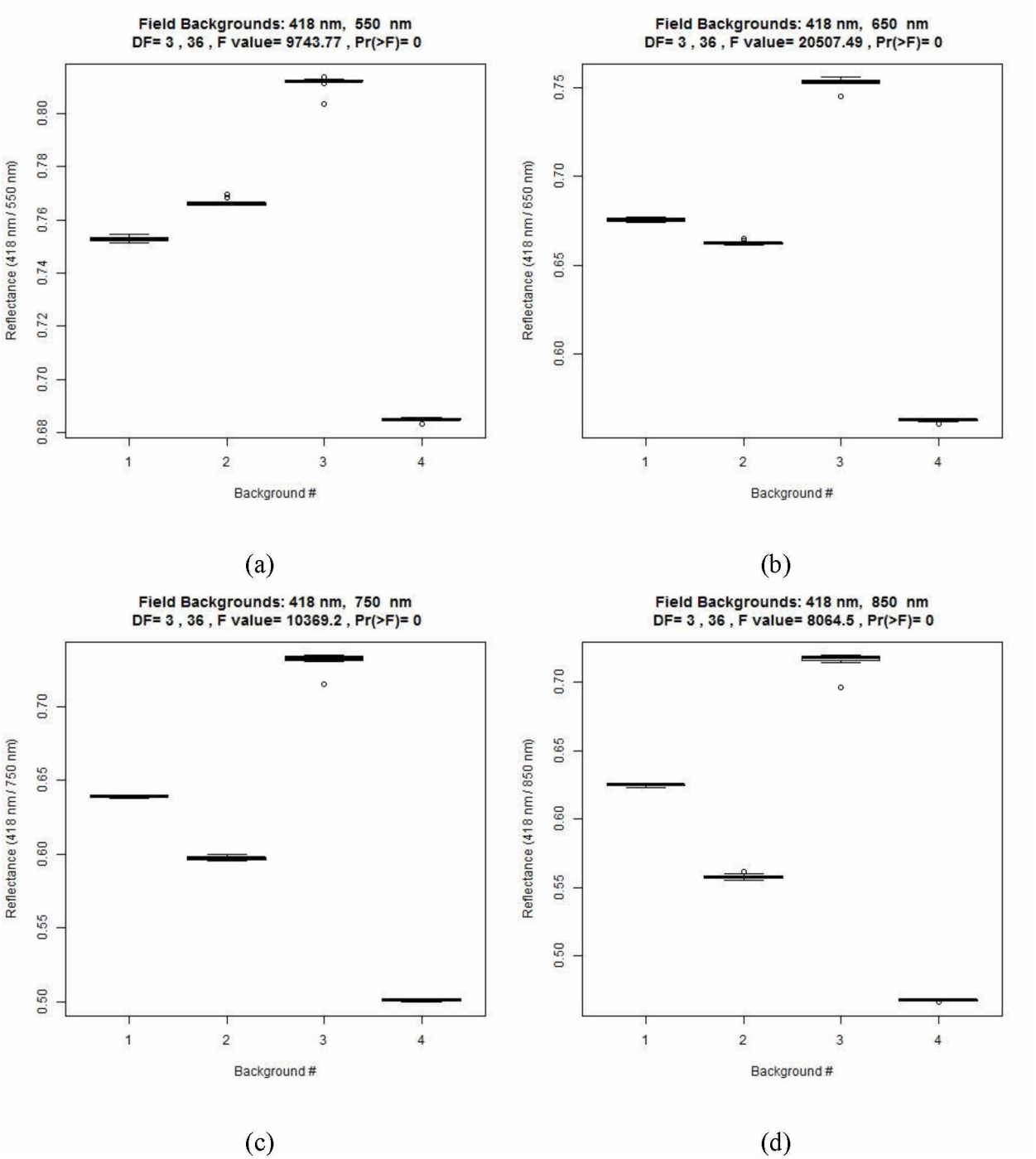

Figure 5.18 Good Condition Asphalt Pavement Beet-Brine Background (a) through (d)

Analysis at the smallest beet-brine application rate recorded in the field, 0.5 mL per 6-inch diameter area, are shown below in Figure 5.19. The 0.5 mL application at maximum concentration is slightly below the maximum rate applied according to AKDOT with the smallest concentration representative of dilution of applied solution.

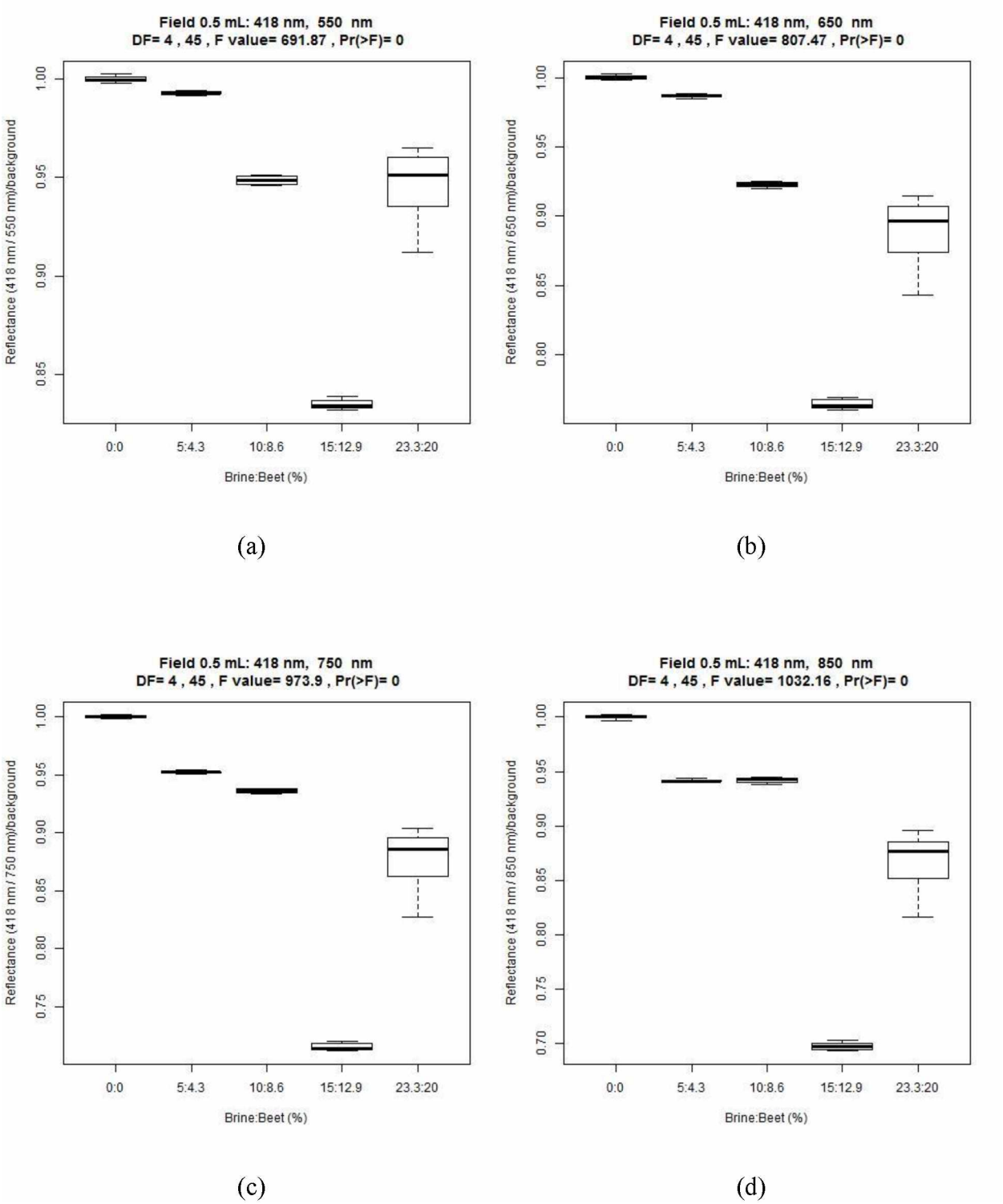

Figure 5.19 0.5 mL Beet-Brine Field Well-Maintained Pavement (a) through (d)

Looking at the ANOVA test for 418 nm compared to 850 nm showed there was a statistically significant difference between concentrations of deicing compound [$F(4,45) = 1032.16$, $p <$

0.001]. Conducting a pairwise comparison using t-tests shows that all the different concentrations were statistically significantly different apart from 10% brine 8.6% beet mixture and 5% brine 4.3% beet mixture which had p=0.64. The trend was expected to be continuous with higher concentration applications producing lower reflectance values however this trend was not recorded. Instead, there is a sharp dip at 15% brine 12.9% beet followed by a resurgence and much larger spread at 23.3% brine 20% beet. This is quite different from lab experimentation and the suspected cause is a combination of the elements that are no longer held constant in a field setting, most predominately initial background reflectance. The wide variation is suspected to be caused by the wild differences in background on a hyperspectral level and the associated normalization done to correct the differences. Increasing the volumetric application, doubling to a 1 mL application over a 6-inch diameter area, are shown below in sets of boxplots in Figure 5.20.

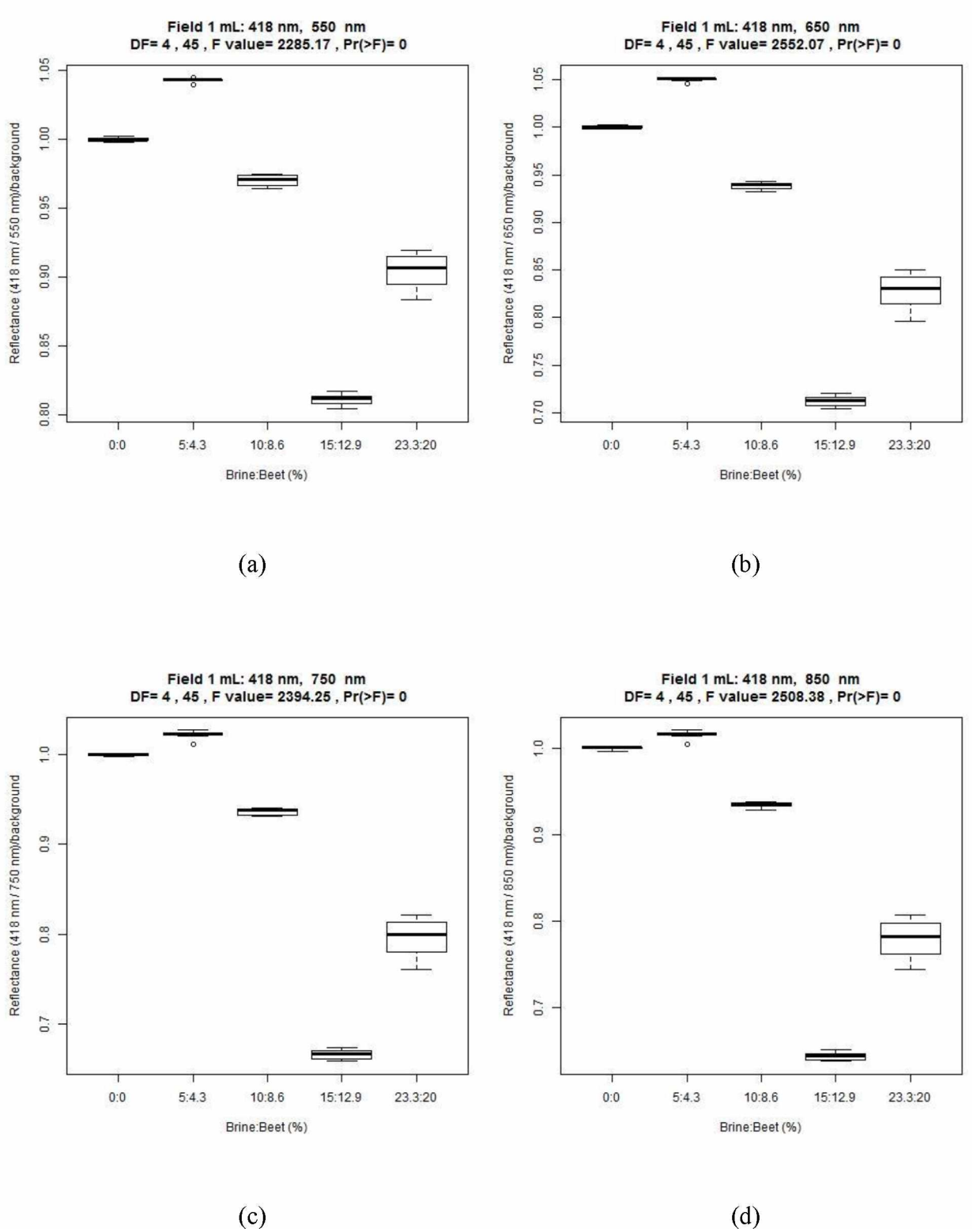

Figure 5.20 1 mL Beet-Brine Field Well-Maintained Pavement (a) through (d)

A comparison of the 418 nm wavelength to 850 nm resulted in a statistically significant difference [$F(4,45) = 2508.4$, $p < 0.001$]. The pairwise comparison indicates that all the different concentrations were statistically significantly different, however the trend among the reflectance values as concentration increases seems to have deteriorated even though the volume of the applications have increased. The trend of 5% brine 4.3% beet having a higher reflectance value compared to its background is not present at higher wavelength comparisons such as comparing 418 nm to 1050 nm. At these higher values the trends shown in Figure 5.19 are mirrored. Further increasing the volumetrics to 5 mL per 6-inch diamter area should theoretically increase the relationships demonstrated in the boxplots. The boxplots are shown below in Figure 5.21.

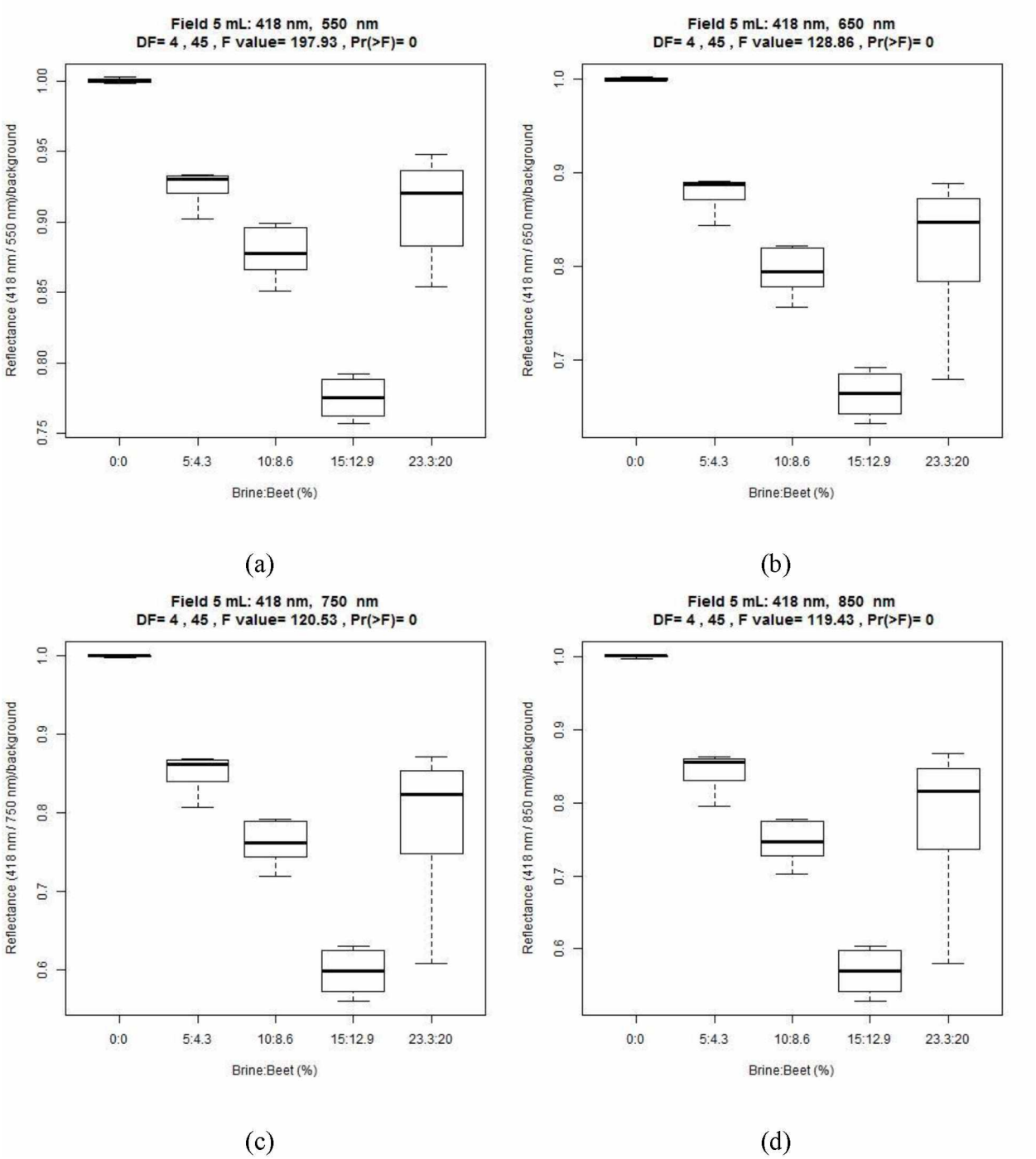

Figure 5.21 5 mL Beet-Brine Field Well-Maintained Pavement (a) through (d)

A comparison of the 418 nm wavelength to 850 nm resulted in a statistically significant difference [$F(4,45) = 119.43$, $p < 0.001$]. Conducting a pairwise comparison using t-tests shows that the majority of different concentrations were statistically significantly different, with the exception of the 5% brine 4.3% beet compared to the 23.3% brine 20% beet having a p=0.06 and

the 10% brine 8.6% beet compared to the 23.3% brine 20% beet having a p=0.26. This lack of statistically significant difference likely stems from the wider range of reflectance values. A problem that developed as the application rates approached values exponentially larger than the AKDOT&PF prescribed amount was compound migration. This was especially true the higher the concentration, which is shown by the increasing box plot size as concentration increases, at a 5 mL application at 23.3% brine 20% beet the chemicals migrated swiftly off the application site due to melt, uneven asphalt pavement, and surface pattern of asphalt pavement.

The highest volumetric amount applied in the field was 10 mL over a 6-inch diameter area which is equivalent to about 2/3 the thinnest film thickness recordable in the lab. At 10 mL applications, too much of the material was leaving the site and thicker applications would not be sustainable. The boxplots are shown below in Figure 5.22.

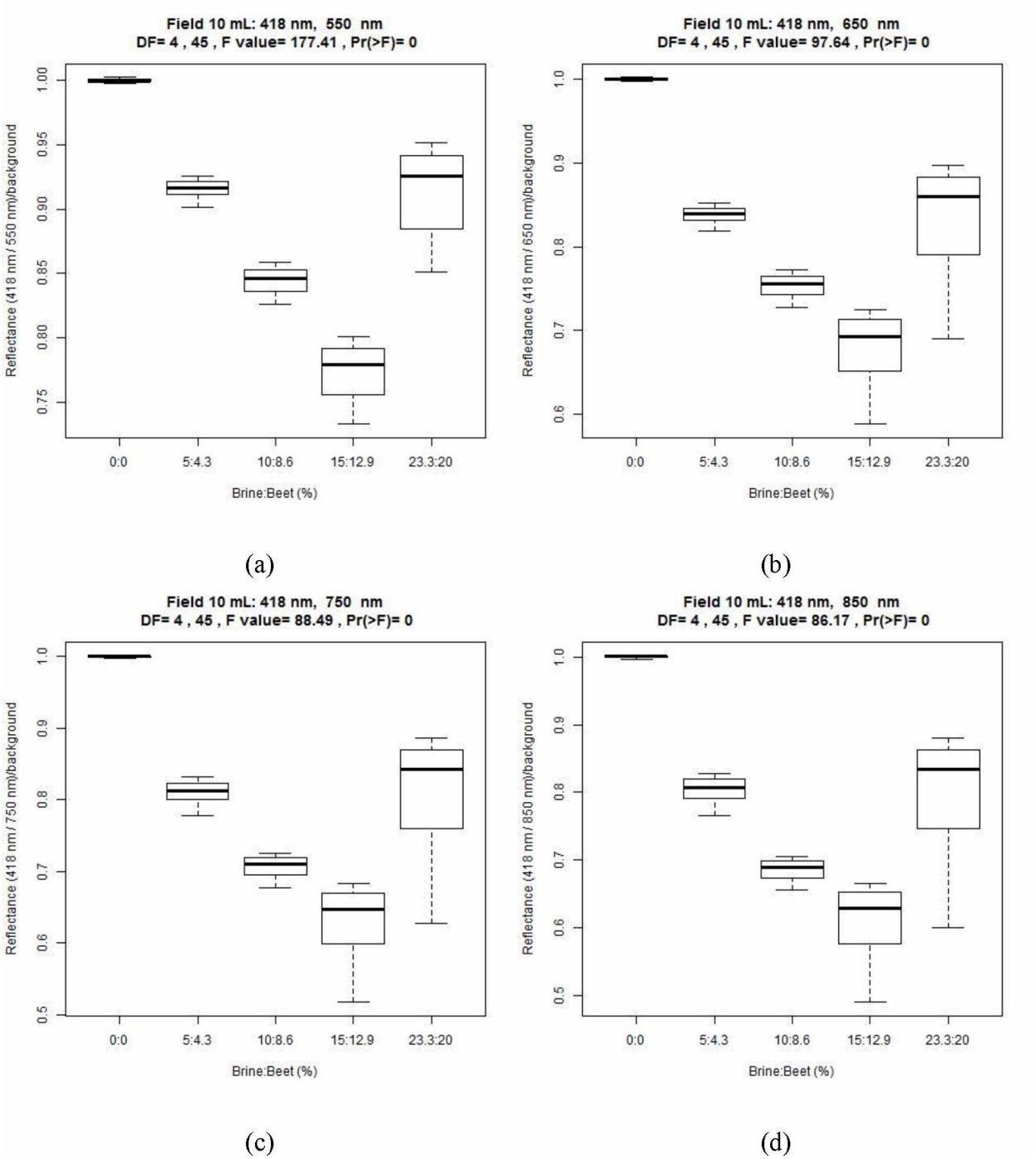

Figure 5.22 10 mL Beet-Brine Field Well-Maintained Pavement (a) through (d)

A comparison of the 418 nm wavelength to 850 nm resulted in a statistically significant difference [$F(4,45) = 86.17$, $p < 0.001$]. Conducting a pairwise comparison using t-tests shows that all of the concentrations were statistically significantly different except the 5% brine 4.3% beet compared to 23.3% brine 20% beet with p=0.80. The trend is continued from previous

iterations of field analysis now with the 15% brine 12.9% beet and 23.3% brine 20% beet having an even wider range of reflectance values likely due to increased material migration.

To diminish the effects of changing background and better explore the relationships generated, the materials were compared with changing volumes but constant concentration. The comparisons begin with the weakest concentration and increase from there starting with 5% brine 4.3% beet solution as shown below.

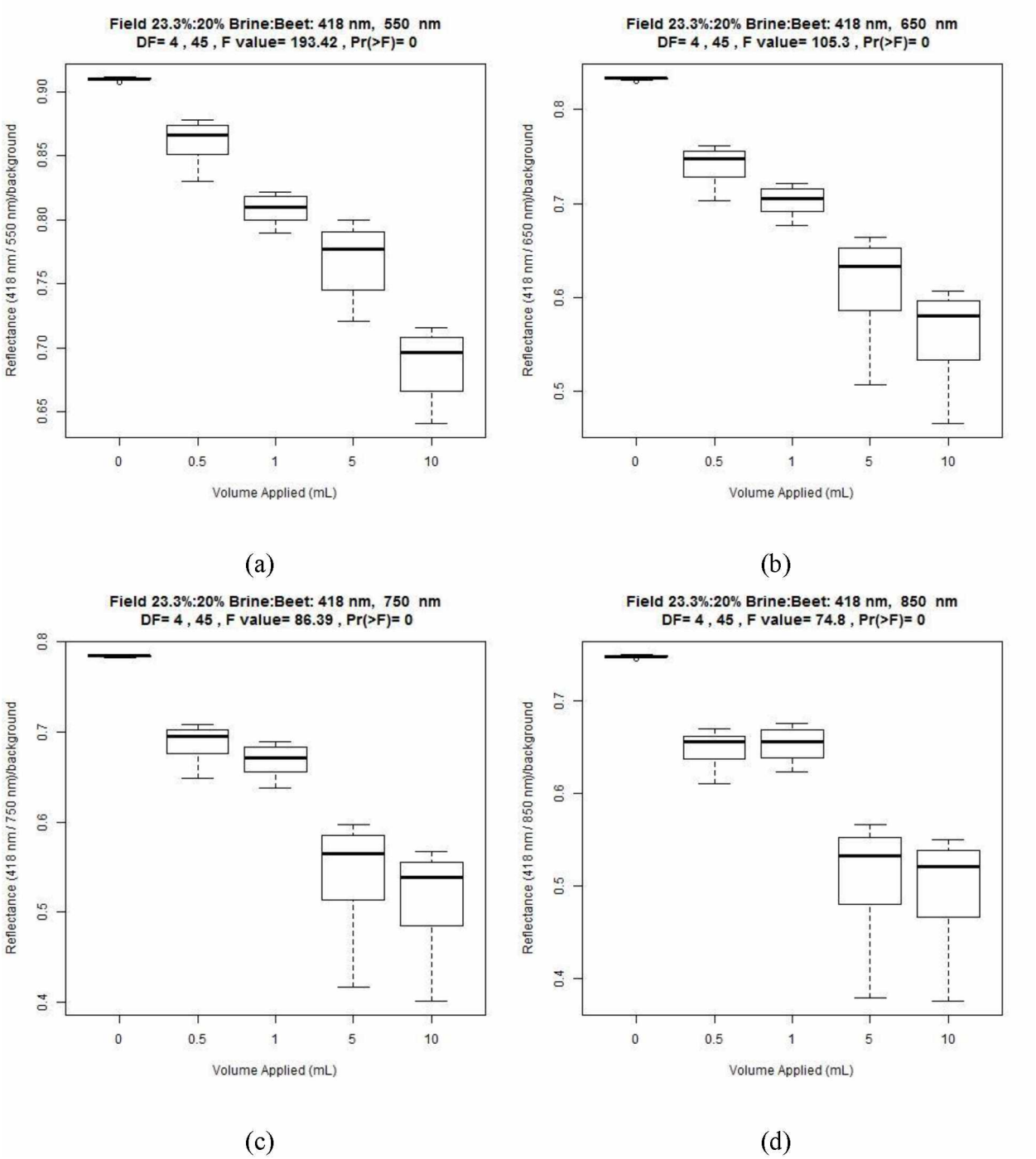

Figure 5.23 23.3% Brine 20% Beet Application Field Well-Maintained Pavement (a) through (d)

This means that instead of comparing different concentrations of the same volume applied, different volumes of the same concentration were compared to each other as shown below in Figure 5.24.

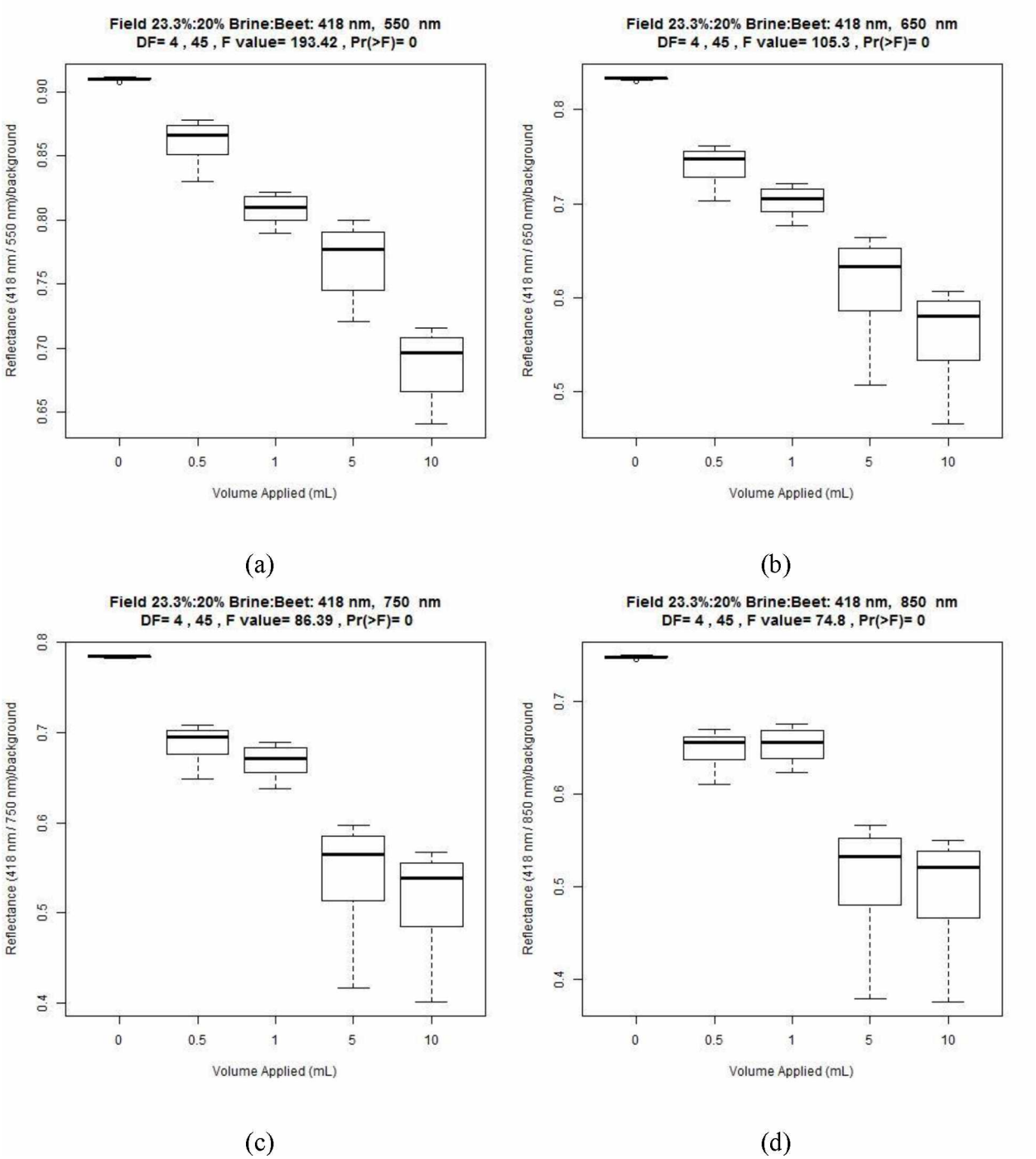

Figure 5.24 23.3% Brine 20% Beet Application Field Well-Maintained Pavement (a) through (d)

A comparison of the 418 nm wavelength to 850 nm resulted in a statistically significant difference [$F(4,45) = 193.42$, $p < 0.001$]. Conducting a pairwise comparison using t-tests shows that all the concentrations were statistically significantly different. These comparisons bare the

closest resemblance to the lab generated ones, only the field generated ones have a lot more noise, and follow the same problems as described by the 5 mL and 10 mL applications.

CHAPTER 6. DISCUSSION AND CONCLUSIONS

The goal of this research project was to explore the possibility of establishing relationships that could represent the presence and concentration of deicing materials applied to winter roads by utilizing spectral imaging hardware. To that end, the methods and data generated for this project represent a first step in the development of an objective method to detect and quantify chlorides and related solutions in roadway environments. Being able to identify concentration and location of brine and beet deicers using spectral imaging would be valuable for practical applications such as winter maintenance and future research such as deicer dispersion and tracking. Monitoring concentration of anti-icing and deicing would allow real-time monitoring to ensure adequate deicing concentrations. As a result, road maintenance crews can avoid conditions where a deicing chemical becomes too diluted and cannot function as intended, possibly refreezing the surface ice making winter roadways more dangerous. Accurate measurements of anti-icing and deicing chemicals would facilitate safer winter roadways as well as more effective use of state materials used to maintain safety and reduce operating budgets. The ability to track and locate surface presence would also be valuable for tracking migration and learn more about the methods by and quantities at which these chemicals migrate within and off the roadway. This is of particular interest as salts and carbohydrates can harm wildlife and some infrastructure.

Initially, the identification and analysis of deicing compounds, most notably sodium chloride and the carbohydrate red beet juice, seemed relatively straight forward. Our research began with the appraisal of current applications of remote sensing, which identified a similar project that had addressed the salinity of soils as it relates to plant health. Our experimentation started in a lab setting in order to maximize controlled variables and slowly expanding from that

point adding more uncertainties that would be realistically found in real world applications of the technology. In the lab setting background, lighting, temperature, runoff, film thickness, and compound were held constant. Utilizing these methods, the older relationship was tested (salt index), and new successful relationships were discovered and developed as well as the expansion of general knowledge of spectral imaging reflectance curves of different materials located on winter roadways.

The new relationships used key wavelengths that experienced a statistically significant change as concentration was adjusted. This involved exploring the application of band math and the development of new spectral analysis techniques to establish trends where the "significant" points of a curve (the peaks and valleys of the curve) were compared to one another.

A possible oversight brought up during analysis of the peaks and valleys was that some of the valleys approached or even exhibited non-reflectance. The reason a reflectance value of zero is problematic is that adding or changing surface materials, in other words possibly increasing the absorbance of a wavelength that is already at or near 0, might be muted or completely undetected as a change response at that particular wavelength. Because changes in reflectance at wavelengths where the value is already near zero might not be detected at all by the spectral equipment currently available, the range of wavelengths used for relationship analysis was expanded to every nm available, from 350 to 2500 nm. This approach eliminated the need for offsetting and normalization generating numerous consistent and repeatable trends for both the brine and beet-brine mixtures. The differences for beet-brine mixtures in a lab setting were much more significant than those developed for purely brine mixtures. The brine mixtures utilized NIR as key wavelengths and had slight overlap when graphed as boxplots while

the beet-brine mixtures utilized the visual spectrum and successfully created linear relationships with up to 1700 of the other wavelengths available.

Advancing to field testing and exploring the effectiveness and repeatability of these relationships as environmental variables changed highlighted the limitations of the hyperspectral equipment and qualifiers for which these lab relationships held true. Some of these problems were foreseen with the materials and hardware, yet these problems were still underestimated when actual field experimentation and testing began.

A major difficulty experienced in this research was the deleterious effects of water on NIR wavelengths. As the deicing compound accomplished its purpose, melting ice, water was created and began to pool on the application site. At certain thicknesses, types, and conditions, water and ice have extremely low reflectance values (i.e., ice and water absorb light and can prevent the identification of other materials contained in solution). Adding salt to water to make a brine results in absorption features and depressed reflectance in the NIR range, making it either impossible to see or massively muted key brine signatures. The best solution to begin seeing parts of the NIR curve for water was to decrease the film thickness, however in doing this it was discovered that the minimum thickness creatable in the laboratory setting was 0.8 mm and maintaining that thickness was a challenge. The thickness could theoretically be decreased further by creating surface striations on the container however the uneven visual markings made this an undesirable solution and research was forced to be limited to a minimum thickness of 0.8 mm. Other dish materials were tested to host the liquid solutions that wouldn't interfere with spectral radiance values however thinner applications were not successfully achieved.

Another issue was utilizing the hardware itself. The machinery was quite expensive with all accessories combined totaling near $100,000 dollars. The equipment had very little people with access due to security reasons which made obtaining and utilizing the equipment difficult. Additionally, the equipment section was going through many changes in terms of who was in charge of the equipment leading to strained access and difficulty in planning out use with other parties using the equipment. Actions were taken to attempt access to alternative machines with no success. The device used in this research last required a calibration in 2017 but because of the uncertain leadership and tumultuous access or funding recalibration has been postponed indefinitely.

Limitations also included accurately creating lab conditions that would mimic field conditions. The first steps in lab testing were a form of proof of concept, pouring liquid until petri dish had full surface coverage which turned out to be 22 mL of solution or 3.6 mm thick solution. This stepping off point revealed many of the problems associated with absorptive properties of water, the obvious solution being use less water. The film thickness could be decreased to a minimum of 5 mL or 0.8 mm before the liquid film would adhere to one side of the petri dish removing the possibility of full surface coverage. An intermediary point of 10 ml or 1.6 mm was used to monitor how changes in film thickness would affect the spectra. The resulting spectra showed more of the NIR spectral curve as volume decreased, however even at the smallest volume repeatable in the lab, the volume of liquid and thereby mg/cm^2 of salt applied was much greater than what AKDOT&PF northern region stated they applied. Techniques to get smaller films were explored by changing petri materials and creating surface striations to prevent the liquid from adhering to itself with limited success. The best solution

created was to fabricate a iced road segment as ice was a surface that would allow application amounts similar to AKDOT&PF winter roadway applications.

Fabrication of a lab-based asphalt pavement road was accomplished using a black PVC endcap to house the simulated winter road. An asphalt pavement core was fabricated using AKDOT&PF specifications and gyratorally compacted, cored, and cut into layer that would fit into the PVC endcaps. The simulated roads were a great success in terms of asphalt pavement spectral reflectance, small easily modifiable roadways, and controlled area. A specified amount of liquid water could then be applied and the specimens could be frozen for specific ice thicknesses. However, a problem arose during testing of deicing compounds. Maintaining the ice layer after fabrication was problematic. The lab research required measuring the reflectance of material in a building in upper campus at UAF however the time it took to align, reference, apply, and record the material the surface ice would begin to melt due to temperature fluctuations instead of deicing application. This highly accelerated melt proved impossible to rectify without access to a walk-in freezer that allowed single occupants for excess of a few hours and internal power outlets. Such facilities were unavailable at time of research and would have been extremely beneficial for lab testing by providing a relevant background material instead of the petri dishes that were used.

Only linear relationships and ratios were explored in the final automated pair comparisons. Even with this simplification, the vast number of pairs required two to three days of computation to successfully execute. The resulting outputs however still produced many successful relationships. Out of the wavelengths available, every point for 350 nm to 2500 nm, pairs were collected that showed a linear trend, either positive or negative, as concentrations changed. For some sampled data sets the number of paired wavelengths that created successfully

linear trends exceeded two million. Of those many points different methods were used to collate and cull the available pairs. The best course of action was to repeat the testing procedure on a new set of the same values thereby confirming repeatability of procedure and relationships. Of the remaining relationships they could be organized in different ways and the order with which these organizations took place could produce different end results for possible finalized identifiers. The R code would produce R squared values, slope values, and count how many times a given wavelength was repeated, the ideas being a larger R squared would produce a better linear trend which would not always be a good qualifier if a more parabolic trend is a better representation, a large slope would theoretically provide more sensitivity to change, and whichever wavelength was repeated the most would be the wavelength most sensitive to changes in concentration. All these procedures resulted in numerous wavelengths that work in a lab setting under idealized lighting conditions, constant temperature, and known values to accurately identify changes in concentration.

The approach that promised the highest likelihood of success was to select the points that had the highest rate of repetition, theoretically representing the wavelengths that would exhibit the greatest sensitivity to changes in concentration and volume. The wavelengths that had the highest number of matching points to their curve that produced a linear trend were then statistically analyzed. For the samples in the lab setting the relationships were extremely strong, there was statistically significant difference between each change in concentration and a consistent trend for both the brine and beet-brine compounds. While numerous sets of points, sometimes even over 1000 for beet-brine in particular, the results had to be culled to reasonable standards. Since brine only had a range of about 90 consecutive points the four that best visually appeared to represent the brine relationship at an even 5 nm spacing were shown in this paper.

Beet-brine solutions, having a much larger range of points available, instead iterated at 100 nm to show changes in accuracy.

Both relationships proved to be highly accurate in a lab setting, however this relationship ran into problems when applied to data gathered in the field. For brine, low concentrations and low volumetric applications tended to have an upward trend while higher applications tended to have a downward trend which matched data gathered in the lab. The lab settings lowest application rates were higher than the field setting's highest application rate which, while not an unreasonable expectation, the hope was that the relationships established in the lab would be strong enough to detect accurate field concentration readings regardless of volume on the surface.

Beet-brine relationships were a lot stronger and numerous than brine relationships in the lab setting. Unfortunately, the field gathered data did not match the accuracy and consistency of lab generated data. Another problem shown by the field data was the added uncertainty of background variation. Different wear, icing, and overall heterogeneity of asphalt pavement all resulted in different reflectance value and overall magnitude shifts in the recorded spectra. Normalization was attempted to rectify these aberrations however the effects were still felt in the overall trends. This is likely due to normalizing to a changing structure is not realistic. If the slight differences in crystalline structure of surface ice that is unperceivable to the human eye, but recorded by the hyperspectrometer, is the reason for these differences, then adding deicer would eventually remove the difference and the normalization would begin hindering the relationship when compared to lower concentrations of deicer.

For completeness, previously discarded analysis methods were also applied to the field data. The salt index equation that was used in soil identification for effective farmland was tested again, even though it had no trend in lab data, produced several relationships that were more statistically significant than the initial field method tested.

In conclusion, this research establishes that changes in concentration of deicers, specifically brine and beet-brine, can be accurately measured, are statistically significantly different at different concentrations, with consistent trends in a controlled lab setting. As more variables are added or changed the lab-based relationships become less effective. Further research could explore which specific elements are the cause, whether it is the changing temperature, application migration, background instability due to melting and changing ice structure, background uncertainty due to asphalt pavement, or perhaps the equations themselves. This research specifically limited its scope to only two variables (i.e., concentration and volume) in the analysis. This research presents a framework for analyzing winter roadways maintenance efforts. New sets of spectra were also produced and analyzed those specific to the components of winter roadways.

It is important for engineers and other such professionals who are responsible for the continued health of a city's infrastructure and the public within it, to be aware of current practices and future technologies that can aid in their work. The technologies used to promote safe winter roads have evolved quickly over the last century, and some of the procedures currently in place today could use further research to determine which of the currently available methods is most efficient.

Future research should focus on field-based data, perhaps focusing on wavelengths which can be acquired through current satellite arrays and focusing on permutations of equations rather than wavelength combinations. In addition, the use a cold room would aid in the fabrication of samples and the specimens that could be tested in a lab setting.

CHAPTER 7. REFERENCES

Alberta's Infrastructure and Transportation. 2006. Road Weather Information System (RWIS) Deployment Plan for Alberts's National Highway System (NHS). http://conf.tac-atc.ca/english/resourcecentre/readingroom/conference/conf2005/docs/s13/lo.pdf

Asfaw, E., Suryabhagavan, K.V., & Argaw, M. (2016, May 19). Soil salinity modeling and mapping using remote sensing and GIS: The case of Wonji sugar cane irrigation farm, Ethiopia. Retrieved December 15, 2017, from https://www.sciencedirect.com/science/article/pii/S1658077X16300042#b0035

Best Practices for Road Weather Management Colorado DOT One Pass Clearing Operations. 2012. http://www.ops.fhwa.dot.gov/publications/fhwahop12046/rwm07_colorado1.htm

City of Fairbanks (n.d.). Public Works Department. Retrieved December 15, 2017, from http://www.fairbanksalaska.us/departments/public-works/

Conger, S.M. 2005. Winter highway maintenance: a synthesis of highway practice. NCHRP Synthesis 344, National Research Council, Washington, D.C.

Corsi, S. R., Geis, S. W., Bowman, G., Failey, G. G., & Rutter, T. D. (2008, October 31). Aquatic Toxicity of Airfield-Pavement Deicer Materials and Implications for Airport Runoff. Retrieved December 15, 2017, from http://pubs.acs.org/doi/pdf/10.1021/es8017732

Dolce, C. (2017, December 12). Snow Has Already Been Recorded in All 50 States, and It Isn't Even Winter Yet. Retrieved December 15, 2017, from https://weather.com/storms/winter/news/2017-12-12-snow-50-states-winter-2017-18

ECOSTRESS Spectral Library (2018, February 2). Jet Propulsion Laboratory. Retrieved from https://speclib.jpl.nasa.gov/

Fay, L., M.Sc, Honarvarnazari, M., Ph.D., Jungwirth, S., M.Sc., Muthumani, A., M.Sc., Cui, N., Ph.D., & Shi, X., Ph.d., P.E. (2015, June). Manual for Environmental Best Practices for Snow and Ice Control (Proj.). Western Transportation Institute. http://clearroads.org/wp-content/uploads/dlm_uploads/Manual_ClearRoads_13-01_FINAL.pdf

Fay, L., Volkening, K., Gallaway, C. and Shi X., in Proceedings (DVD-ROM) of the 87th Annual Meeting of Transportation Research Board (held in Washington D.C., January 2008), eds. Transportation Research Board, (2008), Paper No. 08-1382.

Guidelines for the Selection of Snow and Ice Control Materials to Mitigate Environmental Impacts. 2007. Prepared for the NCHRP Project 6-16.

How Do Weather Events Impact Roads? Federal Highway Administration (2017, February 1). Retrieved February 2, 2019, from https://ops.fhwa.dot.gov/weather/q1_roadimpact.htm

IHS Global Insight (2014, February 24). The Economic Costs of Disruption form a Snowstorm Retrieved December 12, 2017, from https://www.highways.org/wp-content/uploads/2014/02/economic-costs-of-snowstorms.pdf

Kuemmel, D. A., & Hanbali, R. M. (1992, June 1). Accident Analysis of Ice Control Operations (Rep.). Retrieved December 13, 2017, from The Salt Institute website: http://www.trc.marquette.edu/publications/IceControl/ice-control-1992.pdf

Limitations of the Use of Abrasives in Winter Maintenance Operations. Prepared for the Wisconsin Department of Transportation. 2008.

Lysbakken, K.R., and Stotterud, R. "Prewetting Salt with Hot Water," PIARC XII International Winter Roads Congress, Sistriere, Italy, 2006

Manual of Practice for an Effective Anti-Icing Program. (2012, February 08). Federal Highway Administration Retrieved December 15, 2017, from https://www.fhwa.dot.gov/publications/research/safety/95202/005.cfm

McClellan, T., Boone, P. and Coleman, M. 2009. Maintenance Decision Support System (MDSS): Indiana Department of Transportation (INDOT) Statewide Implementation, Final Report. Indiana DOT.

Monteleone, D. (2012). Maintenance & Operations. Retrieved December 15, 2017, from http://dot.alaska.gov/stwdmno/

Nixon, W. A., Kochumman, G., Qiu, L., Qiu, J., & Xiong, J. (2007, May). Evaluation of Using Non-Corrosive Deicing Materials and Corrosion Reducing Treatments For Deicing Salts (Rep. No. IHR Technical Report #463). IIHR - Hydroscience & Engineering.

Ontario Ministry of Transportation. "Making Sand Last: MTO Tests Hot Water Sander" Road Talk, Vol. 14, No. 2, Summer, 2008.

Schuckman, Karen, J. A. (n.d.). *Band Math*. Retrieved from PennState College of Earth and Mineral Sciences: https://www.e-education.psu.edu/geog480/node/524

Snow and Ice. (2017, February 1). Federal Highway Administration Retrieved December 10, 2017, from https://ops.fhwa.dot.gov/weather/weather_events/snow_ice.htm

"Standard Methods for the Examination of Water and Waste Water," (1976). 14th ed., 1976. Available from the American Public Health Association, 1015 18th Street, N.W., Washington, DC 20036.

Staples, J.M., Gamradt, L., Stein, O., Shi, X., 2004. Recommendations for winter traction materials management on roadways adjacent to bodies of water. Montana Department of Transportation. FHWA/MT-04-008/8117-19. http://www.mdt.mt.gov/research/docs/research_proj/traction/final_report.pdf

Sumsion, E. S., & Guthrie, S. W., Ph.D. (2013). Physical and Chemical Effects of Deicers on Concrete Pavement: Literature Review (Rep. No. UT-13.09). Brigham Young University Department of Civil and Environmental Engineering.

Synthesis of Best Practices, Road Salt Management. (2003). Transportation Association of Canada. Retrieved from http://www.tac-atc.ca/english/resourcecentre/readingroom/pdf

Transportation Performance Management. (2017, June 27). Federal Highway Administration Retrieved December 15, 2017, from https://www.fhwa.dot.gov/tpm/about/goals.cfm

Vaa, T. "Implementation of New Sanding Method in Norway." Transportation Research Circular Number E-C063, 2004. http://onlinepubs.trb.org/onlinepubs/circulars/ec063.pdf

Williams, A. L., Stensland, G. J., Peters, C. R., & Osborne, J. (2000). Atmospheric Dispersion Study of Deicing Salt Applied to Roads (Rep.). Champaign, Illinois: Illionois State Water Survey Atmospheric Environment Section.

WINTER MAINTENANCE: Snow removal cost Anchorage, (2017, May 24). Alaska, millions more this winter than previous years. Retrieved December 15, 2017, from https://www.roadsbridges.com/winter-maintenance-snow-removal-cost-anchorage-alaska-millions-more-winter-previous-years

What is NDVI (Normalized Difference Vegetation Index)? (2018, February 24). GIS Geography Retrieved from https://gisgeography.com/ndvi-normalized-difference-vegetation-index/

CHAPTER 8. APPENDIX

```
#The parent code used to extract raw .SED data from a PSR+ 3500 unit and analyze the data
#Number of data frames and concentration numbers can be easily changed depending on
#number of data points applied to
#
#Set wd to whichever folder currently has the files which will be analyzed
#Surface
#setwd("File path name here")
#Home PC
setwd("File path name here")

#Read from .sed file based on spacing using fwf, "View(anysample)" for check
S1=read.fwf("filename.sed",widths=c(-5,5,-33,10),
col.names=c("Wavelength","Reflectance"),header=FALSE, skip=34)
S2=read.fwf("filename.sed",widths=c(-5,5,-33,10),
col.names=c("Wavelength","Reflectance"),header=FALSE, skip=34)
S3=read.fwf("filename.sed",widths=c(-5,5,-33,10),
col.names=c("Wavelength","Reflectance"),header=FALSE, skip=34)
S4=read.fwf("filename.sed",widths=c(-5,5,-33,10),
col.names=c("Wavelength","Reflectance"),header=FALSE, skip=34)
S5=read.fwf("filename.sed",widths=c(-5,5,-33,10),
col.names=c("Wavelength","Reflectance"),header=FALSE, skip=34)
S6=read.fwf("filename.sed",widths=c(-5,5,-33,10),
col.names=c("Wavelength","Reflectance"),header=FALSE, skip=34)
S7=read.fwf("filename.sed",widths=c(-5,5,-33,10),
col.names=c("Wavelength","Reflectance"),header=FALSE, skip=34)
S8=read.fwf("filename.sed",widths=c(-5,5,-33,10),
col.names=c("Wavelength","Reflectance"),header=FALSE, skip=34)
S9=read.fwf("filename.sed",widths=c(-5,5,-33,10),
col.names=c("Wavelength","Reflectance"),header=FALSE, skip=34)
S10=read.fwf("filename.sed",widths=c(-5,5,-33,10),
col.names=c("Wavelength","Reflectance"),header=FALSE, skip=34)
#Average these spectral readings with each other and saves as a named data frame
named_data_frame1=(S1+S2+S3+S4+S5+S6+S7+S8+S9+S10)/10

#Read from .sed file based on spacing using fwf, "View(anysample)" for check
S1=read.fwf("filename.sed",widths=c(-5,5,-33,10),
col.names=c("Wavelength","Reflectance"),header=FALSE, skip=34)
S2=read.fwf("filename.sed",widths=c(-5,5,-33,10),
col.names=c("Wavelength","Reflectance"),header=FALSE, skip=34)
S3=read.fwf("filename.sed",widths=c(-5,5,-33,10),
col.names=c("Wavelength","Reflectance"),header=FALSE, skip=34)
S4=read.fwf("filename.sed",widths=c(-5,5,-33,10),
col.names=c("Wavelength","Reflectance"),header=FALSE, skip=34)
```

```
S5=read.fwf("filename.sed",widths=c(-5,5,-33,10),
col.names=c("Wavelength","Reflectance"),header=FALSE, skip=34)
S6=read.fwf("filename.sed",widths=c(-5,5,-33,10),
col.names=c("Wavelength","Reflectance"),header=FALSE, skip=34)
S7=read.fwf("filename.sed",widths=c(-5,5,-33,10),
col.names=c("Wavelength","Reflectance"),header=FALSE, skip=34)
S8=read.fwf("filename.sed",widths=c(-5,5,-33,10),
col.names=c("Wavelength","Reflectance"),header=FALSE, skip=34)
S9=read.fwf("filename.sed",widths=c(-5,5,-33,10),
col.names=c("Wavelength","Reflectance"),header=FALSE, skip=34)
S10=read.fwf("filename.sed",widths=c(-5,5,-33,10),
col.names=c("Wavelength","Reflectance"),header=FALSE, skip=34)
#Average these spectral readings with each other and saves as a named data frame
named_data_frame2=(S1+S2+S3+S4+S5+S6+S7+S8+S9+S10)/10

#Read from .sed file based on spacing using fwf, "View(anysample)" for check
S1=read.fwf("filename.sed",widths=c(-5,5,-33,10),
col.names=c("Wavelength","Reflectance"),header=FALSE, skip=34)
S2=read.fwf("filename.sed",widths=c(-5,5,-33,10),
col.names=c("Wavelength","Reflectance"),header=FALSE, skip=34)
S3=read.fwf("filename.sed",widths=c(-5,5,-33,10),
col.names=c("Wavelength","Reflectance"),header=FALSE, skip=34)
S4=read.fwf("filename.sed",widths=c(-5,5,-33,10),
col.names=c("Wavelength","Reflectance"),header=FALSE, skip=34)
S5=read.fwf("filename.sed",widths=c(-5,5,-33,10),
col.names=c("Wavelength","Reflectance"),header=FALSE, skip=34)
S6=read.fwf("filename.sed",widths=c(-5,5,-33,10),
col.names=c("Wavelength","Reflectance"),header=FALSE, skip=34)
S7=read.fwf("filename.sed",widths=c(-5,5,-33,10),
col.names=c("Wavelength","Reflectance"),header=FALSE, skip=34)
S8=read.fwf("filename.sed",widths=c(-5,5,-33,10),
col.names=c("Wavelength","Reflectance"),header=FALSE, skip=34)
S9=read.fwf("filename.sed",widths=c(-5,5,-33,10),
col.names=c("Wavelength","Reflectance"),header=FALSE, skip=34)
S10=read.fwf("filename.sed",widths=c(-5,5,-33,10),
col.names=c("Wavelength","Reflectance"),header=FALSE, skip=34)
#Average these spectral readings with each other and saves as a named data frame
named_data_frame3=(S1+S2+S3+S4+S5+S6+S7+S8+S9+S10)/10

#Read from .sed file based on spacing using fwf, "View(anysample)" for check
S1=read.fwf("filename.sed",widths=c(-5,5,-33,10),
col.names=c("Wavelength","Reflectance"),header=FALSE, skip=34)
S2=read.fwf("filename.sed",widths=c(-5,5,-33,10),
col.names=c("Wavelength","Reflectance"),header=FALSE, skip=34)
S3=read.fwf("filename.sed",widths=c(-5,5,-33,10),
col.names=c("Wavelength","Reflectance"),header=FALSE, skip=34)
```

```
S4=read.fwf("filename.sed",widths=c(-5,5,-33,10),
col.names=c("Wavelength","Reflectance"),header=FALSE, skip=34)
S5=read.fwf("filename.sed",widths=c(-5,5,-33,10),
col.names=c("Wavelength","Reflectance"),header=FALSE, skip=34)
S6=read.fwf("filename.sed",widths=c(-5,5,-33,10),
col.names=c("Wavelength","Reflectance"),header=FALSE, skip=34)
S7=read.fwf("filename.sed",widths=c(-5,5,-33,10),
col.names=c("Wavelength","Reflectance"),header=FALSE, skip=34)
S8=read.fwf("filename.sed",widths=c(-5,5,-33,10),
col.names=c("Wavelength","Reflectance"),header=FALSE, skip=34)
S9=read.fwf("filename.sed",widths=c(-5,5,-33,10),
col.names=c("Wavelength","Reflectance"),header=FALSE, skip=34)
S10=read.fwf("filename.sed",widths=c(-5,5,-33,10),
col.names=c("Wavelength","Reflectance"),header=FALSE, skip=34)
#Average these spectral readings with each other and saves as a named data frame
named_data_frame4=(S1+S2+S3+S4+S5+S6+S7+S8+S9+S10)/10

#Read from .sed file based on spacing using fwf, "View(anysample)" for check
S1=read.fwf("filename.sed",widths=c(-5,5,-33,10),
col.names=c("Wavelength","Reflectance"),header=FALSE, skip=34)
S2=read.fwf("filename.sed",widths=c(-5,5,-33,10),
col.names=c("Wavelength","Reflectance"),header=FALSE, skip=34)
S3=read.fwf("filename.sed",widths=c(-5,5,-33,10),
col.names=c("Wavelength","Reflectance"),header=FALSE, skip=34)
S4=read.fwf("filename.sed",widths=c(-5,5,-33,10),
col.names=c("Wavelength","Reflectance"),header=FALSE, skip=34)
S5=read.fwf("filename.sed",widths=c(-5,5,-33,10),
col.names=c("Wavelength","Reflectance"),header=FALSE, skip=34)
S6=read.fwf("filename.sed",widths=c(-5,5,-33,10),
col.names=c("Wavelength","Reflectance"),header=FALSE, skip=34)
S7=read.fwf("filename.sed",widths=c(-5,5,-33,10),
col.names=c("Wavelength","Reflectance"),header=FALSE, skip=34)
S8=read.fwf("filename.sed",widths=c(-5,5,-33,10),
col.names=c("Wavelength","Reflectance"),header=FALSE, skip=34)
S9=read.fwf("filename.sed",widths=c(-5,5,-33,10),
col.names=c("Wavelength","Reflectance"),header=FALSE, skip=34)
S10=read.fwf("filename.sed",widths=c(-5,5,-33,10),
col.names=c("Wavelength","Reflectance"),header=FALSE, skip=34)
#Average these spectral readings with each other and saves as a named data frame
named_data_frame5=(S1+S2+S3+S4+S5+S6+S7+S8+S9+S10)/10

#In order to create a linear equation to look for R^2 and other properties
##Establish x values that correspond to the named data frames, in other words the solution
concentrations

#Here is an example of 0%, 5%, 10%, 15%, and 23.3% values used for brine lab testing
```

```
xentity1=0
xentity2=5
xentity3=10
xentity4=15
xentity5=23.3

#had to add eliminate 0 reflectance value of 0.000001 to eliminate divind by 0 at complete
absorption
#will not impact produced data as change is a complete shift upwards of an impossibly small
percentage
elimate0reflectances=cbind(c(rep(0,2151)),c(rep(0.000001,2151)))

#Each of the data frames needs to be assigned a new name here for easier coding down the line
entity1=named_data_frame1+elimate0reflectances
entity2=named_data_frame2+elimate0reflectances
entity3=named_data_frame3+elimate0reflectances
entity4=named_data_frame4+elimate0reflectances
entity5=named_data_frame5+elimate0reflectances

#creates an empty data frame in which to store successful relationships found
entitysuccess=c()

#in the loops i and j had 349 added to them to change it from channel # to wavelength #
#for loops will iterate wavelength nm by 1 while comparing to a single point on a curve
#the produced values are checked for either positive or negative linear trends
#number of less than or greater than checks dependant on number of concentrations available
for (j in seq(from=1, to=2151, by=1)){
 message(j+349)
 for(i in seq(from=1, to=2151,by=1)){

  if ( ((entity1[i,2]))/((entity1[j,2])) > ((entity2[i,2]))/((entity2[j,2]))
      &((entity2[i,2]))/((entity2[j,2])) > ((entity3[i,2]))/((entity3[j,2]))
      &((entity3[i,2]))/((entity3[j,2])) > ((entity4[i,2]))/((entity4[j,2]))
      &((entity4[i,2]))/((entity4[j,2])) > ((entity5[i,2]))/((entity5[j,2]))
  )
#xvalues and yvalues put into respective frames for linear analysis
  {
   xvalues=c(xentity1,xentity2,xentity3,xentity4,xentity5)

yvalues=c(((entity1[i,2]))/((entity1[j,2])),((entity2[i,2]))/((entity2[j,2])),((entity3[i,2]))/((entity3[j
,2])),((entity4[i,2]))/((entity4[j,2])),((entity5[i,2]))/((entity5[j,2])))
    lm=lm(yvalues~xvalues)

entity=(cbind(i+349,j+349,summary(lm)$coefficients[2,1],summary(lm)$r.squared,summary(lm
)$sigma,summary(lm)$coefficients[1,2],summary(lm)$coefficients[2,2],xentity1,xentity2,xentity
```

```
3,xentity4,xentity5,((entity1[i,2]))/((entity1[j,2])),((entity2[i,2]))/((entity2[j,2])),((entity3[i,2]))/((
entity3[j,2])),((entity4[i,2]))/((entity4[j,2])),((entity5[i,2]))/((entity5[j,2]))))
     entitysuccess=rbind(entitysuccess,entity)
   }


   if ( ((entity1[i,2]))/((entity1[j,2])) < ((entity2[i,2]))/((entity2[j,2]))
       &((entity2[i,2]))/((entity2[j,2])) < ((entity3[i,2]))/((entity3[j,2]))
       &((entity3[i,2]))/((entity3[j,2])) < ((entity4[i,2]))/((entity4[j,2]))
       &((entity4[i,2]))/((entity4[j,2])) < ((entity5[i,2]))/((entity5[j,2]))
   )
   {
    xvalues=c(xentity1,xentity2,xentity3,xentity4,xentity5)

yvalues=c(((entity1[i,2]))/((entity1[j,2])),((entity2[i,2]))/((entity2[j,2])),((entity3[i,2]))/((entity3[j
,2])),((entity4[i,2]))/((entity4[j,2])),((entity5[i,2]))/((entity5[j,2])))
     lm=lm(yvalues~xvalues)

entity=(cbind(i+349,j+349,summary(lm)$coefficients[2,1],summary(lm)$r.squared,summary(lm
)$sigma,summary(lm)$coefficients[1,2],summary(lm)$coefficients[2,2],xentity1,xentity2,xentity
3,xentity4,xentity5,((entity1[i,2]))/((entity1[j,2])),((entity2[i,2]))/((entity2[j,2])),((entity3[i,2]))/((
entity3[j,2])),((entity4[i,2]))/((entity4[j,2])),((entity5[i,2]))/((entity5[j,2]))))
     entitysuccess=rbind(entitysuccess,entity)
   }

  }

}
#order of data, wavelength1, wavelength2, slope, R-squared, RSS (sigma), stddev y, stddev x, x
values, y values!!!
colnames(entitysuccess)=c("Wvl1","Wvl2","slope","R2","sigma","stddev-y","stddev-
x","x0","x1","x2","x3","x4","y0","y1","y2","y3","y4")

#writes as textdocument and excel sheet FOR DESKTOP
#write.table(entitysuccess,"filepathname/txttitle.txt",sep="\t")
#write.csv(entitysuccess,"filepathname/exceltitle.csv",sep="\t")



#Modular code
#
#stddev insertion, goes after any given call to generate a data set
offsetstddev=c()
for(a in seq(from=1,to=2151,by=1)){

coercestddev=c(S1[a,2],S2[a,2],S3[a,2],S4[a,2],S5[a,2],S6[a,2],S7[a,2],S8[a,2],S9[a,2],S10[a,2])
```

```
  thestddev=sd(coercestddev)
  offsetstddev=rbind(offsetstddev, thestddev)
}
plot((S1+S2+S3+S4+S5+S6+S7+S8+S9+S10)/10)
lines(((S1+S2+S3+S4+S5+S6+S7+S8+S9+S10)/10)-offsetstddev, col="red")
lines(((S1+S2+S3+S4+S5+S6+S7+S8+S9+S10)/10)+offsetstddev, col="red")


#Modular code
#
#Produces a table that depicts number of times a wavelength repeats
designated_frame_name=read.csv("stored excel data/exceltitle.csv")
View(table(designated_frame_name[,3]))

#Used to compare data frames and extract duplicated values
excelgathered=c()
excelgathered=rbind(excelcalled22june,excelcalled22jan)
dupli=excelgathered[duplicated(excelgathered[,2:3]),]
View(table(dupli[,3]))
```